UNIVERSITAT DE BARCELONA

Decay of Doubly Strange Hypernuclei

Desintegració d'hipernuclis doblement estranys

Jordi Maneu Victoria

Decay of Doubly Strange Hypernuclei

By

JORDI MANEU VICTORIA

UNIVERSITAT DE BARCELONA

Department of Quantum Physics and Astrophysics
UNIVERSITY OF BARCELONA

A dissertation submitted to the University of Barcelona
in accordance with the requirements of the degree of
DOCTOR OF PHILOSOPHY in the Faculty of Physics.

SEPTEMBER 2019

Decaïment d'hipernuclis doblement estranys

Memòria presentada per optar al grau de doctor per la

Universitat de Barcelona

Programa de doctorat en Física

AUTOR: JORDI MANEU VICTORIA

DIRECTORA: ASSUMPTA PARREÑO GARCIA

TUTOR: DOMÈNEC ESPRIU CLIMENT

UNIVERSITAT DE BARCELONA

Resum

En el model estàndard de la física de partícules els constituents fonamentals de la matèria són els quarks i els leptons, que segueixen l'estadística de Fermi-Dirac. Els quarks experimenten totes les interaccions fonamentals i, a causa de la seva càrrega de color, interaccionen a través de la interacció forta. Dins d'aquest grup de partícules, el quark estrany o quark s és el tercer més lleuger i permet la classificació de les partícules en base al seu contingut d'estranyesa, sent zero per als nucleons i -1, -2 o -3 per als hiperons. Els hiperons son partícules inestables respecte la interacció feble a causa del seu contingut en quarks, i decauen prpincipalment a través de processos que no conserven ni paritat, ni isospin ni estranyesa. Entre ells el més representatiu és potser l'hiperó Λ, sent el més lleuger els seus modes de decaïment a l'espai lliure s'han mesurat amb bona precisió.

Els hipernuclis doble Λ són sistemes de diversos nucleons i dos hiperons Λ i per tant també es tracta de sistemes inestables respecte la interacció feble. Donat que els hiperons es troben immersos en el medi nuclear el principal mode de decaïment mesònic esdevé bloquejat degut al principi d'exclusió de Pauli i això provoca l'aparició de nous mecanismes amb absència de mesons a l'estat final. Entre aquests processos trobem no només aquells mediats per les reaccions $\Lambda N \to NN$, $\Lambda\Lambda \to \Lambda n$ i $\Lambda\Lambda \to \Sigma N$ sinó també, degut a la barreja de canals bariònics ($\Lambda N - \Sigma N$, $\Lambda\Lambda - \Xi N$,$\Lambda\Lambda - \Sigma\Sigma$) possible per la intervenció de la interacció forta, els canals febles $\Sigma N \to NN$, $\Xi N \to \Lambda n$, $\Xi N \to \Sigma N$, $\Sigma\Sigma \to \Lambda n$ i $\Sigma\Sigma \to \Sigma N$.

A causa de la conservació d'estranyesa en les reaccions fortes i electromagnètiques els hipernuclis són de gran utilitat a l'hora de realitzar espectroscopia nuclear. No només això, sinó que fent servir la variació d'estranyesa com a signatura de procesos febles permeten obtenir informació sobre les components amb i sense conservació de paritat de la interacció feble.

Malgrat els sistemes amb una sola partícula Λ s'han estudiat de manera exhaustiva durant més de 20 anys, relativament poc es coneix sobre els sistemes de doble estranyesa, principalment a causa de les dificultats de lligar dues Λ després de la captura de Ξ^-. Aquest projecte completa l'estudi del decaïment dels hipernuclis doble-Λ tot tenint en compte els efectes microscopics de la interacció forta en estats de dos barions en els sectors d'estranyesa -2, -1, i 0, corresponents als possibles estats bari\'o-bari\'o que apareixen en els estats inicial i final. La funció d'ona incial d'estranyesa -2 s'ha obtingut mitjançant la resolució d'una equació de matriu G amb la contribució de potencials bari\'o-bari\'o forts realistes, mentre que les funcions d'ona hiperó-nucleó finals s'han derivat de manera anàloga mitjançant un càlcul microscòpic de matriu T. Conseqüentment s'ha hagut de considerar l'obertura del canal induït per la parella ΞN (amb un llindar energètic més baix que aquell corresponent a la parella $\Sigma\Sigma$). Per evaluar aquests nous canals de desintegració s'ha derivat el potencial que governa la interacció ΞN amb un canvi d'estranyesa $|\Delta S| = 1$ per tal d'incorporar-los a l'estudi de ${}^{\;\;6}_{\Lambda\Lambda}\mathrm{He}$. Aquest potencial està basat en el model d'intercanvi de mesons i inclou els estats fonamentals dels octets pseudoescalar i vector, permetent així el càlcul de l'amplitud de transició.

L'incorporació dels estats $\Xi^- p$ i $\Xi^0 n$ ha requerit el càlcul de noves constants d'acoblament a través de Lagrangians quirals i la simetria de sabor SU(3) en el cas de mesons pseudoescalars i una extensió a la simetria d'spin-sabor SU(6) per al cas dels mesons vector. A més a més, per al cas de les contribucions amb conservació de paritat s'ha utilitzat un *pole model* en que la transició feble es desplaça del vèrtex mesònic a la

línia bariònica.

Addicionalment també s'han construit noves estructures operacionals per tal de tenir en compte els diferents canals de transició d'isospin en funció del mesó intercanviat. Aquestes estructures donen la informació necessària per construir les combinacions de constants d'acoblament que es veuen involucrades en el càlcul de les taxes de desintegració corresponents als nous canals estudiats.

Quan s'incorpora la component $\Lambda\Lambda \to \Xi N \to YN$ als càlculs mitjançant les constants d'acoblament proporcionades pel model de Nijmegen NSC97f s'observa que l'efecte principal per a un estat final Λn prové dels intercanvis de pions i kaons. L'efecte combinat fa disminuir la taxa de desintegració en més d'un factor dos, mentre que el canal ΣN experimenta un increment d'un factor quatre.

Si per contra s'utilitzen les constants d'acoblament obtingudes a partir del model desenvolupat en aquesta tesi s'observa una disminució d'un 30% sobre la desintegració considerant únicament els canals diagonals. Per a estats finals $Lambdan$ s'observa una reducció d'un factor cinc, deguda a una disminució en l'intercanvi de kaons i a un potenciament de l'intercanvi de pions i mesons eta, per als quals hi ha interferència destructiva. Pel que fa als estats finals ΣN, la reducció és d'un 15%.

En general, la component $\Lambda\Lambda - \Xi N$ de la funció d'ona redueix el quocient $\Gamma_{\Lambda n}/(\Gamma_{\Sigma^0 n} + \Gamma_{\Sigma^- p})$ obtingut amb la component $\Lambda\Lambda - \Lambda\Lambda$ en un factor 40, fins a un valor de 0.13 reforçant l'efecte de l'acobalment $\Lambda\Lambda - \Xi N$ en l'inversió de la dominància pel que fa als modes de desintegració $\Lambda n/\Sigma N$.

La nova taxa de desintegració $\Lambda\Lambda \to YN$ estudiada, amb with $YN = \Lambda n$, $\Sigma^0 n$ i $\Sigma^- p$, representa el 3-4% del decaïment no-mesònic induit per un barió i es troba notablement afectada pels efectes de la interacció forta. En particular la importància relativa dels *rates* parcials, en la relació $\Gamma_{\Lambda n}/(\Gamma_{\Sigma^0 n} + \Gamma_{\Sigma^- p})$, es veu invertida quan s'incorpora l'acoblament a estats ΞN en la funció d'ona $\Lambda\Lambda$ inicial correlacionada.

D'aquesta manera malgrat que els efectes introduits per la inclusió d'estats forts addicionals en el decaïment envers estats finals ΛN i ΣN tenen un impacte reduit, són no obstant distingibles i per tant mesures de la desintegració de ${}^{6}_{\Lambda\Lambda}\mathrm{He}$ proporcionarien informació molt necessària respecte la importància dels efectes de la interacció forta en els estats inicial i final i permetrien un millor constrenyiment de les constants d'acoblament bari ó-bari ó-mesó. Prospectivament, la inclusió d'estats intermitjos $\Sigma\Sigma$ contribuirà en aprofundir el nostre coneixement de la física de les reaccions en el sector d'estranyesa $S = -2$ i requerirà, de manera anàloga als estats ΞN, de la derivació de noves constants d'acoblament i operadors d'isospin.

Abstract

Double-Λ hypernuclei are bound systems of several nucleons and two Λ hyperons. These systems are unstable with respect to the weak interaction and chiefly decay through two-body processes that conserve neither parity, isospin or strangeness. Among such processes we can find those mediated by the $\Lambda N \to NN$, $\Lambda\Lambda \to \Lambda n$ and $\Lambda\Lambda \to \Sigma N$ reactions but also, thanks to the baryon channel mixing ($\Lambda N - \Sigma N$, $\Lambda\Lambda - \Xi N$,$\Lambda\Lambda - \Sigma\Sigma$) made possible by the strong interaction, the weak $\Sigma N \to NN$, $\Xi N \to \Lambda n$, $\Xi N \to \Sigma N$, $\Sigma\Sigma \to \Lambda n$ and $\Sigma\Sigma \to \Sigma N$ channels.

This work completes the study of the decay of double-Λ hypernuclei by taking into account the microscopic effects of the strong interaction on two baryon states in strangeness sectors -2, -1 and 0, pertaining to the possible baryon-baryon states appearing in the initial and final states, as previously stated. The initial strangeness -2 wave function is obtained from the solution of a G-matrix equation with the input of realistic strong baryon-baryon potentials, while the final hyperon-nucleon wave functions are derived analogously from a microscopic T-matrix calculation. Consequently the opening of the channel induced by the ΞN pair (with a lower energy threshold than that corresponding to the $\Sigma\Sigma$ pair) had to be considered. In order to evaluate these new decay channels the potential that governs the ΞN interaction with a strangeness variation $|\Delta S| = 1$ had to be derived for its incorporation in the study of the decay of ${}^{6}_{\Lambda\Lambda}\mathrm{He}$. This potential is based on the meson exchange model and includes fundamental states of the pseudoscalar and vector octets.

The inclusion of $\Xi^- p$ and $\Xi^0 n$ states required the derivation of new coupling constants using chiral Lagrangians and SU(3) flavour symmetry (extended to SU(6) spin-flavour symmetry for vector mesons), as well as the construction of new operational structures to account for the different isospin transition channels.

The new $\Lambda\Lambda \to YN$ decay rate studied in this work, with $YN = \Lambda n$, $\Sigma^0 n$ and $\Sigma^- p$, represents 3-4% of the total one-baryon induced non-mesonic decay and is remarkably affected by strong interaction effects. In particular, the relative importance of the partial decay rates, encoded in the ratio $\Gamma_{\Lambda n}/(\Gamma_{\Sigma^0 n} + \Gamma_{\Sigma^- p})$, gets inverted when the mixing to ΞN states is incorporated in the initial correlated $\Lambda\Lambda$ wave function. This sensitivity can be used experimentally to learn about the strong interaction in the strangeness -2 sector.

Per aspera ad scientiam

Agraïments

Amb aquesta tesi finalitza una de les etapes més importants i llargues de la meva vida. Han sigut uns anys d'increïble aprenentatge i unes quantes dificultats però sobretot plens d'un gaudi que espero quedi reflectit en aquestes pàgines.

M'agradaria començar aquesta secció agraint, com no podia ser d'altra manera, la feina i dedicació que ha abocat en aquest projecte la meva directora de tesi, l'Assum, sense la qual aquest escrit i la recerca que encapsula no hauria arribat a ser ni una desena part del que és ara. No només això sinó que totes les hores sota la seva tutela (que ja és dir! física nuclear, màster i doctorat!) han suposat una colossal experiència tant en l'àmbit personal com científic, i em podré donar per satisfet si mai aconsegueixo retornar-li una mínima part.

Si la primera menció correspon per dret a l'Assumpta, no hi ha d'haver dubte que la següent ha de ser per ningú altre que l'Àngels Ramos. D'aquells dies en què va ser la meva professora d'Anàlisi Matemàtica 2 ja n'han passat una bona pila però el seu entusiasme per la física no s'ha vist disminuït en absolut. No hauria pogut arribar mai a pensar que acabaria compartint mesos de recerca amb ella i haver-ho fet ha sigut tot un honor.

Mantenint-nos encara dins del departament de Física Quàntica i Astrofísica provinent del clàssic "Estructura i Constituents de la Matèria" voldria dedicar també algunes paraules als meus companys de despatx, Àxel, Albert i Pere, l'actitud i companyonia dels

quals ha fet que el gresol del doctorat hagi sigut encara més suportable. Tampoc voldria oblidar-me d'en Marc i la Glòria que queden com a custodis del castell.

Si bé dur a terme un doctorat requereix una quantitat de feina gens negligible també és cert que hom no pot estar vint-i-quatre hores al dia, set dies a la setmana treballant. És en aquest àmbit més ociós en què apareixen les converses de sobretaula a l'hora de dinar amb Alberto, Santi, Raúl, David i Òscar, vitals com a estiraments mentals per relaxar la closca i afrontar les tardes amb més energia.

Aquests anys de doctorat no només han suposat un creixement intel·lectual i personal sinó que m'han permès dedicar-me a una afició a la qual li tinc particular estima: córrer. Com en l'aprenentatge la bellesa de córrer rau en una simple premissa: sempre millorar. A dates de l'escriptura d'aquests agraïments són 15319 kilòmetres acumulats a les cames; plens de reptes superats, millors marques personals i sabatilles gastades. Algú us podrà dir que córrer és un esport individual i fins fa un parell d'anys li hauria donat la raó però els integrants de la secció d'atletisme del Club Esportiu Mediterrani han aconseguit que m'alegri d'estar equivocat. Si bé es tracta d'una agrupació amb un valor personal que arriba als núvols m'agradaria destacar en particular un triplet de feres amb els que he compartit molts entrenaments: José, Sergio, Dani sou molt grans i espero que els kilòmetres que hem compartit i compartirem no parin de créixer mai.

Com una bona parella de subjectallibres, si les primeres línies són dedicades a la persona que ha fet possible aquesta tesi aleshores és de simetria que les últimes vagin dedicades a les persones que han sigut cabdals en el meu desenvolupament: la meva família.

Al meu germà, l'Àlex, que ha sigut sempre un exemple a seguir i m'ha ensenyat que no hi ha res millor que el fet d'aprendre pel plaer d'aprendre i que la feina ben feta és la seva pròpia recompensa.

Als meus pares, el papa i la mama, l'Alexandre i la Margarita, que no satisfets amb

donar-m'ho tot m'han donat més i m'han fet costat al llarg de totes les bogeries que he emprés. Sense ells no seria la persona que sóc ara. Al final no hem passat per medicina però amb una mica de sort...

A l'Emma, que encara no ho sap però ha fet que el darrer any de tesi del seu oncle sigui molt més alegre. I si algun dia sent curiositat per aquest treball que es trobi aquestes paraules d'encoratjament: Zawsze możesz na mnie liczyć!

Author's declaration

I declare that the work in this dissertation was carried out in accordance with the requirements of the University's Regulations and Code of Practice for Research Degree Programmes and that it has not been submitted for any other academic award. Except where indicated by specific reference in the text, the work is the candidate's own work. Work done in collaboration with, or with the assistance of, others, is indicated as such. Any views expressed in the dissertation are those of the author.

SIGNED: ..... DATE: .....

TABLE OF CONTENTS

List of Tables

List of Figures

CHAPTER 1

INTRODUCTION

In the Standard Model of Particle Physics the fundamental constituents of matter are quarks and leptons, which collectively follow Fermi-Dirac statistics. Quarks experience all the fundamental interactions and, due to their color charge [1], interact through the strong interaction. Out of this group of particles, the strange quark or *s*-quark is the third lightest quark and allows the classification of the particles belonging to the baryon octet according to their strangeness, being zero for nucleons and -1, -2 or -3 for hyperons. The main objective of strangeness physics is the investigation of the hyperon-nucleon (YN) and hyperon-hyperon (YY) interactions in order to obtain a unified understanding of the baryon-baryon (BB) interaction in the $SU(3)_F$ sector. The current understanding of the nuclear force is phenomenological in nature, but there is no clear physical comprehension at the fundamental level. Studies which extend this force to the strange sector are expected to improve our understanding of the underlying theory governing nuclear interaction.

Hyperons are unstable with respect to the weak interaction due to their quark composition and decay through reactions that do not conserve neither parity, strangeness

nor isospin. The Λ hyperon is the most illustrative example. Being the lightest strange baryon, its weak decay modes in free space, $\Lambda \rightarrow N\pi$, have been measured experimentally with good precision. These mesonic decay channels show that transitions which involve a change in isospin of 3/2 are suppressed with respect to those involving ΔI =1/2 variations[2]. This is the well-known ΔI =1/2 rule of weak hyperon decays. The origin of this suppression is not well understood, and although there are several investigations that try to understand this experimental fact, most of the theoretical work involving weak interactions among hadrons assume the validity of such phenomenological rule.

Since the discovery in 1952 of the first strange fragment in emulsion chamber experiments, many efforts have been put in extending our knowledge of the nuclear chart towards the SU(3) sector. Worldwide, the study of the interactions among nucleons and hyperons has been a priority in the research plan of many experimental facilities. After more than sixty years of Λ-hypernuclear studies, some attention has moved recently to doubly strange systems, with the production of $\Lambda\Lambda$-hypernuclei and more recently, with proposals to study Ξ-hypernuclear spectroscopy.

The most effective way of producing doubly strange hypernuclei is through the (K^-,K^+) reaction, which transfers two strangeness and charge units to the target nucleus. Employing high intensity K^- beams of 1.8 MeV/c and high resolution spectrometers, the E05 experiment at J-PARC [3] plans on producing ${}^{12}_{\Xi}$Be hypernuclei, with the goal of studying their spectroscopy, as well as obtaining information on the Ξ potential depth and the $\Xi N \rightarrow \Lambda\Lambda$ conversion width. On the other hand the E07 experiment at J-PARC[4] aims at producing double-Λ hypernuclei in emulsion, following the capture of Ξ^- hyperons at rest, with ten times more statistics than the KEK-E373 experiment that led to the observation of the ${}^{6}_{\Lambda\Lambda}$He hypernucleus (Nagara event) [5] which established the mild attractive character of the $\Lambda\Lambda$ interaction. A recent analysis of the KEK-E373 experiment also provided direct evidence for the existence of a bound Ξ^- hypernucleus

${}^{15}_{\Xi}$C (Kiso event), produced in the reaction $\Xi^- + {}^{14}$N $\rightarrow {}^{15}_{\Xi}$C $\rightarrow {}^{10}_{\Lambda}$Be $+ {}^{5}_{\Lambda}$He [6, 7].

In hypernuclei, which are bound systems composed of nucleons and one or more hyperons, the Λ is embedded in the nuclear medium and its dominant decay mode, $\Lambda \rightarrow N\pi$, becomes Pauli blocked, as the emerging nucleon tries to access momentum states that are essentially occupied by the surrounding nucleons. Under such circumstances, new decay mechanisms appear, with no mesons in the final state, involving the participation of another baryon. The dominant decay mode for single-Λ hypernuclei with $A > 5$ is $\Lambda N \rightarrow NN$. For double-Λ hypernuclei additional hyperon-induced mechanisms, $\Lambda\Lambda \rightarrow \Lambda n$, $\Lambda\Lambda \rightarrow \Sigma^- p$ and $\Lambda\Lambda \rightarrow \Sigma^0 n$ (referred to as $\Lambda\Lambda \rightarrow YN$ in general henceforth), become possible. Because of the conservation of strangeness in strong and electromagnetic interactions, hypernuclei can be used for nuclear spectroscopy. In addition, using the change in strangeness as a signature of the weak process, the decay of hypernuclei is thus a suitable framework to obtain information not only of the strong baryon-baryon interaction but also on the baryon-baryon interaction in the weak sector, and, using the change of strangeness as signature, one has access to both its parity-conserving (PC) and parity-violating (PV) components. Moreover, the study of multi-strange nuclei is of benefit to the understanding of dense systems, where due to charge neutrality s quarks are preferred.

The inner core of neutron stars have a high chance of containing hyperons, as the density increases hyperonic matter is preferred from an energy point of view. The presence of these hyperons would soften the equations of state (EoS) considerably, consequently lowering the maximum mass these celestial bodies could achieve. This leads to a so-called "hyperon puzzle" due to the unusually high measured masses of millisecond pulsars, that would require new mechanisms to stiffen the EoS: stiffer hyperon-nucleon and/or hyperon-hyperon interactions, repulsive three-body forces with hyperons, new hadronic degrees of freedom that push the onset of appearance of hyperons

to higher densities or the phase transition to quark matter below the hyperon onset [8–10].

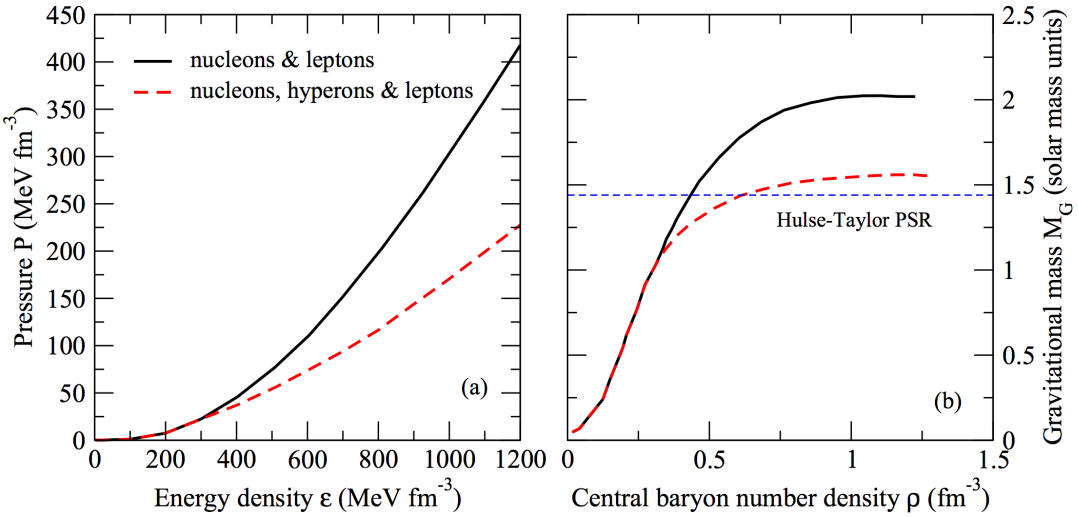

Figure 1.1: Effects of the presence of hyperons on the equation of state and mass of a neutron star. Figures from Ref. [8]

There's also evidence that hyperons play a glue-like role inside the nuclear core, lowering the binding energy and allowing the nucleus to have more neutrons than otherwise possible. Furthermore, the presence of hyperons seems to also induce a reduction in the nuclear radius [11, 12].

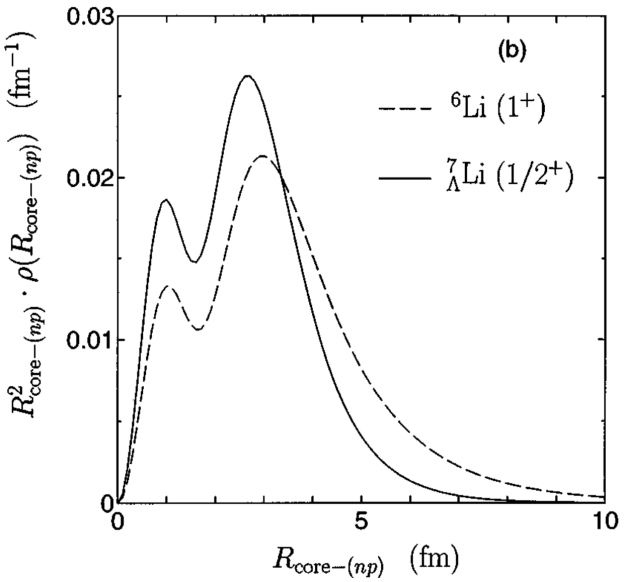

Figure 1.2: Density distributions for the ground states of ^{6}Li and $^7_\Lambda$Li[11].

The decay of single-Λ hypernuclei has been studied thoroughly for more than 20 years, both experimentally and theoretically (see the reviews [13–16]) and a consistent picture of the experimental data[17–23], which includes not only lifetimes but also partial decay widths, the decay asymmetries of the emitted particles, single nucleon, and two-nucleon coincidence spectra, has emerged. Crucial elements for this success have been the inclusion of a scalar-isoscalar component in the weak decay mechanism[24–34], the consideration of final state interactions in the data analysis[24–34], and the estimation of the role played by multiabsorption processes, among others.

Little is known, comparatively, about the double strangeness systems, due to the small yields for binding two Λ particles after Ξ^- capture and the ambiguities in interpreting events owing to the formation of particle-stable excited species. However, this situation might change with the planned experiments at J-PARC which will have much

Table 1.1: Mass and binding energies of helium nucleus and hypernuclei.

	^{4}**He**	$^5_\Lambda$**He**	$^6_{\Lambda\Lambda}$**He**
Mass (Mev)	3738.93	4852.08	5960.97
Binding Energy (MeV)	16.7485	19.2721	26.0639

higher statistics. Some theoretical studies have addressed the weak decay of double-Λ hypernuclei [35–37] since the new hyperonic mechanisms provide new information to constraint the theoretical models.

This work aims at obtaining the weak decay rates of the doubly strange ${}^{6}_{\Lambda\Lambda}$He hypernucleus, focusing especially in the new weak decay modes associated to the presence of two Λ particles, and including all the intermediate baryonic channels allowed by the strong interaction. Specifically, the weak decay process may occur from a $\Lambda\Lambda$, ΞN or $\Sigma\Sigma$ state, which can be excited via the strong interaction from the initial $\Lambda\Lambda$ pair, while the strong interaction also determines the final YN wave function component, which may have transitioned from either a ΛN or a ΣN intermediate state.

For the weak transition we employ the meson-exchange model, built upon the exchange of mesons belonging to the ground state of pseudoscalar and vector octets, thoroughly employed for single-Λ hypernuclei, and extended to the decay of double-Λ hypernuclei in Ref. [35]. The tree-level values for the baryon-baryon-meson coupling constants are derived using SU(3) symmetry for pseudoscalar mesons and the Hidden Local Symmetry for vector mesons. In the computation of the decay rate, the effects of the strong interaction on the initial state are introduced through the solution of a G-matrix equation, with the input of realistic baryon-baryon potentials[38], while the final hyperon-nucleon wave functions are obtained in an analogous way, by solving the corresponding T-matrix equation. The essential development with respect to previous calculations [35] is the consideration of the weak decay processes from the intermediate states than can be coupled to the initial $\Lambda\Lambda$. This requires the use of G-matrix wave functions for the coupled transitions $\Lambda\Lambda$-$\Lambda\Lambda$ and $\Lambda\Lambda$-ΞN (we will see that the $\Lambda\Lambda$-$\Sigma\Sigma$ component is very small and will be neglected in our calculations). Furthermore, the transition potential for the weak $\Xi N - YN$ decay, where Y can be either the Λ or Σ baryon, requires the derivation of novel decay constants. These two new ingredients have

allowed us to obtain an update on the decay rate for the $(\Lambda\Lambda - \Lambda\Lambda) \rightarrow (YN - Y'N)$ channel as well as new results for the $(\Lambda\Lambda - \Xi N) \rightarrow (YN - Y'N)$ channel, where Y' follows the same criteria as Y.

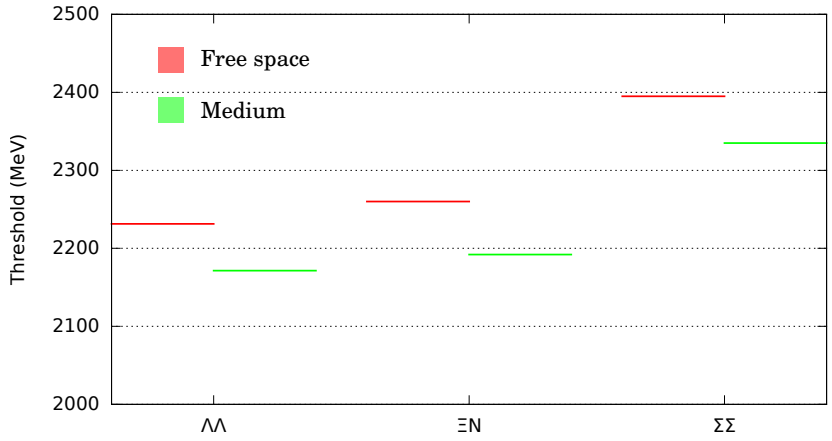

Figure 1.3: Energy thresholds for the $\Lambda\Lambda$, ΞN and $\Sigma\Sigma$ hyperonic states.

It is important to note that since we'll be dealing with strangeness -2 initial states the possible starting pairs will be $\Lambda\Lambda$, ΞN or $\Sigma\Sigma$. In Fig. 1.3 we can observe the two particle thresholds in free space and in the presence of a medium. By considering the medium we lower the thresholds but we do not change its order.

The physical properties and decay modes of the most relevant hyperons for this work are collected in Table 1.2[39]. The weak instability of hyperons precludes a clean extraction of the strong and weak hyperon-nucleon interactions in free space. Consequently, experimental data regarding YN scattering is pretty limited both statistically and in momentum range. Baryon-baryon interaction models are constructed typically as SU(3) flavour extensions of nucleon-nucleon (NN) models which use a large set of NN scattering data, a very poor database of YN scattering points (≤ 40) and the binding energies of light strange bound systems.

Some information on the strong YN interaction can also be obtained from the study of associated Λ-kaon and Σ-kaon production in nucleon-nucleon collisions near threshold

[40–46]. These analysis, nevertheless, present large model dependencies related to the strong interactions between the final particles. Recently, model independent determinations of the low-energy scattering parameters have been successfully obtained through numerical calculations based on Lattice QCD (Quantum Chromodynamics) methods, which rely on extrapolations on the lattice parameter and pion mass[47, 48]. Although promising, an extrapolation of the results to the physical quark masses is still missing, except for the $\Sigma^- n$ channel [48].

With respect to the weak interaction, there was a proposal to measure the Λp production in free space through the $np \to \Lambda p$ mechanism [49–51]. The small cross-sections associated to the process made it impossible to extract any signal for the weak YN interaction. This is the reason why, during the last 60 years or so, the most important source of information on these interactions comes from the study of the spectroscopy and decay of hypernuclei.

The doubly strange baryon Ξ^-, which is the focus of the present work, decays in free space with 99.987% probability through the channel $\Xi^- \to \Lambda\pi^-$, while in the medium the presence of nucleons favors strong and weak non-mesonic decays such as $\Xi^- N \to \Lambda\Lambda, \Sigma\Sigma, \Lambda\Sigma, \Lambda N, \Sigma N$. While the strong $\Xi^- p \to \Lambda\Lambda$ reaction provides information on $\Lambda\Lambda$-hypernuclei, little to no information is available on the V_{Ξ^-} potential. Production experiments provided a shallow potential (-14 MeV), mistakenly interpreted as a bound state of ${}^{12}_{\Lambda}$Be. Calculations with NSC89 and NSC97 Nijmegen models provide a repulsive Ξ^--nucleus potential, while recently constructed ESC04 and ESC08 models give an attractive Ξ^--nucleus potential[52].

The most effective way of producing doubly strange hypernuclei is through the (K^-, K^+) reaction [53], in which the two strangeness and charge units are transferred to the target nucleus. This reaction is one of the most promising when it comes to studying systems with double strangeness. Research into these type of hypernuclei allows to

deepen the knowledge of strong interactions between octet baryons. Ξ hypernuclear spectroscopy is expected to reveal single-particle orbits and determine the Ξ potential depth, which is one of the most important magnitudes to constrain the baryon-baryon interaction models used to describe the cores of neutron stars.

There is evidence of the existence of Ξ hypernuclei in emulsion events, but no bound states have been observed in the experiments conducted so far, due in part to the limited statistical and detector resolution. Other experiments, planned at J-PARC (Ibaraki, Japan), are expected to obtain measures of the energy levels that would give information about the single-particle potential. These experiments are based on a high purity and intensity kaon or pion beams, of energies up to $\sim 2\text{GeV}/c$, which have a high cross-section for the production of $S = -1$ or $S = -2$ hyperons. For example, at the K1.8 beamline at J-PARC the Ξ^- particle is produced through the (K^-,K^+) reaction at 1.8GeV/c where the cross section for the process $p(\text{K}^-,\text{K}^+)\Xi^-$ reaches its maximum value. The produced Ξ^- is stopped inside the iron target, where it forms a Ξ^- atom (with the target nucleus). This atom then emits X-Rays, which are detected by Hyperball-J. The study of these X rays will yield information on the Ξ-nucleus interaction, since the difference between the calculated and the measured X-ray energies is caused by these interactions [54].

Certain considerations must be taken into account for the choice of experimental target. From a physics point of view one must take into account that for a given atomic state the energy shift and width are wider for heavier atoms, although the heavier the atom for the chosen target is, the faster the absorption by the target at the initial state, and thus detection becomes impossible. From the point of view of experimental viability the most important characteristics to bear in mind are: production rate, stopping probability and X-ray absorption in the target.

In addition to the different topics going to be investigated by the PANDA experiment at GSI (Darmstadt, Germany) [55], a high intensity antiproton beam will be used to

generate a $\Xi^+\Xi^-$ pair. This reaction has a cross section of 2μb at 3GeV/c. The goal is to maximize the amount of stopped Ξ^- in the target. The nuclear target presents certain advantages such as a higher cross section and Ξ^- slowing down in dense matter. On the other hand there are some disadvantages like high background and beam losses.

Table 1.2: Properties of the main hyperons involved in the present work including mass (m), isospin, spin, parity ($I(J^P)$), mean life (τ) and charge (q), as well as their main decay modes.

	Physical properties	**Leptonic and radiative decay modes**	**Non-leptonic decay modes**
$\mathbf{\Lambda}$	$m = 1115.883 \pm 0.006$ MeV $I(J^P) = 0(\frac{1}{2}^+)$ $\tau = (2.632 \pm 0.020) \times 10^{-10} s$ $q = 0$	$\Lambda \rightarrow \begin{cases} n\gamma & (1.75 \pm 0.15)\% \\ p\pi^+\gamma & (8.4 \pm 1.4)\% \\ pe\overline{\nu}_e & (8.32 \pm 0.14)\% \\ p\mu\overline{\nu}_\mu & (1.57 \pm 0.35)\% \end{cases}$	$\Lambda \rightarrow \begin{cases} p\pi^- & (63.9 \pm 0.5)\% \\ n\pi^0 & (25.8 \pm 0.5)\% \end{cases}$
$\mathbf{\Sigma^0}$	$m = 1191.642 \pm 0.024$ MeV $I(J^P) = 1(\frac{1}{2}^+)$ $\tau = (7.4 \pm 0.7) \times 10^{-20} s$ $q = 0$	$\Sigma^0 \rightarrow \begin{cases} \Lambda\gamma & 100\% \\ \Lambda\gamma\gamma & < 3\% \\ \Lambda e^+e^- & 5 \times 10^{-3} \end{cases}$	N/A
$\mathbf{\Sigma^-}$	$m = 1197.449 \pm 0.030$ MeV $I(J^P) = 1(\frac{1}{2}^+)$ $\tau = (1.479 \pm 0.011) \times 10^{-10} s$ $q = -1$	$\Sigma^- \rightarrow \begin{cases} n\pi^-\gamma & (4.6 \pm 0.6) \times 10^{-4}\% \\ ne^-\overline{\nu}_e & (1.017 \pm 0.034) \times 10^{-3} \\ n\mu^-\overline{\nu}_\mu & (4.5 \pm 0.4) \times 10^{-4} \\ \Lambda e^-\overline{\nu}_e & (5.73 \pm 0.27) \times 10^{-5} \end{cases}$	$\Sigma^- \rightarrow n\pi^-$ $(99.848 \pm 0.005)\%$
$\mathbf{\Xi^-}$	$m = 1321.71 \pm 0.07$ MeV $I(J^P) = \frac{1}{2}(\frac{1}{2}^+)$ $\tau = (1.639 \pm 0.015) \times 10^{-10} s$ $q = -1$	$\Xi^- \rightarrow \begin{cases} \Xi^-\gamma & (1.27 \pm 0.23) \times 10^{-4} \\ \Lambda e\overline{\nu}_e & (5.63 \pm 0.31) \times 10^{-4} \\ \Lambda\mu\overline{\nu}_\mu & (3.5^{+3.5}_{-2.2}) \times 10^{-4} \\ \Sigma^0 e\overline{\nu}_e & (8.7 \pm 1.7) \times 10^{-5} \\ \Sigma^0\mu\overline{\nu}_\mu & < 8 \times 10^{-4} \\ \Xi^0 e\overline{\nu}_e & < 2 - 3 \times 10^{-3} \end{cases}$	$\Xi^- \rightarrow \Lambda\pi^-$ $(99.887 \pm 0.035)\%$

CHAPTER 2

BARYON-BARYON INTERACTIONS AT LOW ENERGIES

Quantum chromodynamics (QCD) is a non-abelian description of strong interactions, using quarks and gluons as basic degrees of freedom. This theory is born, partially, due to the success of the the abelian gauge theory describing the interaction between charged particles, Quantum Electrodynamics (QED). The QCD analog of electric charge is a notion called color, related to the strong interactions of quarks and gluons. This property was proposed shortly after the existence of quarks was first suggested in 1964 by George Zweig and Murray Gell-Mann[56, 57] in order to explain the coexistence of quarks with identical quantum states inside some hadrons, which would violate the Pauli exclusion principle.

While QED and QCD share a formal similarity there exist two crucial differences between the two theories: color confinement and asymptotic freedom. The phenomenon of color confinement may be understood in comparison to the behaviour of the photon field in QED. While the electrical field between charged particles decreases in strength rapidly as they are separated, the gluon field between two color charges forms a narrow flux tube instead and as such the strong force between the pair is constant regardless

of their separation. Eventually, as the particles become separated from one another, a point is reached in which it is more energetically favourable to produce another $q\overline{q}$ pair rather than extend the flux tube further. In counterpart, asymptotic freedom means that as the energy scale of the interactions between quarks and gluons increases (or as the length scale decreases) the interactions between particles becomes weaker, which entails perturbation theory is only applicable at short distances.

While these difficulties preclude rigorous QCD predictions there exist two cases in which reliable theoretical predictions may be obtained from this theory: the high and low energy limits.

As stated, due to colour confinement, QCD may not be treated perturbatively at low energies. To proceed, one must then construct an effective field theory with hadronic degrees of freedom that preserves the symmetries of the underlying theory.

The SU(3) group is integral to strong interactions, since it is the gauge group of QCD, and the $SU(3)_L$ x $SU(3)_R$ direct product is the chiral symmetry group of QCD for vanishing u-, d-, and s-quark masses. We shall remind here that quarks are spin-1/2 fermions with six different flavours on top of the three possible colours.

There is a large energy gap between the three light quarks (u, d, s) and the three heavy ones (c, b, t). Since the masses of the three lightest quarks are well below the typical hadronic scale (1 GeV) one might simplify the problem by considering that $m_u, m_d, m_s \to 0$ in the description of low-energy QCD. Under this assumption, the QCD Lagrangian is then given by

$$\mathscr{L}_{QCD} = \sum_{l=u,d,s} \overline{q}_l i\gamma^\mu D_\mu q_l - \frac{1}{4}\mathscr{G}_{\mu\nu,a}\mathscr{G}_a^{\mu\nu}, \tag{2.1}$$

in terms of the covariant derivative

$$D_\mu = \partial_\mu - ig\sum_{a=1}^{8}\frac{\lambda_a}{2}\mathscr{A}_{\mu,a} \tag{2.2}$$

and the field strength tensor, which corresponds to

$$\mathcal{G}_{\mu\nu,a} = \partial_\mu \mathcal{A}_{\nu,a} - \partial_\nu \mathcal{A}_{\mu,a} + g f_{abc} \mathcal{A}_{\mu,b} \mathcal{A}_{\nu,c}, \tag{2.3}$$

being $\mathcal{A}_{\mu,a}$ the eight independent gauge potentials (as it is known, the number of generators may be related to the dimension through the formula $N^2 - 1$, and as such for $N = 3$ we obtain eight generators), f_{abc} the totally antisymmetric structure constants of SU(3), and λ_a the Gell-Mann matrices which satisfy the following commutation relation $\left[\frac{\lambda_a}{2}, \frac{\lambda_b}{2}\right] = i f_{abc} \frac{\lambda_c}{2}$.

The idea of chirality is defined by the right-handed (R) and left-handed (L) projection operators

$$P_R = \frac{1}{2}\left(1 + \gamma_5\right) = P_R^\dagger, \tag{2.4}$$

$$P_L = \frac{1}{2}\left(1 - \gamma_5\right) = P_L^\dagger, \tag{2.5}$$

with γ_5 being the chirality matrix $\gamma_5 = i\gamma^0\gamma^1\gamma^2\gamma^3$ which satisfies $\{\gamma^\mu, \gamma_5\} = 0$ and $\gamma_5^2 = 1$. Both P_R and P_L matrices satisfy the completeness, idempotence and orthogonality relations,

$$P_R + P_L = 1, \tag{2.6}$$

$$P_R^2 = P_R, \tag{2.7}$$

$$P_L^2 = P_L, \tag{2.8}$$

$$P_R P_L = P_L P_R = 0. \tag{2.9}$$

These operators project the Dirac field to its chiral right- and left-handed components:

$$q_R = P_R q, \tag{2.10}$$

$$q_L = P_L q. \tag{2.11}$$

To understand why these chirality states are called right- and left-handed one must examine the helicity (defined as the projection of the spin onto the direction of momentum)

eigenstates of the Dirac equation. For ultrarelativistic or massless particles with mass m and energy E, helicity and chirality become the same concept:

$$u(p) = \sqrt{\frac{E+m}{2E}} \begin{pmatrix} \chi \\ \frac{\vec{\sigma}\vec{p}}{E+m}\chi \end{pmatrix} \xrightarrow{E>>m} \sqrt{\frac{1}{2}} \begin{pmatrix} \chi \\ \vec{\sigma}\hat{p}\chi \end{pmatrix}, \tag{2.12}$$

where the spin in the rest frame is assumed to be either parallel or antiparallel to the direction of momentum $\vec{\sigma}\cdot\hat{p}\chi$. On the other hand, the projector operators in the representation of Dirac matrices can be expressed as:

$$P_R = \frac{1}{2}\begin{pmatrix} 1_{2\times2} & 1_{2\times2} \\ 1_{2\times2} & 1_{2\times2} \end{pmatrix},\ P_L = \frac{1}{2}\begin{pmatrix} 1_{2\times2} & -1_{2\times2} \\ -1_{2\times2} & 1_{2\times2} \end{pmatrix}. \tag{2.13}$$

One can see that in the zero-mass limit these operators project to the positive and negative helicity eigenstates, which means that in this particular limit chirality equals helicity.

Before writing the QCD Lagrangian in the chiral limit it is useful to decompose the q fields in terms of its q_R and q_L components as follows

$$\overline{q}\Gamma_i q = \overline{q}_R\Gamma_i q_R + \overline{q}_L\Gamma_i q_L. \tag{2.14}$$

Applying this expression to the term containing the contraction of the covariant derivative yields a decoupled expression for a quadratic quark form in which only the sum of two terms connecting left-handed with left-handed and right-handed with right-handed quark fields appear:

$$\mathscr{L}_{QCD} = \sum_{l=u,d,s} \left(\overline{q}_{R,l} i\gamma^\mu D_\mu q_{R,l} + \overline{q}_{L,l} i\gamma^\mu D_\mu q_{L,l}\right) - \frac{1}{4}\mathscr{G}_{\mu\nu,a}\mathscr{G}_a^{\mu\nu}. \tag{2.15}$$

Since the covariant derivative is flavour-independent, $\mathscr{L}^0_{QCD}$ is invariant under chiral flavour transformations, that is:

$$\begin{pmatrix} u_{R,L} \\ d_{R,L} \\ s_{R,L} \end{pmatrix} \mapsto U_{R,L} \begin{pmatrix} u_{R,L} \\ d_{R,L} \\ s_{R,L} \end{pmatrix} = \exp\left(-i\sum_{a=1}^{8}\Theta_a^{R,L}\frac{\lambda_a}{2}\right) e^{-i\Theta^{R,L}} \begin{pmatrix} u_{R,L} \\ d_{R,L} \\ s_{R,L} \end{pmatrix}. \tag{2.16}$$

Applying Noether's theorem[58] to this Lagrangian exhibiting global $U(3)_L \times U(3)_R$ symmetry one would expect a total of $2 \times (8+1)$ $((L,R) \times ((N^2-1)+1))$conserved currents. These may be identified using the method of Gell-Mann and Lévy[59], which consists of promoting this global symmetry to a local one, thus yielding the left and right currents:

$$L^{\mu,a} = \overline{q}_L \gamma^\mu \frac{\lambda^a}{2} q_L, \ \partial_\mu L^{\mu,a} = 0, \tag{2.17}$$

$$R^{\mu,a} = \overline{q}_R \gamma^\mu \frac{\lambda^a}{2} q_R, \ \partial_\mu R^{\mu,a} = 0. \tag{2.18}$$

2.1 Chiral Perturbation Theory

Chiral Perturbation Theory (ChPT) provides a systematic method for discussing the consequences of the global flavour symmetries of QCD at low energies by means of an effective field theory (EFT), developed so as to determine the low-energy hadronic observables. This effective Lagrangian is expressed in terms of the hadronic degrees of freedom which, at low energies show up as observable asymptotic states. At low energies these are just the members of the pseudoscalar octet, regarded as the Goldstone bosons of the spontaneous breaking of the chiral $SU(3)_L \times SU(3)_R$ symmetry.

EFTs are low-energy approximations to more fundamental theories, as such they are described with a set of variables suited (i.e. convenient for calculations) for the particular energy region of interest. As QCD cannot be solved analytically and standard perturbation theory cannot be applied for energies below 1 GeV, quarks and gluons are not efficient degrees of freedom and light hadronic states, such as mesons and baryons, have to be used instead.

To construct an EFT one has to write down the effective Lagrangian, which includes all terms that are compatible with the symmetries (and the breaking thereof) of the underlying theory. The coefficients of these terms are calculable from the underlying theory but since QCD cannot be solved as of yet, in the case of chiral perturbation theory

the parameters are taken as free parameters which one has to fit to experimental data.

In the case of chiral symmetry pion fields can be described in terms of an exponential parametrization, but since this description contains infinite terms an energy expansion is necessary in order to make it manageable. At low energies the matrix elements of the terms of the expansion are small, since each derivative contributes with a factor of q when matrix elements are taken. From dimensional analysis one can determine the behaviour of the coefficient of an operator with n derivatives as $\frac{1}{M^{n-4}}$, and as such the effect of an n-derivative vertex is $\frac{q^n}{M^{n-4}}$, which for large n will be suppressed for energies smaller than M.

The description of the interaction between two baryons of the $(1/2)^+$ octet through the exchange of either a pseudoscalar or a vector meson, needs the knowledge of the interaction Lagrangian connecting two baryons and a meson for each of the vertices involved in the corresponding diagram. In particular, the formalism for the construction of such meson-exchanging Lagrangians was developed by Callan, Coleman, Wes and Zumino in 1968 [60, 61]. In these types of realizations whenever functions of the Goldstone bosons appear, they are always accompanied by at least one space-time derivative (terms with no derivatives will not be relevant to describe the dynamics of the system, as they would contribute as a constant). Since the interaction with Goldstone bosons must vanish at zero momentum in the chiral limit the expansion of the Lagrangian at low energies is in powers of derivatives and pion masses.

The end-game is the construction of the most general theory describing the dynamics of the Goldstone bosons associated with the spontaneous symmetry breakdown in QCD. This effective Lagrangian should be invariant under $\mathrm{SU(3)}_L \times \mathrm{SU(3)}_R \times \mathrm{U(1)}_V$.

The dynamical variables are collected in matrix form as follows

$$\phi = \begin{pmatrix} \frac{1}{\sqrt{2}}\pi^0 + \frac{1}{\sqrt{6}}\eta & \pi^+ & K^+ \\ \pi^- & -\frac{1}{\sqrt{2}}\pi^0 + \frac{1}{\sqrt{6}}\eta & K^0 \\ K^- & \overline{K}^0 & -\frac{2}{\sqrt{6}}\eta \end{pmatrix}, \tag{2.19}$$

defining the SU(3) matrix U(ϕ) as:

$$U(\phi) = \exp\left(\sqrt{2}\, i \frac{\phi}{f_\pi}\right). \tag{2.20}$$

An expansion in terms of powers of momentum should be performed. As such, the basic building blocks of one such expansion will be the U matrix and its successive derivatives. This fulfils the aforementioned $\mathrm{SU}(3)_L \times \mathrm{SU}(3)_R \times \mathrm{U}(1)_V$ symmetry requirement, but in order to also satisfy Lorentz invariance only even powers of these derivatives may be present. As such the Lagrangian may be expressed as:

$$\mathscr{L} = \mathscr{L}^{(0)} + \mathscr{L}^{(2)} + \mathscr{L}^{(4)} + \ldots \tag{2.21}$$

The first term of this Lagrangian preserves the requested symmetries, with the leading term being $\mathscr{L}^{(2)}$, involving the derivatives of U. Consequently the most general effective Lagrangian density with the minimal number of derivatives reads:

$$\mathscr{L}^{(2)} = \frac{f_\pi}{4} \mathrm{Tr}(\partial_\mu U \partial^\mu U^\dagger). \tag{2.22}$$

The derivative of the chiral field transforms

$$U \mapsto RUL^\dagger \tag{2.23}$$

$$\partial_\mu U \mapsto \partial_\mu (RUL^\dagger) = \partial_\mu RUL^\dagger + R\partial_\mu UL^\dagger + RU\partial_\mu L^\dagger = R\partial_\mu UL^\dagger. \tag{2.24}$$

Similarly one may find:

$$U^\dagger \mapsto LU^\dagger R^\dagger \tag{2.25}$$

$$\partial_\mu U^\dagger \mapsto L\partial_\mu U^\dagger R^\dagger \tag{2.26}$$

Treating baryons as matter fields coupled to mesons and external sources allows us to incorporate them into a chiral perturbation theory. Similarly to the meson fields, the baryon fields should transform non-linearly under the chiral $SU(3)_L \times SU(3)_R$ but linearly under the vector subgroup $SU(2)_V$. When constructing the Lagrangian involving baryons, it is more convenient to work with the square root of the unitary matrix U, u, $U = u^2$, with the matrix u transforming in the following way:

$$u \mapsto \sqrt{LUR^\dagger} = LuK^\dagger(L,R,U) = K(L,R,U)uR^\dagger, \tag{2.27}$$

where $K(L,R,U) \in SU(3)$ depends on L, R and U non trivially. Therefore this transformation is local since U is defined as an exponential of a matrix which collects continuous functions in a Minkowski space. This is in contrast to what happens to U where its transformation under $SU(3)_L \times SU(3)_R$ is global. This local character of the transformation makes mandatory the introduction of a covariant derivative, $D^\mu = \partial^\mu + \Gamma^\mu$, which transforms in the same way as the baryon fields.

The baryon octet is collected in a traceless 3×3 matrix B where each member of the octet is represented by a Dirac spinor field:

$$B = \begin{pmatrix} \frac{1}{\sqrt{2}}\Sigma^0 + \frac{1}{\sqrt{6}}\Lambda & \Sigma^+ & p \\ \Sigma^- & -\frac{1}{\sqrt{2}}\Sigma^0 + \frac{1}{\sqrt{6}}\Lambda & n \\ \Xi^- & \Xi^0 & -\frac{2}{\sqrt{6}}\Lambda \end{pmatrix}, \tag{2.28}$$

transforming under $SU(3)_L \times SU(3)_R$ as $B \mapsto KBK^\dagger$. Hence, turning to the covariant derivative, D^μ acting on B, $D^\mu B = \partial^\mu B + [\Gamma^\mu, B]$, should transform as $D^\mu B \mapsto K D^\mu B$. Indeed, this is a usual property that could not take place unless the chiral connection (Γ^μ) were defined as

$$\Gamma^\mu = \frac{1}{2}\left(u^\dagger\left(\partial^\mu - ir^\mu\right)u + u^\dagger\left(\partial^\mu - il^\mu\right)u\right) \tag{2.29}$$

which transforms as $\Gamma^\mu \mapsto K\Gamma^\mu K^\dagger - (\partial_\mu K)K^\dagger$. Apart from Γ^μ, there is another $O(p)$ building block, known as chiral *vielbein* which can be written as

$$u^\mu = u^\dagger\left(\partial^\mu - ir^\mu\right)u - u^\dagger\left(\partial^\mu - il^\mu\right)u, \tag{2.30}$$

that also fulfils the transformation law $u^\mu \mapsto Ku^\mu K^\dagger$. Now, we are able to proceed to introduce the most general effective Lagrangian for meson-baryon (MB) systems

$$\mathscr{L}^{MB}_{eff}(B,U) = \sum_{n=1}^{\infty}\mathscr{L}^{(n)}_{\phi B} = \mathscr{L}^{(1)}_{\phi B} + \mathscr{L}^{(2)}_{\phi B} + \mathscr{L}^{(3)}_{\phi B} + ... \tag{2.31}$$

2.1.1 Pseudoscalar mesons

From this expression one appreciates that the effective MB Lagrangian comes not only in even powers of momenta, such as in meson ChPT, but also odd powers are possible due to Dirac structures. Each $\mathscr{L}^{(n)}_{\phi B}$ term consist of bilinears of the B field with the chiral order $\mathscr{O}(p^n)$. At lowest order ($\mathscr{O}(p)$), one finds that for pseudoscalar mesons, $J^P = 0^-$, the Lagrangian reads

$$\begin{aligned}\mathscr{L}^{S}_{BB\phi} = &\,\mathrm{Tr}\left[\overline{B}\left(i\gamma_\mu D^\mu - M_0\right)B\right] + D\,\mathrm{Tr}\left[\overline{B}\gamma^\mu\gamma_5\left\{u_\mu, B\right\}\right] \\ &+ F\,\mathrm{Tr}\left[\overline{B}\gamma^\mu\gamma_5\left[u_\mu, B\right]\right]\end{aligned} \tag{2.32}$$

where $F = 0.52$ MeV and $D = 0.85$ MeV are the octet baryon to meson couplings, whose numerical values are found through the use of the five known experimental data on hyperon semileptonic decay constants[62, 63]. M_0 is the baryonic mass matrix, B ($\overline{B^i_j} = (B^j_i)^\dagger\gamma_4$) is the matrix representing the inbound (outbound) baryons and $\nabla_\mu B = \partial_\mu B + \left[\Gamma_\mu, B\right]$ the covariant derivative introduced to account for gauge invariance. The dependence on the meson fields is contained in the Γ_μ and u_μ operators:

$$\Gamma_\mu = \frac{1}{2}\left(u^\dagger\partial_\mu u + u\partial_\mu u^\dagger\right) \quad u_\mu = \frac{i}{2}\left(u\partial_\mu u^\dagger - u^\dagger\partial_\mu u\right), \tag{2.33}$$

where u is defined as $u = \mathrm{e}^{i\frac{\phi}{\sqrt{2}f_\pi}} \simeq 1 + i\frac{1}{\sqrt{2}f_\pi}\phi$, with $f_\pi = 93$ MeV the pion decay constant, and ϕ the self-adjoint matrix of inbound pseudoscalar mesons,

$$\phi = \begin{pmatrix} \frac{1}{\sqrt{2}}\pi^0 + \frac{1}{\sqrt{6}}\eta & \pi^+ & K^+ \\ \pi^- & -\frac{1}{\sqrt{2}}\pi^0 + \frac{1}{\sqrt{6}}\eta & K^0 \\ K^- & \overline{K}^0 & -\frac{2}{\sqrt{6}}\eta \end{pmatrix}. \tag{2.34}$$

One should note that, while the calculation for the exchange of pseudoscalar mesons other than the pion require the use of $\mathrm{SU}(3)_f$ symmetry, the inclusion of vector mesons in the formalism requires the use of SU(6) = $\mathrm{SU}(2)_s$ × $\mathrm{SU}(3)_f$ spin-flavour symmetry ($\mathrm{SU}(6)_W$ for the weak vertices), as will be explained in the next Section.

2.1.2 Vector mesons

The interaction between baryons and vector mesons has not been as extensively studied as the one involving pseudoscalar mesons, but one can use the Hidden Local Symmetry (HLS) model[64], to accommodate vector mesons consistently with chiral symmetry.

The Hidden Local Symmetry model is based on a G×H symmetry where the global symmetry G corresponds to $\mathrm{SU}()_L \times \mathrm{SU}()_R$ and the local symmetry H=$\mathrm{SU}()_V$ is the hidden local symmetry. The G×H symmetry is spontaneously broken down to a diagonal sum H which is nothing but the H of the G/H of the non-linear sigma model.

The ρ-meson is such a dynamical gauge boson of the hidden local $\mathrm{SU}(2)_v$ symmetry in the $\mathrm{SU}(2)_L \times \mathrm{SU}(2)_R/\mathrm{SU}(2)_v$ non-linear chiral Lagrangian.

In order to incorporate these mesons in our formalism, the following Lagrangian is used:

$$\begin{aligned} \mathscr{L}^S_{BBV} = &-g\{\langle\overline{B}\gamma_\mu[V_8^\mu, B]\rangle + \langle\overline{B}\gamma_\mu B\rangle\langle V_8^\mu\rangle + \frac{1}{4M}\big(F\langle\overline{B}\sigma_{\mu\nu}[\partial^\mu V_8^\nu - \partial^\nu V_8^\mu, B]\rangle \\ &+ D\langle\overline{B}\sigma_{\mu\nu}\{\partial^\mu V_8^\nu - \partial^\nu V_8^\mu, B\}\rangle\big) + \langle\overline{B}\gamma_\mu B\rangle\langle V_0^\mu\rangle + \frac{C_0}{4M}\langle\overline{B}\sigma_{\mu\nu}V_0^{\mu\nu}B\rangle\}, \end{aligned} \tag{2.35}$$

which may be obtained from the generalization of the HLS formalism in SU(2) to the SU(3) sector. There, V_8 and V_0 are the octet and singlet terms in the vector meson matrix respectively,

$$V_\mu = \frac{1}{2}\begin{pmatrix} \rho^0+\omega & \sqrt{2}\rho^+ & \sqrt{2}K^{*+} \\ \sqrt{2}\rho^- & -\rho^0+\omega & \sqrt{2}K^{*0} \\ \sqrt{2}K^{*-} & \sqrt{2}\overline{K}^{*0} & \sqrt{2}\phi \end{pmatrix}_\mu , \tag{2.36}$$

The octet and singlet matrices can be obtained by considering the mixing of the octet and singlet components of the physical ω and ϕ meson, which under the ideal mixing assumption leads to[65]:

$$\omega = \sqrt{\frac{1}{3}}\omega_8 + \sqrt{\frac{2}{3}}\omega_0, \tag{2.37}$$

$$\phi = -\sqrt{\frac{2}{3}}\phi_8 + \sqrt{\frac{1}{3}}\phi_0, \tag{2.38}$$

yielding:

$$V_8 = \tfrac{1}{2}\begin{pmatrix} \rho^0+\sqrt{\frac{1}{3}}\omega_8 & \sqrt{2}\rho^+ & \sqrt{2}K^{*+} \\ \sqrt{2}\rho^- & -\rho^0+\sqrt{\frac{1}{3}}\omega_8 & \sqrt{2}K^{*0} \\ \sqrt{2}K^{*-} & \sqrt{2}\overline{K}^{*0} & \frac{2}{\sqrt{3}}\phi_8 \end{pmatrix}, \quad V_0 = \tfrac{1}{2}\begin{pmatrix} \sqrt{\frac{2}{3}}\omega_0 & 0 & 0 \\ 0 & \sqrt{\frac{2}{3}}\omega_0 & 0 \\ 0 & 0 & \sqrt{\frac{2}{3}}\phi_0 \end{pmatrix}. \tag{2.39}$$

The SU(3) D and F constants take now the values $D = 2.4$ and $F = 0.82$, and the constant C_0 is chosen such that the value for the ϕNN vertex is null (according to naive expectations based in the Okubo Zweig Iizuka, *OZI*, rule) which translates into a value of $3F - D$, and the anomalous magnetic coupling of the ωNN vertex gives $\kappa_\omega \simeq 3F - D$[66]. The baryon mass is represented in Eq. (2.35) by M, while g takes the form:

$$g = \frac{m}{\sqrt{2}f_\pi}, \tag{2.40}$$

where m is the mass of the exchanged meson.

2.2 Weak baryon-baryon-meson interaction

In this section the formalism for the calculation of the weak baryon-baryon-meson vertices will be presented. First we will take a look at the parity-violating amplitudes for both pseudoscalar and vector mesons. Next we will introduce the so-called Pole Model as a means to calculate the parity-conserving contributions.

2.2.1 Parity-violating contribution

2.2.1.1 Pseudoscalar mesons

The starting point to derive the weak vertices is the heavy baryon chiral perturbation Hamiltonian introduced by Jenkins and Manohar in the early ninenties [67, 68] to account for strangeness changing amplitudes, all the while neglecting those terms in which the decuplet baryon matrix appears.

Using a lowest-order chiral analysis one can only generate parity-violating amplitudes, since the weak chiral Lagrangian describing parity-conserving transitions has the wrong transformation property under the combined action of the charge and parity (CP) operators [69]. The effective Lagrangian:

$$\mathscr{L}^{W}_{BB\phi} = \sqrt{2}\left(h_D \,\mathrm{Tr}\left[\overline{B}\left\{\xi^\dagger h \xi, B\right\}\right] + h_F \,\mathrm{Tr}\left[\overline{B}\left[\xi^\dagger h \xi, B\right]\right]\right), \tag{2.41}$$

is written in terms of the dimensionless constants $h_D = -1.69\times10^{-7}$ and $h_F = 3.26\times10^{-7}$, which can be fitted to reproduce known meson decay amplitudes and the s-wave non-leptonic weak decays of the baryon octet members [68]. The h operator is a 3×3 matrix with a single non-zero element, $h_{23} = 1$, which accounts for strangeness variations of $|\Delta S| = 1$. The operator ξ plays a role equivalent to the one of the u operator in the strong Lagrangian defined in the previous section.

2.2.1.2 Vector mesons

For the weak vertices the introduction of the SU(6)$_W$ group is necessary. This group describes the product of the SU(3) flavour group with the SU(2)$_W$ spin group, which is the proper group to consider when dealing with particles in motion, as the ones involved in weak decay processes [70]. In this representation the meson fields are expressed in terms of a quark-antiquark product ϕ_b^a, where the upper and lower indices refer to the spin-flavour antiquark and quark combinations respectively:

$$\phi_b^a = \varepsilon q_b \overline{q}_a \text{ with} \begin{cases} \varepsilon = 1 & \text{if both a and b even} \\ \varepsilon = -1 & \text{otherwise.} \end{cases} \tag{2.42}$$

The labels used correspond to the fundamental representation of SU(6)$_W$, and as such, both indices range from 1 to 6. The spin up and spin down u quarks are assigned to 1 and 2 respectively, the d quarks are assigned to 3 and 4 and the strange quarks to 5 and 6.

For the baryons one must define the symmetric tensors

$$B^{abc} \equiv \frac{1}{6} \sum_{\substack{perm \\ a,b,c}} S^a(1) S^b(2) S^c(3) \tag{2.43}$$

$$B_{abc} = \overline{B}^{abc} = \frac{1}{6} \sum_{\substack{perm \\ a,b,c}} \overline{S}^a(1) \overline{S}^b(2) \overline{S}^c(3), \tag{2.44}$$

where the constants a, b and c run over the same numerical values stated before. The couplings may be found by expressing the Hamiltonian in terms of the SU(6)$_W$ tensors. This Hamiltonian is the product of two currents, each belonging to the 35 representation, and using the Clebsch-Gordan series one can extract the parity-conserving and parity-violating pieces of the Hamiltonian. As discussed before, imposing the right CP transformation leads to only PV contributions, which can be expressed in terms of

reduced matrix elements for the product of the appropriate representations:

$$2a_T : \left[(\overline{B}B)_{35} \times M_{35}\right]_{280_a} \tag{2.45}$$

$$2a_V : \left[(\overline{B}B)_{35} \times M_{35}\right]_{\overline{280}_a} \tag{2.46}$$

$$b_T : \left[(\overline{B}B)_{405} \times M_{35}\right]_{280_a} \tag{2.47}$$

$$b_V : \left[(\overline{B}B)_{405} \times M_{35}\right]_{\overline{280}_a} \tag{2.48}$$

$$c_V : \left[(\overline{B}B)_{35} \times M_{35}\right]_{35_a}, \tag{2.49}$$

with the constants b_T, b_V and c_V determined directly through the pion decay amplitudes from either a Λ or Σ initial state, while a_T and a_V are extracted from factorization calculations[71]:

$$a_T = \frac{1}{3}a_V = \frac{3}{5}G\cos\theta_c \sin\theta_c \langle\rho^0|V_\mu^3|0\rangle\langle p|A^{\mu 3}|p\rangle, \tag{2.50}$$

$$b_V = -b_T = 6\left(\frac{1}{\sqrt{3}}A_{\Lambda p} + A_{\Sigma^+ p}\right), \tag{2.51}$$

$$c_V = 3\left(\sqrt{3}A_{\Lambda p} + A_{\Sigma^+ p}\right). \tag{2.52}$$

The values $A_{\Sigma^+ p} = -3.27 \times 10^{-7}$ and $A_{\Lambda p} = 3.25 \times 10^{-7}$ obtained from data on the experimental angular distribution of the decay products and on the polarization of the final baryon [72] are used. The final general expression accounting for the weak PV baryon-baryon-vector meson couplings is:

$$\begin{aligned}
H_{PV}^{\Delta S} =& a_T[\overline{B}^{ij2}B_{ij1}\overline{\phi}_3^6 - \overline{B}^{ij3}B_{ij6}\overline{\phi}_2^1 - \overline{B}^{ij1}B_{ij2}\overline{\phi}_4^5 + \overline{B}^{ij4}B_{ij5}\overline{\phi}_1^2] \\
&+ a_V[\overline{B}^{ij2}B_{ij5}\overline{\phi}_3^2 - \overline{B}^{ij3}B_{ij2}\overline{\phi}_2^5 - \overline{B}^{ij1}B_{ij6}\overline{\phi}_4^1 + \overline{B}^{ij4}B_{ij1}\overline{\phi}_1^6] \\
&+ b_T[\overline{B}^{ij2}B_{i16}\overline{\phi}_3^j - \overline{B}^{ij3}B_{i16}\overline{\phi}_2^j - \overline{B}^{23i}B_{ij6}\overline{\phi}_j^1 + \overline{B}^{23i}B_{1ij}\overline{\phi}_j^6 \\
&- \overline{B}^{i1j}B_{25i}\overline{\phi}_4^j + \overline{B}^{ij4}B_{i25}\overline{\phi}_1^j + \overline{B}^{i14}B_{ij5}\overline{\phi}_j^2 - \overline{B}^{i14}B_{ij2}\overline{\phi}_j^5] \\
&+ b_V[\overline{B}^{ij2}B_{i25}\overline{\phi}_3^j - \overline{B}^{ij3}B_{i25}\overline{\phi}_2^j + \overline{B}^{i23}B_{ij5}\overline{\phi}_j^2 - \overline{B}^{23i}B_{ij2}\overline{\phi}_j^5 \\
&- \overline{B}^{1ij}B_{16i}\overline{\phi}_4^j + \overline{B}^{ij4}B_{16i}\overline{\phi}_1^j - \overline{B}^{14i}B_{ij6}\overline{\phi}_j^1 + \overline{B}^{i14}B_{1ij}\overline{\phi}_j^6] \\
&+ c_V[\overline{B}^{ijk}B_{ij6}\overline{\phi}_4^k - \overline{B}^{ij4}B_{ijk}\overline{\phi}_k^6 - \overline{B}^{ijk}B_{ij5}\overline{\phi}_3^k + \overline{B}^{ij3}B_{ijk}\overline{\phi}_k^5],
\end{aligned} \tag{2.53}$$

where the SU(6)$_W$ tensor terms must be expanded in terms of the physical fields to write down the $\langle B'M|H_{PV}|B\rangle$ elements of interest.

2.2.2 Parity-conserving contribution

As stated above, the use of the weak effective Hamiltonian at lowest order allows us to obtain only the parity-violating amplitudes. The standard method to compute the parity-conserving amplitudes is based in the pole model[73], according to which the weak transition is shifted from the meson vertex to the baryonic (and mesonic) line. The starting point is to consider the transition amplitude for the non-leptonic emission of a meson, $B \to B' M_i(q)$

$$\langle B' M_i(q)|H_W|B\rangle = \int \mathrm{d}^4x\, \mathrm{e}^{iqx}\theta(x^0)\langle B'|[\partial A_i(x), H_W]|B\rangle, \tag{2.54}$$

where $A_i(x)$ is the axial current associated to the meson field and H_W is the weak interaction Lagrangian. Inserting a complete set of states $\sum_n |n\rangle\langle n|$ into Eq. (2.54) leads to a series of contributions among which the dominant one corresponds to the baryon $(1/2)^+$ pole terms, that become singular in the SU(3) soft-meson limit and represent the leading contribution to the PC amplitudes [72]:

$$\begin{aligned}\langle B' M_i(q)|H_W|B\rangle \sim &\sum_n \left[\delta(\vec{p}_n - \vec{p}_{B'} - \vec{q})\right)\frac{\langle B'|A_i^\mu(0)|n\rangle\langle n|H_W(0)|B\rangle}{p_B^0 - p_n^0}\Bigg] \\ &+ \sum_{n'}\left[\delta(\vec{p}_B - \vec{p}_{n'} - \vec{q}\,)\frac{\langle B'|H_W(0)|n'\rangle\langle n'|A_i^\mu(0)|B\rangle}{p_B^0 - q^0 - p_{n'}^0}\right].\end{aligned} \tag{2.55}$$

An illustrative portrayal of this equation may be found in the following figure. One may easily identify the first sum term of the equation to the diagram with the weak vertex shifted onto the baryonic line before the strong vertex, and in the same manner relate the diagram with the weak baryonic-line vertex after the strong one with the second summation.

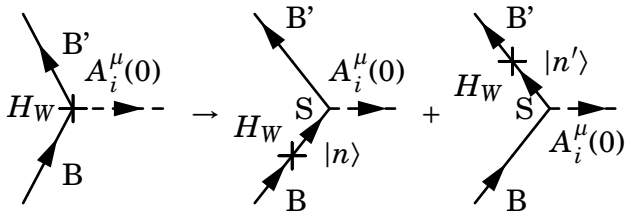

Figure 2.1: Diagrammatic representation of Eq. (2.55)

For the calculation of the weak pole vertices it is necessary to express the physical states in terms of the baryon octet fields $|B_i\rangle$, as well as the meson states in terms of $|M_i\rangle$[74]. Furthermore, the mesonless weak transition between baryons, $\langle B|H_W(0)|B'\rangle$, can be computed using low-energy theorems for mesons. These theorems express the matrix element for the emission of a meson of zero (or small) four-momentum in terms of the corresponding matrix element in the absence of the soft meson and some equal-time commutators of currents[75]. They are based in the existence of certain symmetry in a given physical process, which give rise to degenerate multiplets (a state containing an arbitrary number of Goldstone bosons) with couplings related by the symmetry. Therefore, we will be able to relate the strong scattering amplitudes to the weak vertices,

$$\lim_{q\to 0}\langle B \xrightarrow{PV} B'M_i\rangle = \lim_{q\to 0}\langle B'M_i|H_{PV}|B\rangle = -\frac{i}{f_\pi}\langle B'|[F_i,H_6]|B\rangle, \tag{2.56}$$

where, following Cabibbo's theory, we have assumed that the weak hamiltonian transforms like the sixth component of an octet, H_6, according to the CP invariance of $H_W^{\Delta S=1}$, and F_i are the corresponding $SU(3)$ generators.

To compute the last term of Eq. (2.56), one can use the completely antisymmetric, f_{ijk}, and symmetric, d_{ijk}, SU(3) coefficients[76] to express the action of the F_i generator on a baryon field,

$$F_i|B_j\rangle = if_{ijk}|B_k\rangle, \tag{2.57}$$

and the weak transition between baryon fields in terms of two reduced matrix elements,

A and B,

$$\langle B_k|H_6|B_j\rangle = iAf_{6jk} + Bd_{6jk}, \tag{2.58}$$

which can be determined by a fit to experimental data for specific PV transitions, for which we choose the $\Sigma^+ \to p + \pi^0$ ($A_{\Sigma^+ p}$) and $\Lambda \to p + \pi^-$ ($A_{\Lambda p}$) processes,

$$A_{\Sigma^+ p} = \frac{i}{4f_\pi}(B - A), \tag{2.59}$$

$$A_{\Lambda p} = -\frac{i}{f_\pi}\frac{-3A - B}{4\sqrt{3}}. \tag{2.60}$$

Combining these expressions, we obtain:

$$-\frac{i}{f_\pi}A = A_{\Sigma^+ p} - \sqrt{3}A_{\Lambda p}, \tag{2.61}$$

$$-\frac{i}{f_\pi}B = -\sqrt{3}A_{\Lambda p} - 3A_{\Sigma^+ p}. \tag{2.62}$$

Therefore, when inserting the above relations in Eq. (2.58), one can obtain the weak PC baryon transitions required in the pole model, $B_j \leftrightarrow B_k$, in terms of the $\Sigma^+ \to p + \pi^0$ and $\Lambda \to p + \pi^-$ PV amplitudes.

One should note that, in principle, contributions to the PC amplitudes coming from the poles in the meson propagator are also possible. These contributions have not been included, in part due to their small contribution in comparison to those of baryon poles, but also due to the uncertainty in the phase between baryon and meson pole terms[73].

With all this input we will be able to derive the baryon-baryon-meson coupling constants which will appear in the calculation of the hypernuclear decay rate.

CHAPTER 3

HYPERNUCLEAR DECAY RATE

Traditionally, hypernuclear decay studies have been focused into the decay of single-Λ hypernuclei. These studies have relied chiefly in three observables: total decay rates, partial decay rates (*i.e.* $\Lambda n \to nn$, $\Lambda p \to np$) and asymmetry.

In this context asymmetry refers to the angular asymmetry in the distribution of the decay particles coming from the nonmesonic weak decay of polarized hypernuclei with respect to their polarization axis, and can be theoretically understood in terms of the interference between parity-conserving and parity-violating amplitudes. The observable used to evaluate the asymmetry is the intensity of the outgoing nucleons, which may be expressed in terms of the transition operator of the weak decay, as well as the states of the outgoing particles, residual nucleus and the initial hypernucleus.

In the present work, however, focus will be placed solely in total and partial (induced by $\Lambda\Lambda$, $\Xi^0 n$, $\Xi^- p$ pairs) decay rates of $S = -2$ hypernuclei and as such no further detail will be given on asymmetry.

3.1 Decay Rate

In order to describe the nonmesonic weak decay of hypernuclei one requires the knowledge of the initial and final wave functions, as well as the two-body mechanism. Further details on both of these basic ingredients will be given in Chapter 4 and 5 respectively.

The nonmesonic decay rate of a hypernucleus decaying into a residual nucleus and two outgoing baryons is given by

$$\Gamma_{nm} = \int \frac{d^3k_1}{(2\pi)^3} \int \frac{d^3k_2}{(2\pi)^3} \sum_{\substack{M_I\{R\} \\ \{1\}\{2\}}} (2\pi)\delta(M_H - E_R - E_1 - E_2) \times \frac{1}{2J+1} |\mathscr{M}_{fi}|^2, \tag{3.1}$$

where M_H, E_R, E_1 and E_2 correspond to the mass of the hypernucleus, the energy of the residual $(A-2)$-particle system, and the total asymptotic energies of the emitted baryons, respectively. The integration variables $\vec{k}_1$ and $\vec{k}_2$ stand for the momenta of the two particles in the final state. Note that the momentum conserving delta function has been used to integrate over the momentum of the residual nucleus. The sum, together with the factor $1/(2J+1)$, indicates an average over the initial hypernucleus spin projections, M_I, and a sum over all quantum numbers of the residual $(A-2)$-particle system, $\{R\}$, as well as the spin and isospin projection of the emitted final particles, {1} and {2} (henceforth referred to as $\overline{\sum}$). $\mathscr{M}_{fi}$ stands for the transition amplitude from an initial hypernuclear state (${}^{6}_{\Lambda\Lambda}$He in the present study) to a final state composed of a residual nuclear core plus two outgoing baryons. When a transformation to the total momentum, $\vec{P} = \vec{k}_1 + \vec{k}_2$, and relative momentum, $\vec{k} = (\vec{k}_1 - \vec{k}_2)/2$ of the two outgoing particles is performed the expression for Γ_{nm} becomes

$$\Gamma_{nm} = \int \frac{d^3P}{(2\pi)^3} \int \frac{d^3k}{(2\pi)^3} \times \overline{\sum} (2\pi)\delta(M_H - E_R - E_1 - E_2) |\mathscr{M}_{fi}|^2. \tag{3.2}$$

We will write the hypernuclear transition amplitude, $\mathscr{M}_{fi}$, in terms of the elementary two-body transitions, $B_1 B_2 \to B_{1'} B_{2'}$. Working in a shell-model framework, the Λ hyperons and nucleons are described, in a first approximation, by harmonic oscillator

single-particle orbitals. The oscillator parameter of the Λ particle ($b_\Lambda = 1.6$ fm) is chosen to simulate the probability to find two Λ particles in ${}^{6}_{\Lambda\Lambda}$He, ${}^{10}_{\Lambda\Lambda}$Be and ${}^{13}_{\Lambda\Lambda}$B hypernuclei for which experimental binding energies are available[77], while that of the nucleon ($b_N = 1.4$ fm) is fixed by the ^{4}He charge form factor which determines the size of the nuclear core. In addition, a weak coupling scheme is assumed, by virtue of which the Λ hyperons couple only to the ground state of the nuclear core. Therefore, in the case of the ${}^{6}_{\Lambda\Lambda}$He hypernucleus studied here, with quantumspin and isospin numbers $J_I = M_I = 0$, $T_I = M_{T_I} = 0$, the state will be given by

$$|{}^{6}_{\Lambda\Lambda}\mathrm{He}\rangle = |\Lambda\Lambda\rangle^{J_{\Lambda\Lambda}=M_{\Lambda\Lambda}=0}_{T_{\Lambda\Lambda}=M_{T_{\Lambda\Lambda}}=0} \otimes |{}^{4}\mathrm{He}\rangle^{J_c=M_c=0}_{T_c=M_{T_c}=0}\,, \tag{3.3}$$

where antisymmetry forces the two Λ hyperons to be in a $^1S_0$ state, since they are assumed to be in the lowest s-shell ($1s_{1/2}$) before the weak decay occurs. This is so because, in general, a Λ in an excited orbital will rapidly decay into the ground state through electromagnetic or strong de-excitation processes, which are orders of magnitude faster than those mediated by the weak interaction.

The ${}^{6}_{\Lambda\Lambda}$He has two Λ hyperons and four nucleons and therefore the most important decay channel for such a nucleus is the one induced by one nucleon, $\Lambda N \to NN$. The evaluation of the $\Lambda N \to NN$ transition rate requires to decompose the nonstrange nuclear core as one nucleon coupled to a conveniently antisymmetrized three-particle system, while decoupling one of the two Λ particles, so that the initial ΛN pair can convert into a final NN pair. The details and final expression for the hypernuclear decay amplitude in terms of two-body $\Lambda N \to NN$ ones can be found in Ref. [35]. Here, we focus on the $\Lambda\Lambda \to YN$ decay mode, which is the one we improve with respect to earlier calculations. In this case, the Λ hyperon does not need to be decoupled from the cluster, neither a nucleon from the core. The residual 4-particle system, which coincides with the ^{4}He nucleus, contains no strangeness, while the final two-particle state contains one hyperon than can be either a Λ ($|YT_Y\rangle = |00\rangle$), a Σ^- ($|Yt_Y\rangle = |1-1\rangle$) or a Σ^0 ($|Yt_Y\rangle = |10\rangle$).

The $\Lambda\Lambda \to YN$ amplitude is then given by

$$\begin{aligned}\mathscr{M}_{\Lambda\Lambda\to YN} &= \langle \vec{k}_N s_N t_N, \vec{k}_Y s_Y t_Y; {}^4\mathrm{He}|\hat{O}|{}^6_{\Lambda\Lambda}\mathrm{He}\rangle|\tfrac{1}{2}-\tfrac{1}{2}\rangle_\Lambda \\ &= \sum_{S,M_S} \langle \tfrac{1}{2}s_N, \tfrac{1}{2}s_Y|SM_S\rangle\langle \tfrac{1}{2}t_N, Y t_Y|TM_T\rangle \\ &\times \langle \vec{K}|\Psi^{CM}_{\Lambda\Lambda}\rangle\langle \vec{k}, SM_S, TM_T|\hat{O}|\Psi^{rel}_{\Lambda\Lambda}, S_0M_{S_0}, T_0M_{T_0}\rangle \ , \end{aligned} \tag{3.4}$$

where the initial $\Lambda\Lambda$ wave function has been written as a product of relative and center-of -mass wave functions, $\Psi^{rel}_{\Lambda\Lambda}$ and $\Psi^{CM}_{\Lambda\Lambda}$, respectively, and $\vec{k}$ and $\vec{K}$ are the relative and total momentum of the emitted YN pair. The amplitude $\langle \vec{k}, SM_S, TM_T|\hat{O}|\Psi^{rel}_{\Lambda\Lambda}, S_0M_{S_0}, T_0M_{T_0}\rangle$ represents the two-body transition matrix element. The spin quantum numbers of the $\Lambda\Lambda$ pair are $S_0 = M_{S_0} = 0$, due to antisymmetrization, while its isospin quantum numbers are $T_0 = 1/2$, $M_{T_0} = -1/2$, which contain the coupling to the isospurion field $|\frac{1}{2}-\frac{1}{2}\rangle_\Lambda$ introduced to account for the $\Delta I = ½$ rule in the weak transition. The isospin quantum numbers of the emitted pair fulfil $T = T_0 = 1/2$ and $M_T = M_{T_0} = -1/2$ by isospin conservation.

These two-body matrix elements are calculated using a two-body interaction potential and the inclusion of initial and final correlated wave functions which are derived through the resolution of the G-matrix formalism for the former and the Lippmann-Schwinger equation for the latter.

In the case of the $\Lambda\Lambda \to YN$ decay, and since the strong interaction allows for the conversion to other baryon-baryon channels, the weak interaction will take place not only from the initial $\Lambda\Lambda$ pair, but also from pairs containing other members of the baryon octet, $\Xi^- p$, $\Xi^0 n$ and $\Sigma^+\Sigma^-$, which will in turn decay weakly into either $\Sigma^0 n$, Λn or $\Sigma^- p$ states. Moreover, the strong interaction acting between the final baryons will produce additional $YN - Y'N$ transitions, with Y, Y' being Λ or Σ hyperons.

The two-body weak potential is based on a meson-exchange model, according to which, every $\Lambda\Lambda \to YN$ and $\Xi N \to YN$ transition can be understood in terms of the exchange

of mesons between the interacting particles, with masses related to the inverse of the interaction range and with quantum numbers allowed by the symmetries governing the underlying dynamics. Within this model, a transition can be understood as a product of a strong vertex and a weak one, where the change in strangeness occurs, connected through the meson propagator (see Fig. 4.2 next chapter). Only a limited number of vertice can be accessed from experiments, for instance, the ones involving pions. The calculation corresponding to the exchange of pseudoscalar mesons other than the pion requires the use of $SU(3)_f$ symmetry to obtain the baryon-baryon-meson vertices, while the inclusion of vector mesons in the formalism requires the use of the generalization of the Hidden Local Symmetry (HLS) formalism extended to the SU(3) sector[78] ($SU(6)_W$ for the weak vertices). The formalism and the results for our specific decay channels are presented in the next chapter.

One might also use the less model dependent effective field theory approach to describe the four-fermion weak interaction, which would replace those vector meson exchanges by contact terms [29–32]. These approaches are organized as an expansion of increasing dimension (powers of some *small* ratio of physical scales), providing a more systematic and controllable framework to study the weak process. The size of the coefficients in the expansion is constrained by fitting to accurate experimental data. At present, there are no precise measurements for the required weak transitions in the strangeness -2 sector, and the effective field theory approach is not feasible. Therefore, one has to rely on model determinations of the decay mechanism as the one employed in the present work.

CHAPTER 4

THE WEAK Λ-INDUCED DECAY

As discussed in the previous chapter the $\Lambda\Lambda \to YN$ transition can be explained through the exchange of a meson connecting a strong and a weak vertex, where the strangeness variation occurs. Each one of these transitions is governed by underlying symmetries and conservation laws that determine which quantum numbers are allowed and set an interaction range compatible with the exchanged meson.

For the zero charge transition channel, since the strong interaction allows for the conversion to other baryon-baryon channels, the weak interaction will take place not only from the initial $\Lambda\Lambda$ pair, but from pairs containing other members of the baryon octet, $\Xi^- p$, $\Xi^0 n$, $\Sigma^0\Sigma^0$ or $\Sigma^+\Sigma^-$, which will in turn decay weakly into either $\Sigma^0 n$, Λn or $\Sigma^- p$ states. Moreover, the strong interaction acting between the final baryons will produce additional $\Lambda N - \Sigma N$ transitions.

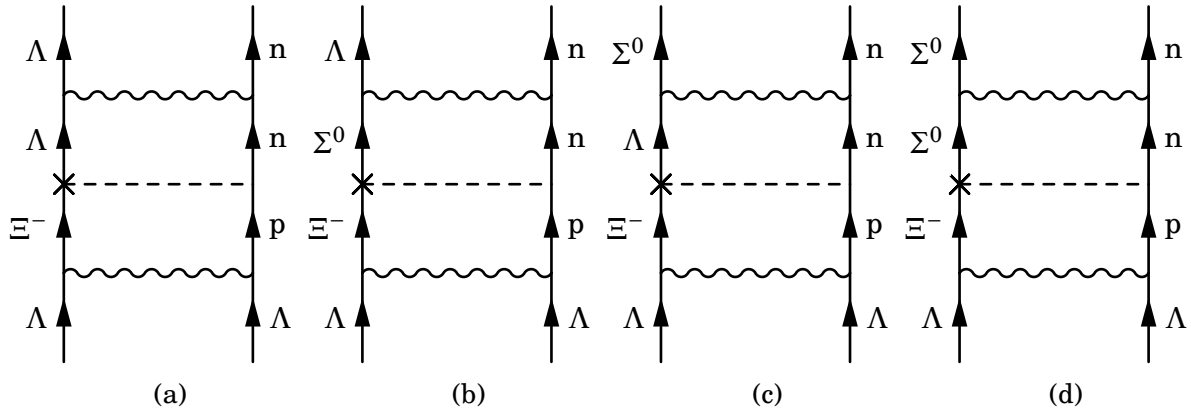

Figure 4.1: Examples of decay diagrams involving $\Lambda\Lambda - \Xi^- p$ mixing states originating from the strong interaction. Wiggly lines represent the strong interaction between baryons, while dashed lines represent weak transitions with the weak vertex denoted by a cross.

As heretofore been mentioned, the vector meson exchanges could be replaced by contact terms in effective field theory methods but these types of approaches would require experimental data that as of yet does not exist for the $S = -2$ sector. For all calculations performed from this point onwards the frame of reference depicted in Fig. 4.2 will be used.

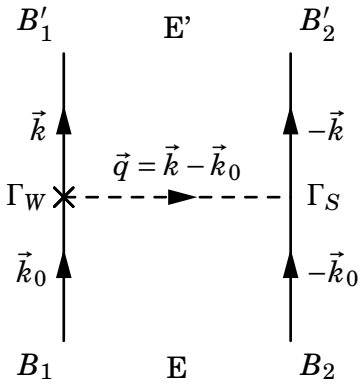

Figure 4.2: Diagrammatric representation of a $B_1 B_2 \to B'_1 B'_2$ transition within a one-meson exchange model. The cross represents an insertion of a weak vertex.

4.1 The One-Meson Exchange Potential

The evaluation of the two-body transition matrix elements of Eq. (3.4) requires the knowledge of the operator that triggers the weak $\Delta S = -1$ transition from an initial baryon pair to a final one. In the meson exchange description employed here these transitions are assumed to proceed via the exchange of virtual mesons belonging to the pseudoscalar and vector meson octets. The corresponding transition potential is obtained from the amplitude displayed in Fig. 4.2, which is written as

$$\mathscr{M} = \int d^4x\, d^4y\, \overline{\Psi}_{1'}(x)\Gamma_1\Psi_1(x)\Delta_\phi(x-y)\overline{\Psi}_{2'}(y)\Gamma_2\Psi_2(y), \tag{4.1}$$

with Γ_i being the Dirac operators characteristic of the baryon-baryon-meson vertices and $\Delta_\phi(x-y)$ the meson (ϕ) propagator:

$$\Delta_\phi(x-y) = \int \frac{d^4q}{(2\pi)^4} \frac{\mathrm{e}^{iq(x-y)}}{(q^0)^2 - \vec{q}^{\,2} - m_\phi^2}. \tag{4.2}$$

Combining the above two expressions, performing a change to center-of-mass (c.m.) and relative variables and integrating over the c.m., time and energy variables, one obtains the amplitude in terms of the vertices that come from the matrix elements between fields, $\overline{\Psi}(x)\Gamma\Psi(x)$. In Table 4.1 we show the strong and weak Γ operators for pseudoscalar (PS) and vector (V) mesons. The constants A, B, α, β and ϵ correspond to the weak baryon-baryon-meson (BBM) couplings, while g ($g^{\mathrm{V}}, g^{\mathrm{T}}$) represents the strong (vector, tensor) one. The γ matrices are taken under the Dirac representation. Note the presence of a γ_5 factor in the PV vertices.

We take the non-relativistic reduction of this transition amplitude and the static $q^0 = 0$ limit, allowing us to identify $\mathscr{M}(\vec{q})$ with $V(\vec{q})$, which is the Fourier transform of the transition potential in coordinate space. As we detail below, the general structure of this potential for pseudoscalar meson exchange reads:

$$V^\phi(\vec{q}) = \sum_k \left(A_k^{Y,\phi} + \frac{B_k^{Y,\phi}}{2\overline{M}} \vec{\sigma}_1\vec{q} \right) \frac{\vec{\sigma}_2\vec{q}}{\vec{q}^{\,2} + m_\phi^2} \hat{O}_k^Y, \tag{4.3}$$

Table 4.1: Pseudoscalar (PS) and vector (V) Γ vertices entering Eq. (4.1) (in units of $G_F {m_\pi}^2 = 2.21 \times 10^{-7}$).

	PS	**V**
Strong	$\mathrm{i}g\gamma_5$	$\left[g^{\mathrm{V}}\gamma^\mu + \mathrm{i}\dfrac{g^{\mathrm{T}}}{2M}\sigma^{\mu\nu}q_\nu\right]$
Weak	$\mathrm{i}(A + B\gamma_5)$	$\left[\alpha\gamma^\mu - \beta\mathrm{i}\dfrac{\sigma^{\mu\nu}q_\nu}{2\overline{M}} + \varepsilon\gamma^\mu\gamma_5\right]$

where $\overline{M}$ is the average mass of the baryons involved in the weak vertex, m_ϕ is the mass of the exchanged meson and the index k in the sum runs over the different isospin structures associated to each type of meson. Similarly, the potential for vector meson exchange reads:

$$V^v(\vec{q}) = \sum_k \left(\mathrm{i}\frac{A_k^{Y,v}}{2M}(\vec{\sigma}_1 \times \vec{\sigma}_2)\vec{q} + B_k^{Y,v} + \frac{C_k^{Y,v}}{4M\overline{M}}(\vec{\sigma}_1 \times \vec{q})(\vec{\sigma}_2 \times \vec{q}) \right) \frac{1}{\vec{q}^{\,2} + m_v^2} \hat{O}_k^Y . \tag{4.4}$$

The explicit expressions for the A, B and C constants, in terms of strong and weak coupling constants, will be given at the end of this section.

4.1.1 Spin Structure

So far we have seen the interaction potential in momentum space, but in order to use the initial and final state wave functions, which are calculated in coordinate space (as we shall see in Chapter 5), one must Fourier transform the above expression to obtain the potential in configuration space:

$$\begin{aligned} V(\vec{r}) &= \sum_i \sum_\alpha V_\alpha^{(i)}(\vec{r}) = \sum_i \sum_\alpha V_\alpha^{(i)}(r)\widehat{O}_\alpha \widehat{I}_\alpha^{(i)} \\ &= \sum_i \Big[V_C^{(i)}(r)\widehat{I}_C^{(i)} + V_{SS}^{(i)}(r)\vec{\sigma}_1\vec{\sigma}_2\widehat{I}_{SS}^{(i)} + V_T^{(i)}(r)S_{12}(\hat{r})\widehat{I}_T^{(i)} + \\ &\quad + \Big(n^i \vec{\sigma}_2 \cdot \hat{r} + (1 - n^i)\left[\vec{\sigma}_1 \times \vec{\sigma}_2\right] \cdot \hat{r} \Big) V_{PV}^{(i)}(r)\widehat{I}_{PV}^{(i)} \Big], \end{aligned} \tag{4.5}$$

where the i index runs over the different mesons exchanged with each number representing either π, ρ, K, K^*, η or ω and α being an index that represents the different spin operators. As such the $\widehat{O}_\alpha$ operator may take the following forms:

- Central spin-independent (C): $\widehat{1}$ (only for vector mesons)
- Central spin-dependent (SS): $\vec{\sigma}_1\vec{\sigma}_2$
- Tensor (T): $S_{12}(\vec{r}) = 3\vec{\sigma}_1\hat{r}\vec{\sigma}_2\hat{r} - \vec{\sigma}_1\vec{\sigma}_2$
- Parity-Violating (PV): $\mathrm{i}\vec{\sigma}_2\hat{r}$ (for pseudoscalar mesons)
- Parity-Violating, $[\vec{\sigma}_1 \times \vec{\sigma}_2]\cdot\hat{r}$ (for vector mesons)

Additionally in Eq. (4.5) $n^i = 1(0)$ for pseudoscalar (vector) mesons. Thus, the explicit expressions for the $\langle (L'S)JM_J|\widehat{O}_\alpha|(L_rS_0)JM_J\rangle$ coefficients appearing in the transition amplitude will be given. The quantum numbers L_r, S_0, J and M_J correspond to the initial strangeness $S = -2$ state, while L', S, J and M_J dovetail with the final YN system. Each vertex also incorporates a monopole form factor in order to account for the finite size and structure of the particles involved, with the expression[35]:

$$F_i(\vec{q}^{\,2}) = \frac{\Lambda_i^2 - \mu_i^2}{\Lambda_i^2 + \vec{q}^{\,2}}, \tag{4.6}$$

where the value of the cut-off, Λ_i, depends on the meson (with mass μ_i) exchanged. The utilization of form factors prompts the successive regularization[79]:

$$V_C(r;\mu_i) \to V_C(r;\mu_i) - V_C(r;\Lambda_i) - \Lambda_i \frac{\Lambda_i^2 - \mu_i^2}{2} \frac{\mathrm{e}^{-\Lambda_i r}}{4\pi}\left(1 - \frac{2}{\Lambda_i r}\right), \tag{4.7}$$

$$V_{SS}(r;\mu_i) \to V_{SS}(r;\mu_i) - V_{SS}(r;\Lambda_i) - \Lambda_i \frac{\Lambda_i^2 - \mu_i^2}{2} \frac{\mathrm{e}^{-\Lambda_i r}}{4\pi}\left(1 - \frac{2}{\Lambda_i r}\right), \tag{4.8}$$

$$V_T(r;\mu_i) \to V_T(r;\mu_i) - V_T(r;\Lambda_i) - \Lambda_i \frac{\Lambda_i^2 - \mu_i^2}{2} \frac{\mathrm{e}^{-\Lambda_i r}}{4\pi}\left(1 + \frac{2}{\Lambda_i r}\right), \tag{4.9}$$

$$V_{PV}(r;\mu_i) \to V_{PV}(r;\mu_i) - V_{PV}(r;\Lambda_i) - \Lambda_i \frac{\Lambda_i^2 - \mu_i^2}{2} \frac{\mathrm{e}^{-\Lambda_i r}}{4\pi}. \tag{4.10}$$

The values for the cut-offs used in the present work have been collected in Table 4.2, and are modified from those extracted from the Nijmegen soft-core hyperon-nucleon

Table 4.2: Cut-offs for the vertices involved in the calculation of the $\Lambda\Lambda \to YN$ and $\Xi N \to YN$ decay rates.

Meson	$\Lambda_{\mathbf{i}}$ **(MeV)**
π	1749.87
η	1749.87
ρ	1231.64
ω	1310.31
k	1788.58
k^*	1649.28

potentials[38, 80], which use an exponential form factor, in order to match the monopole-type form factor used in the present work.

4.1.1.1 Central transition

Since the operator for the central transition is $\widehat{O}_\alpha = \widehat{1}$:

$$\langle (L'S)JM_J|\widehat{1}|(L_rS_0)JM_J\rangle = \delta_{L_rL'}\delta_{S_0S}. \tag{4.11}$$

4.1.1.2 Spin-Spin transition

$$\langle (L'S)JM_J|\vec{\sigma}_1\vec{\sigma}_2|(L_rS_0)JM_J\rangle = (2S(S+1)-3)\delta_{L_rL'}\delta_{S_0S}. \tag{4.12}$$

4.1.1.3 Tensor transition

$$\langle (L'S)JM_J|\left[3\vec{\sigma}_1\hat{r}\vec{\sigma}_2\hat{r}-\vec{\sigma}_1\vec{\sigma}_2\right]|(L_rS_0)JM_J\rangle = S^J_{L_rL'}\delta_{L_rL'}\delta_{S_0S}, \tag{4.13}$$

where the $S^J_{L_rL'}$ coefficients are given in Table 4.3.

Table 4.3: Coefficients involved in the calculation of the tensor transition spin matrix elements.

$\mathbf{S^J_{L_rL'}}$	$\mathbf{L'=J+1}$	$\mathbf{L'=J}$	$\mathbf{L'=J-1}$
$\mathbf{L_r=J+1}$	$\frac{-2(J+2))}{2J+1}$	0	$\frac{6\sqrt{J(J+1)}}{2J+1}$
$\mathbf{L_r=J}$	0	2	0
$\mathbf{L_r=J-1}$	$\frac{6\sqrt{J(J+1)}}{2J+1}$	0	$\frac{-2(J+2))}{2J+1}$

4.1.1.4 Parity-Violating transition

There exist two possible operators for the parity-violating transition depending on whether the exchanged meson belongs to the pseudoscalar or the vector octet. For pseudoscalar mesons $\widehat{O}_\alpha = \vec{\sigma}_2\widehat{r}$, and thus:

$$\begin{aligned}\langle (L'S)JM_J|\vec{\sigma}_2\widehat{r}|(L_rS_0)JM_J\rangle &= (-1)^{J+1-L'}\sqrt{6}\sqrt{2S_0+1}\sqrt{2L_r+1}\sqrt{2S+1}\\ &\times\langle 10L_r0|L'0\rangle\begin{pmatrix}\frac{1}{2} & \frac{1}{2} & S_0\\ S & 1 & \frac{1}{2}\end{pmatrix}\begin{pmatrix}L' & L_r & 1\\ S_0 & S & J\end{pmatrix}.\end{aligned} \tag{4.14}$$

Conversely if the exchanged meson belongs to the vector octet $\widehat{O}_\alpha = [\vec{\sigma}_1\times\vec{\sigma}_2]\cdot\widehat{r}$

$$\begin{aligned}\langle (L'S)JM_J|[\vec{\sigma}_1\times\vec{\sigma}_2]\cdot\widehat{r}|(L_rS_0)JM_J\rangle &= \mathrm{i}(-1)^{J-L'+S}6\sqrt{6}\sqrt{2S_0+1}\sqrt{2L_r+1}\sqrt{2S+1}\\ &\times\langle 10L_r0|L'0\rangle\begin{pmatrix}L' & L_r & 1\\ S_0 & S & J\end{pmatrix}\begin{pmatrix}1 & 1 & 1\\ \frac{1}{2} & \frac{1}{2} & S\\ \frac{1}{2} & \frac{1}{2} & S_0\end{pmatrix}.\end{aligned} \tag{4.15}$$

In both cases the 2×3 array denotes a Wigner 3-j symbol, which may be given in terms of the Clebsch-Gordan coefficients by:

$$\begin{pmatrix}j_1 & j_2 & j_3\\ m_1 & m_2 & m_3\end{pmatrix} \equiv \frac{(-1)^{j_1-j_2-m_3}}{\sqrt{2j_3+1}}\langle j_1m_1j_2m_2|j_3(-m_3)\rangle \tag{4.16}$$

4.1.2 Isospin Structure

In order to build the isospin operators $\hat{O}_k^Y$ one needs to know the isospin nature of the meson being exchanged (isoscalar for η and ω, isodoublet for K and K^*, and isovector for π and ρ) and the specific baryons involved in the two-body weak transition. Note that the $\Delta I = 1/2$ rule is implemented through the insertion of an isospurion $|\,\frac{1}{2}\,-\frac{1}{2}\rangle$ in the initial state. We focus on developing the isospin structure for the transitions $\Xi N \to YN$, with $Y = \Lambda, \Sigma$, which are the new contributions considered in the present work. Attending only to the isospin quantum numbers, the general structure of the $\Xi N \to YN$ matrix element is:

$$\begin{aligned} & g_1^{Y,\phi}\langle Y\, t_Y, \tfrac{1}{2}\, t_{Nf}|\hat{O}_1^Y|0\, t_\Xi - \tfrac{1}{2}, \tfrac{1}{2}\, t_{Ni}\rangle \times \langle 0\, t_\Xi - \tfrac{1}{2}|\tfrac{1}{2}\, t_\Xi, \tfrac{1}{2} - \tfrac{1}{2}\rangle \\ & + g_2^{Y,\phi}\langle Y\, t_Y, \tfrac{1}{2}\, t_{Nf}|\hat{O}_2^Y|1\, t_\Xi - \tfrac{1}{2}, \tfrac{1}{2}\, t_{Ni}\rangle \times \langle 1\, t_\Xi - \tfrac{1}{2}|\tfrac{1}{2}\, t_\Xi, \tfrac{1}{2} - \tfrac{1}{2}\rangle \\ & + g_3^{Y,\phi}\langle Y\, t_Y, \tfrac{1}{2}\, t_{Nf}|\hat{O}_3^Y|1\, t_\Xi - \tfrac{1}{2}, \tfrac{1}{2}\, t_{Ni}\rangle \times \langle 1\, t_\Xi - \tfrac{1}{2}|\tfrac{1}{2}\, t_\Xi, \tfrac{1}{2} - \tfrac{1}{2}\rangle. \end{aligned} \tag{4.17}$$

where the isospurion has been coupled to the isospin $\frac{1}{2}$ of the Ξ giving states with isospin $I = 0, 1$, which in turn couple to the initial nucleon isospin ($t_{Ni} = \frac{1}{2}$ for a p and $-\frac{1}{2}$ for a n) to give the final YN state.

We first examine those cases where the final state is of the ΛN type, i.e. $|Y\, t_Y\rangle = |0\, 0\rangle$. The possible isospin operators can be argued to be

$$\widehat{O}_1^\Lambda \equiv \mathbb{I}_1 \otimes \mathbb{I}_2, \tag{4.18}$$

$$\widehat{O}_2^\Lambda \equiv \vec{\mathbb{T}}_{01} \otimes \vec{\tau}_2, \tag{4.19}$$

$$\widehat{O}_3^\Lambda \equiv 0, \tag{4.20}$$

where $\vec{\tau}$ stands for the Pauli matrices and $\vec{\mathbb{T}}_{01}$ is an operator that allows the transition from a $I = 1$ state to a $I = 0$ one. Its spherical coordinates have the following matrix elements

$$\langle 00|\mathbb{T}_{01}^k|1m\rangle = (-1)^k\langle 0\, 0, 1 - k|1\, m\rangle = (-1)^k\delta_{m,-k}. \tag{4.21}$$

We note that, in the case of a ΛN final state, we have set the $\widehat{O}_3^{\Lambda}$ operator to zero to account for the fact that there is only one possible scalar operator ($\widehat{O}_2^{\Lambda}$) connecting the initial $|1\,t_\Xi - \frac{1}{2}, \frac{1}{2}\,t_{Ni}\rangle$ pair with the final $\langle 0\,0, \frac{1}{2}\,t_{Nf}|$ one. In the case of a ΣN final state, we have $|Y\,t_Y\rangle = |1 t_Y\rangle$ and the corresponding appropriate set of operators is:

$$\widehat{O}_1^{\Sigma} \equiv \vec{\mathbb{T}}_{10} \otimes \vec{\tau}_2, \tag{4.22}$$

$$\widehat{O}_2^{\Sigma} \equiv \mathbb{I}_1 \otimes \mathbb{I}_2, \tag{4.23}$$

$$\widehat{O}_3^{\Sigma} \equiv \vec{\mathbb{T}}_{11} \otimes \vec{\tau}_2, \tag{4.24}$$

where $\vec{\mathbb{T}}_{10}$ mediates transitions from isospin 0 to isospin 1, with matrix elements

$$\langle 1m|\mathbb{T}_{10}^k|00\rangle = \delta_{m,k}\ , \tag{4.25}$$

as can be inferred taking the adjoint in Eq. (4.21). Likewise $\vec{\mathbb{T}}_{11}$ induces transitions from an initial $I = 1$ state to a final $I = 1$ one. Its matrix elements are given by:

$$\langle 1m'|\mathbb{T}_{11}^k|1m\rangle = \sqrt{2}\langle 1m'|1m1k\rangle\ . \tag{4.26}$$

In the following, we will write the isospin coefficients $g_i^{Y,\phi}$ ($i = 1,2,3$) in terms of the weak and strong coupling constants characteristic of the meson exchanged in either the $\Xi N \to \Lambda N$ or $\Xi N \to \Sigma N$ process. The Appendix A contains an example calculation of the weak and strong coupling constants that are used in the formalism.

In the case of the isoscalar mesons (η or ω) only the $\mathbb{I}_1 \otimes \mathbb{I}_2$ operator contributes to the transition. Therefore, for ΛN final states, the transition will match the following structure

$$g_1^{\Lambda,\eta}\langle \tfrac{1}{2}\,t_{Nf}|\tfrac{1}{2}\,t_{Ni}\rangle\langle 0\,t_\Xi - \tfrac{1}{2}|\tfrac{1}{2}\,t_\Xi, \tfrac{1}{2} - \tfrac{1}{2}\rangle. \tag{4.27}$$

The Clebsch-Gordan coefficient will only be non-zero when the initial state contains a Ξ^0 hyperon. By matching the former expression with that for the $\Xi^0 n \to \Lambda n$ transition, one

obtains the corresponding relation between the isospin coupling and the product of weak and strong coupling constants. Thus, one has:

$$g_1^{\Lambda,\eta} = \sqrt{2}\, g^W_{\Xi^0\Lambda\eta} g^S_{NN\eta} \,, \tag{4.28}$$

$$g_2^{\Lambda,\eta} = 0 \,, \tag{4.29}$$

$$g_3^{\Lambda,\eta} = 0 \,. \tag{4.30}$$

and similarly for the ω meson.

Considering now the case of ΣN final states, only the O_2^Σ operator can contribute to the isoscalar meson exchange. Hence, following similar steps as in the previous case but for the $\Xi^0 n \to \Sigma^0 n$ transition, we find:

$$g_1^{\Sigma,\eta} = 0, \tag{4.31}$$

$$g_2^{\Sigma,\eta} = \sqrt{2}\, g^W_{\Xi^0\Sigma^0\eta} g^S_{NN\eta}, \tag{4.32}$$

$$g_3^{\Sigma,\eta} = 0. \tag{4.33}$$

Let us now turn to the isovector (π or ρ) mesons. For ΛN final states the first isospin structure does not contribute because the isovector meson cannot connect an isospin 0 initial state with the final Λ at the weak vertex. The combined analysis of the $\Xi^0 p \to \Lambda p$, $\Xi^0 n \to \Lambda n$ and $\Xi^- p \to \Lambda n$ amplitudes therefore determines:

$$g_1^{\Lambda,\pi} = 0, \tag{4.34}$$

$$g_2^{\Lambda,\pi} = -\frac{1}{\sqrt{2}}\, g^W_{\Xi^-\Lambda\pi^-}\, g^S_{np\pi^-} = -g^W_{\Xi^-\Lambda\pi^-} g^S_{NN\pi} \,, \tag{4.35}$$

$$g_3^{\Lambda,\pi} = 0 \,, \tag{4.36}$$

where the generic strong coupling $g^S_{NN\pi} = g^S_{pp\pi^0} = -g^S_{nn\pi^0} = g^S_{np\pi^-}/\sqrt{2}$ has been employed in the last two terms. Similarly, for the ΣN final states one finds:

$$g_1^{\Sigma,\pi} = \sqrt{2}\, g^W_{\Xi^0\Sigma^0\pi^0} g^S_{NN\pi}, \tag{4.37}$$

$$g_2^{\Sigma,\pi} = 0, \tag{4.38}$$

$$g_3^{\Sigma,\pi} = g^W_{\Xi^-\Sigma^-\pi^0} g^S_{NN\pi} \,. \tag{4.39}$$

Finally, the case of the isodoublet (K or K^*) mesons involves the exchange of an isospin $\frac{1}{2}$ particle. After including the isospurion, as seen in Eq. (4.17), the isospin conserving transitions are then mediated by isoscalar or isovector operators. In the case of ΛN final states, working out the $\Xi^0 p \to \Lambda p$ and $\Xi^0 n \to \Lambda n$ amplitudes (and the $\Xi^- p \to \Lambda n$ one as a consistency check), we find:

$$g_1^{\Lambda,K} = \frac{1}{\sqrt{2}} g^S_{\Xi\Lambda K}\left(2g^W_{ppK^0} + g^W_{pnK^+}\right), \tag{4.40}$$

$$g_2^{\Lambda,K} = -\frac{1}{\sqrt{2}} g^S_{\Xi\Lambda K} g^W_{npK^+}\ , \tag{4.41}$$

$$g_3^{\Lambda,K} = 0\ , \tag{4.42}$$

written in terms of the generic strong coupling $g^S_{\Xi\Lambda K} = g^S_{\Xi^0\Lambda K^0} = g^S_{\Xi^-\Lambda K^+}$.

Other weak processes are possible in the case of K-exchange when the weak vertex is the ΞNK one. Those processes involve an interchange of particles either in the initial or final state of the amplitude but the operators mediating the transition are the same as before. Therefore, after analyzing the $p\Xi^0 \to \Lambda p$, $n\Xi^0 \to \Lambda n$ and $p\Xi^- \to \Lambda n$ amplitudes, we find:

$$\tilde{g}_1^{\Lambda,K} = -\frac{1}{\sqrt{2}} g^S_{\Lambda NK}\left(g^W_{\Xi^0 nK^0} - 2g^W_{\Xi^0 pK^+}\right), \tag{4.43}$$

$$\tilde{g}_2^{\Lambda,K} = \frac{1}{\sqrt{2}} g^S_{\Lambda NK} g^W_{\Xi^0 nK^0}\ , \tag{4.44}$$

$$\tilde{g}_3^{\Lambda,K} = 0\ , \tag{4.45}$$

written in terms of the generic strong coupling $g^S_{\Lambda NK} = g^S_{\Lambda pK^+} = g^S_{\Lambda nK^0}$.

For the ΣN final state, we find

$$g_1^{\Sigma,K} = -\frac{1}{\sqrt{2}} g^S_{\Xi\Sigma K} g^W_{pnK^+}, \tag{4.46}$$

$$g_2^{\Sigma,K} = \frac{1}{\sqrt{2}} g^S_{\Xi\Sigma K}\left(g^W_{pnK^+} + 2g^W_{ppK^0}\right), \tag{4.47}$$

$$g_3^{\Sigma,K} = \frac{1}{\sqrt{2}} g^S_{\Xi\Sigma K} g^W_{pnK^+}\ , \tag{4.48}$$

written in terms of the generic strong coupling $g^S_{\Xi\Sigma K} = g^S_{\Xi^0\Sigma^0 K^0} = -g^S_{\Xi^-\Sigma^- K^0}/\sqrt{2} = -g^S_{\Xi^-\Sigma^0 K^+}$.

For the processes in which the weak vertex is the ΞNK in the ΞN baryon line, which involve an interchange of particles in the initial or final state, we find:

$$\tilde{g}_1^{\Sigma,K} = \frac{1}{\sqrt{2}} g^S_{\Sigma NK} g^W_{\Xi^0 n\overline{K}^0}, \tag{4.49}$$

$$\tilde{g}_2^{\Sigma,K} = -\frac{1}{\sqrt{2}} g^S_{\Sigma NK} \left(g^W_{\Xi^0 n\overline{K}^0} - 2 g^W_{\Xi^0 p K^-} \right), \tag{4.50}$$

$$\tilde{g}_3^{\Sigma,K} = -\frac{1}{\sqrt{2}} g^S_{\Sigma NK} g^W_{\Xi^0 n\overline{K}^0}, \tag{4.51}$$

written in terms of the generic strong coupling $g^S_{\Sigma NK} = g^S_{p\Sigma^+ K^-} = -g^S_{n\Sigma^0\overline{K}^0} = g^S_{p\Sigma^+\overline{K}^0}/\sqrt{2} = g^S_{n\Sigma^- K^-}/\sqrt{2}$.

In summary, in the expression of Eq. (4.3) for the potential mediated by pseudoscalar mesons, the constants $A_k^{Y,\phi}$ and $B_k^{Y,\phi}$ correspond to the $g_k^{Y,\phi}$ coefficients just derived, which contain products of weak and strong couplings. The weak coupling constants employed should be the parity-violating ones in the case of the $A_k^{Y,\phi}$ constants and the parity-conserving ones in the case of the $B_k^{Y,\phi}$ ones.

Similarly, the $A_k^{Y,v}$, $B_k^{Y,v}$ and $C_k^{Y,v}$ couplings appearing in the vector meson exchange potential of Eq. (4.4), correspond to the $g_k^{Y,v}$ coefficients, but taking into account the following considerations:

- $A_k^{Y,v}$ contains the parity-violating weak coupling constant times the sum of the vector and tensor strong coupling constants.

- $B_k^{Y,v}$ contains the parity-conserving weak vector coupling constant times the strong vector one.

- $C_k^{Y,v}$ contains the sum of the parity-conserving vector and tensor weak coupling constants times the sum of the vector and tensor strong coupling constants.

Table 4.4: Strong pseudoscalar meson couplings to the octet baryons, where D and F are the couplings of the pseudoscalar Lagrangian of Eq. (4.52) and $\overline{M}$ denotes the average mass of the baryons at the baryon-baryon-meson vertex.

Coupling	**Analytic value**	$\mathbf{g^S_{BB\phi}}$
$NN\pi$	$\frac{D+F}{2f_\pi}2\overline{M}$	13.83
$NN\eta$	$\frac{3F-D}{2\sqrt{3}f_\pi}2\overline{M}$	4.14
ΛNK	$-\frac{3D+F}{2\sqrt{3}f_\pi}2\overline{M}$	−15.37
$\Lambda\Lambda\eta$	$-\frac{D}{\sqrt{3}f_\pi}2\overline{M}$	−11.77
$\Lambda\Sigma\pi$	$\frac{D}{\sqrt{3}f_\pi}2\overline{M}$	12.19
ΣNK	$\frac{D-F}{2f_\pi}2\overline{M}$	3.78
$\Sigma\Sigma\pi$	$\frac{F}{f_\pi}2\overline{M}$	13.36
$\Sigma\Sigma\eta$	$\frac{D}{\sqrt{3}f_\pi}2\overline{M}$	12.60
$\Xi\Lambda K$	$\frac{3F-D}{2\sqrt{3}f_\pi}2\overline{M}$	5.36
$\Xi\Sigma K$	$-\frac{D+F}{2f_\pi}2\overline{M}$	−18.47
$\Xi\Xi\pi$	$-\frac{D-F}{\sqrt{2}f_\pi}2\overline{M}$	−4.68
$\Xi\Xi\eta$	$-\frac{3F+D}{2\sqrt{3}f_\pi}2\overline{M}$	−19.77

4.2 Strong baryon-baryon-meson couplings

4.2.1 Pseudoscalar mesons

As discussed in Chapter 2, the strong Lagrangian corresponding to the exchange of a pseudoscalar meson has the following form:

$$\begin{aligned}\mathscr{L}^S_{BB\phi} = &\,\mathrm{Tr}\left[\overline{B}\left(i\gamma^\mu\nabla_\mu\right)B\right] - M_B\,\mathrm{Tr}\left[\overline{B}B\right] \\ &+ D\,\mathrm{Tr}\left[\overline{B}\gamma^\mu\gamma_5\left\{u_\mu,B\right\}\right] + F\,\mathrm{Tr}\left[\overline{B}\gamma^\mu\gamma_5\left[u_\mu,B\right]\right],\end{aligned} \tag{4.52}$$

which allows us to derive the Yukawa-type coupling constants of the baryons to the pseudoscalar mesons displayed in Table 4.4.

4.2.2 Vector mesons

The Lagrangian used to implement the exchange of vector mesons is the following:

$$\begin{aligned}\mathscr{L}^{S}_{BBV} = &-g\{\langle\overline{B}\gamma_\mu[V_8^\mu,B]\rangle + \langle\overline{B}\gamma_\mu B\rangle\langle V_8^\mu\rangle + \frac{1}{4M}\big(F\langle\overline{B}\sigma_{\mu\nu}[\partial^\mu V_8^\nu - \partial^\nu V_8^\mu,B]\rangle \\ &+ D\langle\overline{B}\sigma_{\mu\nu}\{\partial^\mu V_8^\nu - \partial^\nu V_8^\mu,B\}\rangle\big) + \langle\overline{B}\gamma_\mu B\rangle\langle V_0^\mu\rangle + \frac{C_0}{4M}\langle\overline{B}\sigma_{\mu\nu}V_0^{\mu\nu}B\rangle\}.\end{aligned} \tag{4.53}$$

The Yukawa couplings involving vector mesons are displayed in Table 4.5.

4.3 Weak baryon-baryon-meson vertices

In this section the coupling constants for the weak baryon-baryon-meson vertices will be presented. In line with the formalism discussed in Chapter 2, we will first take a look at the parity-violating amplitudes for both pseudoscalar and vector mesons while introducing the parity-conserving contributions next.

4.3.1 Parity-violating contribution

4.3.1.1 Pseudoscalar mesons

As a reminder, the effective Lagrangian used will be:

$$\mathscr{L}^{W}_{BB\phi} = \sqrt{2}\big(h_D\,\mathrm{Tr}\left[\overline{B}\left\{\xi^\dagger h\xi,B\right\}\right] + h_F\,\mathrm{Tr}\left[\overline{B}\left[\xi^\dagger h\xi,B\right]\right]\big), \tag{4.54}$$

with the dimensionless constants being $h_D = -1.69\times10^{-7}$ and $h_F = 3.26\times10^{-7}$. The Lagrangian of Eq. (4.54) allows one to find the weak PV coupling constants of the baryons to the pseudoscalar mesons displayed in Table 4.6. Refer to the Appendix section A.2 for an example calculation.

4.3.1.2 Vector mesons

For the weak vertices we have used the SU(6)$_W$ group, in which meson fields are expressed in terms of a quark-antiquark product and baryons are defined as symmetric

Table 4.5: Vector (V) and tensor (T) strong vector-meson couplings to the octet baryons components, with g, D, F and C_0 being the couplings of the strong BBV Lagrangian of Eq. (4.53).

Coupling	**Analytic value**	$\mathbf{g^S_{BBV}}$
$NN\rho\ (V)$	$-\frac{1}{2}g$	2.95
$NN\rho\ (T)$	$-\frac{D+F}{2}g$	9.49
$NN\omega\ (V)$	$\frac{2\sqrt{2}+3}{2\sqrt{3}}g$	3.54
$NN\omega\ (T)$	$\frac{\sqrt{2}C_0+D+F}{2\sqrt{3}}g$	5.62
$\Lambda NK^*\ (V)$	$-\frac{\sqrt{3}}{2}g$	−5.11
$\Lambda NK^*\ (T)$	$-\frac{D+3F}{2\sqrt{3}}g$	−8.27
$\Lambda\Lambda\omega\ (V)$	$\frac{\sqrt{2}+1}{\sqrt{3}}g$	8.22
$\Lambda\Lambda\omega\ (T)$	$\frac{\sqrt{2}C_0+2D}{6\sqrt{3}}g$	2.77
$\Lambda\Sigma\rho\ (V)$	0	0
$\Lambda\Sigma\rho\ (T)$	$\frac{D}{\sqrt{3}}g$	8.17
$\Sigma NK^*\ (V)$	$-\frac{1}{2}g$	−2.95
$\Sigma NK^*\ (T)$	$\frac{D-F}{2}g$	4.66
$\Sigma\Sigma\rho\ (V)$	$-g$	−5.89
$\Sigma\Sigma\rho\ (T)$	$-Fg$	−4.83
$\Sigma\Sigma\omega\ (V)$	$\frac{\sqrt{2}+1}{\sqrt{3}}g$	8.22
$\Sigma\Sigma\omega\ (T)$	$\frac{\sqrt{2}C_0+2D}{2\sqrt{3}}g$	8.31
$\Xi\Lambda K^*\ (V)$	$-\frac{\sqrt{3}}{2}g$	5.11
$\Xi\Lambda K^*\ (T)$	$\frac{D-3F}{2\sqrt{3}}g$	0.10
$\Xi\Sigma K^*\ (V)$	$-\frac{1}{2}g$	−2.95
$\Xi\Sigma K^*\ (T)$	$-\frac{D+F}{2}g$	−9.49
$\Xi\Xi\rho\ (V)$	$\frac{1}{2}g$	2.95
$\Xi\Xi\rho\ (T)$	$-\frac{F-D}{2}g$	−4.66
$\Xi\Xi\omega\ (V)$	$\frac{2\sqrt{2}+1}{2\sqrt{3}}g$	6.51
$\Xi\Xi\omega\ (T)$	$\frac{D-F}{2\sqrt{3}}g$	2.69

Table 4.6: Weak parity-violating pseudoscalar meson couplings to the octet baryons.

Coupling	**Analytic value**	$\mathbf{g^{PV}_{BB\phi}}$
pnK^+	$h_D + h_F$	1.57×10^{-7}
ppK^0	$h_F - h_D$	4.95×10^{-7}
nnK^0	$2h_F$	6.52×10^{-7}
$\Xi^0 n\overline{K}^0$	0	0
$\Xi^0 pK^-$	0	0
$\Xi^0\Lambda\pi^0$	$\frac{3h_F - h_D}{2\sqrt{3}}$	3.31×10^{-7}
$\Xi^-\Lambda\pi^-$	$\frac{h_D - 3h_F}{\sqrt{6}}$	-4.68×10^{-7}
$\Xi^0\Lambda\eta$	$\frac{h_D - 3h_F}{2}$	-5.73×10^{-7}
$\Xi^0\Sigma^0\pi^0$	$-\frac{h_D + h_F}{2}$	-7.84×10^{-8}
$\Xi^-\Sigma^-\pi^0$	$\frac{h_D + h_F}{\sqrt{2}}$	1.11×10^{-7}
$\Xi^-\Sigma^0\pi^-$	$-\frac{h_D + h_F}{\sqrt{2}}$	-1.11×10^{-7}
$\Xi^0\Sigma^0\eta$	$\frac{\sqrt{3}(h_D + h_F)}{2}$	1.36×10^{-7}
$\Xi^-\Sigma^-\eta$	$\frac{\sqrt{3}(h_D + h_F)}{\sqrt{2}}$	1.92×10^{-7}

tensors. The final general expression accounting for the weak PV baryon-baryon-vector meson couplings is:

$$
\begin{aligned}
H_{PV}^{\Delta S} =& a_T[\overline{B}^{ij2}B_{ij1}\overline{\phi}_3^6 - \overline{B}^{ij3}B_{ij6}\overline{\phi}_2^1 - \overline{B}^{ij1}B_{ij2}\overline{\phi}_4^5 + \overline{B}^{ij4}B_{ij5}\overline{\phi}_1^2] \\
&+ a_V[\overline{B}^{ij2}B_{ij5}\overline{\phi}_3^2 - \overline{B}^{ij3}B_{ij2}\overline{\phi}_2^5 - \overline{B}^{ij1}B_{ij6}\overline{\phi}_4^1 + \overline{B}^{ij4}B_{ij1}\overline{\phi}_1^6] \\
&+ b_T[\overline{B}^{ij2}B_{i16}\overline{\phi}_3^j - \overline{B}^{ij3}B_{i16}\overline{\phi}_2^j - \overline{B}^{23i}B_{ij6}\overline{\phi}_j^1 + \overline{B}^{23i}B_{1ij}\overline{\phi}_j^6 \\
&- \overline{B}^{i1j}B_{25i}\overline{\phi}_4^j + \overline{B}^{ij4}B_{i25}\overline{\phi}_1^j + \overline{B}^{i14}B_{ij5}\overline{\phi}_j^2 - \overline{B}^{i14}B_{ij2}\overline{\phi}_j^5] \\
&+ b_V[\overline{B}^{ij2}B_{i25}\overline{\phi}_3^j - \overline{B}^{ij3}B_{i25}\overline{\phi}_2^j + \overline{B}^{i23}B_{ij5}\overline{\phi}_j^2 - \overline{B}^{23i}B_{ij2}\overline{\phi}_j^5 \\
&- \overline{B}^{1ij}B_{16i}\overline{\phi}_4^j + \overline{B}^{ij4}B_{16i}\overline{\phi}_1^j - \overline{B}^{14i}B_{ij6}\overline{\phi}_j^1 + \overline{B}^{i14}B_{1ij}\overline{\phi}_j^6] \\
&+ c_V[\overline{B}^{ijk}B_{ij6}\overline{\phi}_4^k - \overline{B}^{ij4}B_{ijk}\overline{\phi}_k^6 - \overline{B}^{ijk}B_{ij5}\overline{\phi}_3^k + \overline{B}^{ij3}B_{ijk}\overline{\phi}_k^5],
\end{aligned}
\tag{4.55}
$$

The resulting expressions and numerical results of the weak PV coupling constants of baryons to vector mesons are shown in Table 4.7.

4.3.2 Parity-conserving contribution

Since the use of the weak effective Hamiltonian only allows for the generation of parity-violating amplitudes, in order to compute the parity-conserving ones the pole model is employed.

Table 4.7: Weak parity-violating vector meson couplings to the octet baryons.

Coupling	**Analytic value**	$\mathbf{g^{PV}_{BBV}}$
pnK^{*+}	$\frac{1}{9}(-b_T+2b_V-5c_V)$	-6.72×10^{-7}
ppK^{*0}	$\frac{1}{9}\left(8a_T+b_T-\frac{1}{2}b_V+c_V\right)$	1.38×10^{-7}
nnK^{*0}	$\frac{1}{9}\left(-2a_T-\frac{1}{2}b_T+b_V+c_V\right)$	-4.34×10^{-7}
$\Xi^0n\overline{K}^{*0}$	0	0
Ξ^0pK^{*-}	$\frac{1}{9}(b_T-2b_V)$	2.79×10^{-7}
$\Xi^0\Lambda\rho^0$	$\frac{\sqrt{3}}{9}\left(a_T+\frac{1}{4}b_T-\frac{1}{4}b_V+\frac{1}{2}c_V\right)$	1.31×10^{-7}
$\Xi^-\Lambda\rho^-$	$\frac{\sqrt{6}}{9}\left(-a_V+\frac{1}{4}b_T-\frac{1}{4}b_V+\frac{1}{2}c_V\right)$	2.84×10^{-7}
$\Xi^0\Lambda\omega$	$\frac{1}{3}\left(\frac{1}{3}a_T+\frac{1}{4}b_T-\frac{1}{4}b_V+\frac{1}{6}c_V\right)$	1.69×10^{-7}
$\Xi^0\Sigma^0\rho^0$	$\frac{1}{9}\left(-5a_T-\frac{7}{4}b_T+\frac{5}{4}b_V-\frac{5}{2}c_V\right)$	-4.25×10^{-7}
$\Xi^-\Sigma^-\rho^0$	$-\frac{5\sqrt{2}}{18}(2a_T+c_V)$	-2.07×10^{-7}
$\Xi^-\Sigma^0\rho^-$	$\frac{\sqrt{2}}{9}\left(-5a_V+\frac{1}{4}b_T-\frac{1}{4}b_V+\frac{5}{2}c_V\right)$	5.56×10^{-7}
$\Xi^0\Sigma^0\omega$	$\frac{\sqrt{3}}{27}\left(-5a_T-\frac{1}{4}b_T-\frac{1}{4}b_V-\frac{5}{2}c_V\right)$	-8.47×10^{-8}
$\Xi^-\Sigma^-\omega$	$-\frac{5\sqrt{6}}{27}\left(a_T+\frac{1}{2}c_V\right)$	-1.20×10^{-7}

The expressions of the weak PC coupling constants of baryons to pseudoscalar and vector mesons are shown in Tables 4.8 and 4.9, respectively. The strong coupling constants in the expressions of Table 4.8 should be replaced by the numerical values listed in Table 4.4, to obtain the weak PC couplings involving pseudoscalar mesons. Analogously the weak PC vector and tensor couplings involving vector mesons are obtained by inserting, respectively, the vector and tensor values of the strong coupling constants listed in Table 4.5 into the expressions of Table 4.9.

Table 4.8: Weak baryon-baryon-pseudoscalar meson parity-conserving couplings, $g^{PC}_{BB\phi}$.

Coupling	**Analytic value**
pnK^+	$g^S_{\Lambda pK^+}\frac{1}{m_n-m_\Lambda}\frac{-A_{\Lambda p}}{\sqrt{2}}+g^S_{\Sigma^0 pK^+}\frac{1}{m_n-m_{\Sigma^0}}\frac{-A_{\Sigma^+ p}}{\sqrt{2}}$
ppK^0	$g^S_{p\Sigma^+\overline{K}^0}\frac{1}{m_p-m_{\Sigma^+}}A_{\Sigma^+ p}$
nnK^0	$g^S_{n\Lambda\overline{K}^0}\frac{1}{m_n-m_\Lambda}\frac{-A_{\Lambda p}}{\sqrt{2}}+g^S_{n\Sigma^0\overline{K}^0}\frac{1}{m_n-m_{\Sigma^0}}\frac{-A_{\Sigma^+ p}}{\sqrt{2}}$
$\Xi^0 n\overline{K}^0$	$g^S_{\Lambda nK^0}\frac{1}{m_{\Xi^0}-m_\Lambda}\frac{1}{\sqrt{2}}\left(A_{\Lambda p}-\sqrt{3}A_{\Sigma^+ p}\right)+g^S_{\Sigma^0 nK^0}\frac{1}{m_{\Xi^0}-m_{\Sigma^0}}\frac{-1}{2\sqrt{2}}\left(A_{\Sigma^+ p}+\sqrt{3}A_{\Lambda p}\right)+g^S_{\Xi^0\Lambda K^0}\frac{1}{m_n-m_\Lambda}\frac{-A_{\Lambda p}}{\sqrt{2}}+g^S_{\Xi^0\Sigma^0 K^0}\frac{1}{m_n-m_{\Sigma^0}}\frac{-A_{\Sigma^+ p}}{\sqrt{2}}$
$\Xi^0 pK^-$	$g^S_{\Lambda pK^+}\frac{1}{m_{\Xi^0}-m_\Lambda}\frac{1}{\sqrt{2}}\left(A_{\Lambda p}-\sqrt{3}A_{\Sigma^+ p}\right)+g^S_{\Sigma^0 pK^+}\frac{1}{m_{\Xi^0}-m_{\Sigma^0}}\frac{-1}{2\sqrt{2}}\left(A_{\Sigma^+ p}+\sqrt{3}A_{\Lambda p}\right)+g^S_{\Xi^0\Sigma^+ K^+}\frac{1}{m_p-m_{\Sigma^+}}A_{\Sigma^+ p}$
$\Xi^0\Lambda\pi^0$	$g^S_{\Xi^0\Xi^0\pi^0}\frac{1}{m_\Lambda-m_{\Xi^0}}\frac{1}{\sqrt{2}}\left(A_{\Lambda p}-\sqrt{3}A_{\Sigma^+ p}\right)+g^S_{\Lambda\Sigma^0\pi^0}\frac{1}{m_{\Xi^0}-m_{\Sigma^0}}\frac{-1}{2\sqrt{2}}\left(A_{\Sigma^+ p}+\sqrt{3}A_{\Lambda p}\right)$
$\Xi^-\Lambda\pi^-$	$g^S_{\Sigma^-\Lambda\pi^+}\frac{1}{m_{\Xi^-}-m_{\Sigma^-}}\frac{1}{2}\left(\sqrt{3}A_{\Lambda p}+A_{\Sigma^+ p}\right)+g^S_{\Xi^-\Xi^0\pi^+}\frac{1}{m_\Lambda-m_{\Xi^0}}\frac{1}{\sqrt{2}}\left(A_{\Lambda p}-\sqrt{3}A_{\Sigma^+ p}\right)$
$\Xi^0\Lambda\eta$	$\left(g^S_{\Xi^0\Xi^0\eta}-g^S_{\Lambda\Lambda\eta}\right)\frac{1}{m_\Lambda-m_{\Xi^0}}\frac{1}{\sqrt{2}}\left(A_{\Lambda p}-\sqrt{3}A_{\Sigma^+ p}\right)$
$\Xi^0\Sigma^0\pi^0$	$g^S_{\Xi^0\Xi^0\pi^0}\frac{1}{m_{\Sigma^0}-m_{\Xi^0}}\frac{-1}{2\sqrt{2}}\left(A_{\Sigma^+ p}+\sqrt{3}A_{\Lambda p}\right)+g^S_{\Sigma^0\Lambda\pi^0}\frac{1}{m_{\Xi^0}-m_\Lambda}\frac{1}{\sqrt{2}}\left(A_{\Lambda p}-\sqrt{3}A_{\Sigma^+ p}\right)$
$\Xi^-\Sigma^-\pi^0$	$\left(g^S_{\Xi^-\Xi^-\pi^0}-g^S_{\Sigma^-\Sigma^-\pi^0}\right)\frac{1}{m_{\Sigma^-}-m_{\Xi^-}}\frac{1}{2}\left(\sqrt{3}A_{\Lambda p}+A_{\Sigma^+ p}\right)$
$\Xi^-\Sigma^0\pi^-$	$\left(g^S_{\Sigma^-\Sigma^0\pi^+}\frac{1}{m_{\Xi^-}-m_{\Sigma^-}}+\frac{-1}{\sqrt{2}}g^S_{\Xi^-\Xi^0\pi^+}\frac{1}{m_{\Sigma^0}-m_{\Xi^0}}\right)\frac{1}{2}\left(\sqrt{3}A_{\Lambda p}+A_{\Sigma^+ p}\right)$
$\Xi^0\Sigma^0\eta$	$\left(g^S_{\Xi^0\Xi^0\eta}-g^S_{\Sigma^0\Sigma^0\eta}\right)\frac{1}{m_{\Sigma^0}-m_{\Xi^0}}\frac{-1}{2\sqrt{2}}\left(A_{\Sigma^+ p}+\sqrt{3}A_{\Lambda p}\right)$
$\Xi^-\Sigma^-\eta$	$\left(g^S_{\Xi^-\Xi^-\eta}-g^S_{\Sigma^-\Sigma^-\eta}\right)\frac{1}{m_{\Sigma^-}-m_{\Xi^-}}\frac{1}{2}\left(\sqrt{3}A_{\Lambda p}+A_{\Sigma^+ p}\right)$

Table 4.9: Weak baryon-baryon-vector meson parity-conserving couplings, g^{PC}_{BBV}.

Coupling	Analytic value
pnK^{*+}	$g^S_{\Lambda pK^{*+}}\frac{1}{m_n-m_\Lambda}\frac{-A_{\Lambda p}}{\sqrt{2}}+g^S_{\Sigma^0 pK^{*+}}\frac{1}{m_n-m_{\Sigma^0}}\frac{-A_{\Sigma^+ p}}{\sqrt{2}}$
ppK^{*0}	$g^S_{p\Sigma^+\overline{K}^{*0}}\frac{1}{m_p-m_{\Sigma^+}}A_{\Sigma^+ p}$
nnK^{*0}	$g^S_{n\Lambda\overline{K}^{*0}}\frac{1}{m_n-m_\Lambda}\frac{-A_{\Lambda p}}{\sqrt{2}}+g^S_{n\Sigma^0\overline{K}^{*0}}\frac{1}{m_n-m_{\Sigma^0}}\frac{-A_{\Sigma^+ p}}{\sqrt{2}}$
$\Xi^0 n\overline{K}^{*0}$	$g^S_{\Lambda nK^{*0}}\frac{1}{m_{\Xi^0}-m_\Lambda}\frac{1}{\sqrt{2}}\left(A_{\Lambda p}-\sqrt{3}A_{\Sigma^+ p}\right)+g^S_{\Sigma^0 nK^{*0}}\frac{1}{m_{\Xi^0}-m_{\Sigma^0}}\frac{-1}{2\sqrt{2}}\left(A_{\Sigma^+ p}+\sqrt{3}A_{\Lambda p}\right)+g^S_{\Xi^0\Lambda K^{*0}}\frac{1}{m_\Lambda-m_n}\frac{-A_{\Lambda p}}{\sqrt{2}}+g^S_{\Xi^0\Sigma^0 K^{*0}}\frac{1}{m_{\Sigma^0}-m_n}\frac{-A_{\Sigma^+ p}}{\sqrt{2}}$
$\Xi^0 pK^{*-}$	$g^S_{\Lambda pK^{*+}}\frac{1}{m_{\Xi^0}-m_\Lambda}\frac{1}{\sqrt{2}}\left(A_{\Lambda p}-\sqrt{3}A_{\Sigma^+ p}\right)+g^S_{\Sigma^0 pK^{*+}}\frac{1}{m_{\Xi^0}-m_{\Sigma^0}}\frac{-1}{2\sqrt{2}}\left(A_{\Sigma^+ p}+\sqrt{3}A_{\Lambda p}\right)+g^S_{\Xi^0\Sigma^+ K^{*+}}\frac{1}{m_p-m_{\Sigma^+}}A_{\Sigma^+ p}$
$\Xi^0\Lambda\rho^0$	$g^S_{\Xi^0\Xi^0\rho^0}\frac{1}{m_\Lambda-m_{\Xi^0}}\frac{1}{\sqrt{2}}\left(A_{\Lambda p}-\sqrt{3}A_{\Sigma^+ p}\right)+g^S_{\Lambda\Sigma^0\rho^0}\frac{1}{m_{\Xi^0}-m_{\Sigma^0}}\frac{-1}{2\sqrt{2}}\left(A_{\Sigma^+ p}+\sqrt{3}A_{\Lambda p}\right)$
$\Xi^-\Lambda\rho^-$	$g^S_{\Sigma^-\Lambda\rho^+}\frac{1}{m_{\Xi^-}-m_{\Sigma^-}}\frac{1}{2}\left(\sqrt{3}A_{\Lambda p}+A_{\Sigma^+ p}\right)+g^S_{\Xi^-\Xi^0\rho^+}\frac{1}{m_\Lambda-m_{\Xi^0}}\frac{1}{\sqrt{2}}\left(A_{\Lambda p}-\sqrt{3}A_{\Sigma^+ p}\right)$
$\Xi^0\Lambda\omega$	$\left(g^S_{\Xi^0\Xi^0\omega}-g^S_{\Lambda\Lambda\omega}\right)\frac{1}{m_\Lambda-m_{\Xi^0}}\frac{1}{\sqrt{2}}\left(A_{\Lambda p}-\sqrt{3}A_{\Sigma^+ p}\right)$
$\Xi^0\Sigma^0\rho^0$	$g^S_{\Xi^0\Xi^0\rho^0}\frac{1}{m_{\Sigma^0}-m_{\Xi^0}}\frac{-1}{2\sqrt{2}}\left(A_{\Sigma^+ p}+\sqrt{3}A_{\Lambda p}\right)+g^S_{\Sigma^0\Lambda\rho^0}\frac{1}{m_{\Xi^0}-m_\Lambda}\frac{1}{\sqrt{2}}\left(A_{\Lambda p}-\sqrt{3}A_{\Sigma^+ p}\right)$
$\Xi^-\Sigma^-\rho^0$	$\left(g^S_{\Xi^-\Xi^-\rho^0}-g^S_{\Sigma^-\Sigma^-\rho^0}\right)\frac{1}{m_{\Sigma^-}-m_{\Xi^-}}\frac{1}{2}\left(\sqrt{3}A_{\Lambda p}+A_{\Sigma^+ p}\right)$
$\Xi^-\Sigma^0\rho^-$	$\left(g^S_{\Sigma^-\Sigma^0\rho^+}\frac{1}{m_{\Xi^-}-m_{\Sigma^-}}+\frac{-1}{\sqrt{2}}g^S_{\Xi^-\Xi^0\rho^+}\frac{1}{m_{\Sigma^0}-m_{\Xi^0}}\right)\frac{1}{2}\left(\sqrt{3}A_{\Lambda p}+A_{\Sigma^+ p}\right)$
$\Xi^0\Sigma^0\omega$	$\left(g^S_{\Xi^0\Xi^0\omega}-g^S_{\Sigma^0\Sigma^0\omega}\right)\frac{1}{m_{\Sigma^0}-m_{\Xi^0}}\frac{-1}{2\sqrt{2}}\left(A_{\Sigma^+ p}+\sqrt{3}A_{\Lambda p}\right)$
$\Xi^-\Sigma^-\omega$	$\left(g^S_{\Xi^-\Xi^-\omega}-g^S_{\Sigma^-\Sigma^-\omega}\right)\frac{1}{m_{\Sigma^-}-m_{\Xi^-}}\frac{1}{2}\left(\sqrt{3}A_{\Lambda p}+A_{\Sigma^+ p}\right)$

CHAPTER 5

THE STRONG INTERACTION AND THE BARYON-BARYON WAVE FUNCTION

In this chapter we discuss how to incorporate the strong interaction effects into the calculation of the weak decay amplitude. We employ the G-matrix formalism to obtain the correlated wave function for the initial hyperon-hyperon state, which takes into account the Pauli blocking effects on the nucleon of the intermediate ΞN pair. For the description of the final YN system, the relevant strong interaction effects in the evaluation of decay rates are those associated with their mutual interaction, which can be addressed by solving the corresponding $T-$matrix equation. The propagation of these two baryons through the residual nuclear medium induces additional final state interactions, which modify energy and angular spectra of the emitted particles. Using an intranuclear cascade code (Monte-Carlo), one can then compare to experimental data at the level of the detected particle spectra. Since our interest with the present calculation is to estimate decay rates, we will omit the involved analysis of the particle spectra and focus only on the interaction between the two weakly emitted baryons. Note that, given

Table 5.1: Possible $^{2S+1}L_J$ channels involved in the weak process $\Lambda\Lambda \underset{S}{\rightarrow} B_1B_2 \underset{W}{\longrightarrow} B_1'B_2' \underset{S}{\rightarrow} YN$, contributing to the weak (W) decay of ${}^{6}_{\Lambda\Lambda}$He, where the first and last transitions are mediated by the strong (S) interaction. Each state has been labelled by the relevant hyperon.

$\Lambda\Lambda$	$\underset{S}{\rightarrow}$	$B_1\,B_2$	$\underset{W}{\longrightarrow}$	$B_1'\,B_2'$	$\underset{S}{\rightarrow}$	YN
(Λ)		$(\tilde{Y})$		(Y')		(Y)
$^{2S+1}L_J$		$^{2\tilde{S}+1}\tilde{L}_J$		$^{2\tilde{S}'+1}\tilde{L}'_J$		$^{2S'+1}L'_J$
$^1S_0$	$\rightarrow$	$^1S_0$	$\rightarrow$	$^1S_0$	$\rightarrow$	$^1S_0$
$^1S_0$	$\rightarrow$	$^1S_0$	$\rightarrow$	$^3P_0$	$\rightarrow$	$^3P_0$

the angular quantum numbers of the $\Lambda\Lambda$ initial state, $^1S_0$, the possible $^{2S+1}L_J$ channels involved in the process $\Lambda\Lambda \rightarrow B_1B_2 \rightarrow B_1'B_2' \rightarrow YN$ are the only ones listed in Table 5.1, where conservation of total angular momentum, as well as conservation of parity for the strong $^1S_0 \rightarrow {}^1S_0$ and $^3P_0 \rightarrow {}^3P_0$ transitions, have been taken into account. The symbols in between brackets denote the labels that will represent the different baryon-baryon channels in the two-body states.

5.1 Final State Interactions

When one introduces the effect of the strong interaction, the wave function describing the relative motion gets modified with respect to the free wave function. Let the Hamiltonian be $H = H_0 + V$, with H_0 the Hamiltonian describing the situation in which the two systems do not interact and V being the interaction potential. If we denote by Φ the plane wave solution, $|\vec{k}YS'M_S'\rangle$ with momentum $\vec{k}$ and spin S, of the Hamiltonian H_0 with energy E, *i.e.* $H_0\Phi = E\Phi$, then the possible solutions for Ψ are given by the Lippmann-Schwinger equation,

$$|\Psi^{(\pm)}\rangle = |\Phi\rangle + \frac{V|\Psi^{(\pm)}\rangle}{E - H_0 \pm i\epsilon}, \tag{5.1}$$

where the positive (negative) solution corresponds to a plane wave plus an outgoing (incoming) spherical wave at sufficiently large distances.

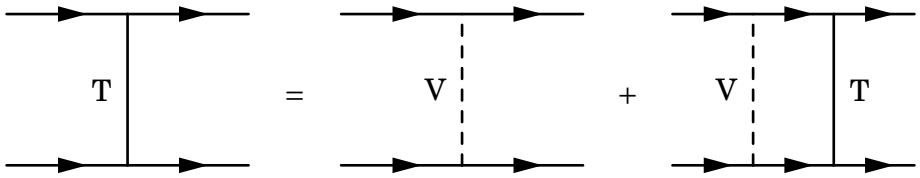

Figure 5.1: Diagrammatic representation of the Lippmann-Schwinger equation.

An alternative formulation of the Lippmann-Schwinger equation written in terms of the transition matrix T yields

$$|\Psi^{(+)}\rangle = |\Phi\rangle + \frac{T|\Phi\rangle}{E - H_0 + i\epsilon}, \tag{5.2}$$

$$\langle\Psi^{(-)}| = \langle\Phi| + \frac{\langle\Phi|T}{E - H_0 - i\epsilon}, \tag{5.3}$$

where the T operator fulfils

$$T = V + V\frac{T}{E - H_0 + i\epsilon}. \tag{5.4}$$

Projecting into coordinate space and inserting a complete set of states on the r.h.s in Eq. (5.3) we find:

$$\begin{aligned}\langle\Psi^{(-)}_{\vec{k}} Y S' M'_S|\vec{r}\rangle &= \langle\vec{k} Y S' M'_S|\vec{r}\rangle \\ &+ \sum_{\tilde{S}'\tilde{M}'_S}\sum_{Y'}\int d^3k' \frac{\langle\vec{k} Y S' M'_S|T|\vec{k}' Y' \tilde{S}' \tilde{M}'_S\rangle\langle\vec{k}' Y' \tilde{S}' \tilde{M}'_S|\vec{r}\rangle}{E - H_0 - i\epsilon},\end{aligned} \tag{5.5}$$

where the quantum numbers follow the notation used in Table 5.1. We perform a partial wave decomposition in the coupled $(LS)J$ representation of the wave functions $\langle\Psi^{(-)}_{\vec{k}} Y S' M'_S|\vec{r}\rangle$ and $\langle\vec{k} Y S' M'_S|\vec{r}\rangle$, the latter being the adjoint of the free plane wave, $\mathrm{e}^{-i\vec{k}\vec{r}}\langle Y S' M'_S|$, and obtain:

$$\begin{aligned}\Psi^{(-)*}_{\vec{k}\,Y}(\vec{r})\chi^{S'}_{M'_S} =& 4\pi \sum_{JM}\sum_{L' M'_L \tilde{L}' \tilde{S}'}\sum_{Y'}(-i)^{\tilde{L}'}\Psi^{(-)*J}_{Y L' S', Y' \tilde{L}' \tilde{S}'}(k,r) Y_{L' M'_L}(\hat{k}) \\ &\times \langle L' M'_L S' M'_S|JM\rangle \mathscr{J}^{\dagger JM}_{\tilde{L}' \tilde{S}'}(\hat{r}),\end{aligned} \tag{5.6}$$

where the generalized spherical harmonic $\mathscr{J}^{\dagger}$ is defined as

$$\mathscr{J}^{\dagger JM}_{\tilde{L}'\tilde{S}'}(\hat{r}) = \sum_{\tilde{M}'_L \tilde{M}'_S} \langle \tilde{L}'\tilde{M}'_L \tilde{S}'\tilde{M}'_S | JM \rangle Y^*_{\tilde{L}'\tilde{M}'_L}(\hat{r}). \tag{5.7}$$

The partial wave decomposition for the free plane wave may be obtained by replacing $\Psi^{(-)*J}_{YL'S',Y'\tilde{L}'\tilde{S}'}(k,r)$ with $j_{L'}(kr)\delta_{Y'Y}\delta_{\tilde{L}'L'}\delta_{\tilde{S}'S'}$ in Eq. (5.6), where $j_{L'}(kr)$ is the spherical Bessel wave function.

For the T matrix elements one can write

$$\begin{aligned}\langle \vec{k} Y S' M'_S | T | \vec{k}' Y' \tilde{S}' \tilde{M}'_S \rangle = \sum_{JM} \sum_{L'M'_L} \sum_{\tilde{L}'\tilde{M}'_L} & Y_{L'M'_L}(\hat{k}) Y^*_{\tilde{L}'M'_{\tilde{L}}}(\hat{k}') \\ & \times \langle L' M'_L S' M'_S | JM \rangle \langle \tilde{L}' \tilde{M}'_L \tilde{S}' \tilde{M}'_S | JM \rangle \\ & \times \langle kY(L'S')JM | T | k'Y'(\tilde{L}'\tilde{S}')JM \rangle \ .\end{aligned} \tag{5.8}$$

Inserting the previous equation, together with the partial wave decomposition of the wave functions in Eq. (5.5), one obtains the equation that determines the partial wave components of the correlated wave function:

$$\begin{aligned}\Psi^{(-)*J}_{YL'S',Y'\tilde{L}'\tilde{S}'}(k,r) = & \, j_{L'}(kr)\delta_{Y'Y}\delta_{\tilde{L}'L'}\delta_{\tilde{S}'S'} + \\ & + \int k'^2 dk' \frac{\langle kY(L'S')JM|T|k'Y'(\tilde{L}'\tilde{S}')JM\rangle j_{\tilde{L}'}(k'r)}{E(k) - E(k') + i\epsilon} \ ,\end{aligned} \tag{5.9}$$

where the partial wave T-matrix elements fulfill the integral equation:

$$\begin{aligned}\langle kY(L'S')JM|T|k'Y'(\tilde{L}'\tilde{S}')JM\rangle = & \langle kY(L'S')JM|V|k'Y'(\tilde{L}'\tilde{S}')JM\rangle + \\ & + \sum_{L''S''Y''} \int k''^2 dk'' \langle kY(L'S')JM|V|k''Y''(L''S'')JM\rangle \\ & \times \frac{\langle k''Y''(L''S'')JM|T|k'Y'(\tilde{L}'\tilde{S}')JM\rangle}{E(k) - E(k'') + i\epsilon} \ .\end{aligned} \tag{5.10}$$

Note that, since the $\Lambda\Lambda$ pair is in a $^1S_0$ state, conservation of angular momentum and parity prevents a change of the spin and orbital angular momentum quantum numbers between the pre- and post-strong transition states, as seen in Table 5.1. Consequently, the above equations could be simplified by applying $L'' = \tilde{L}' = L'$, $\tilde{M}_{L'} = M_{L'}$, $S'' = \tilde{S}' = S'$ and $\tilde{M}_{S'} = M_{S'}$.

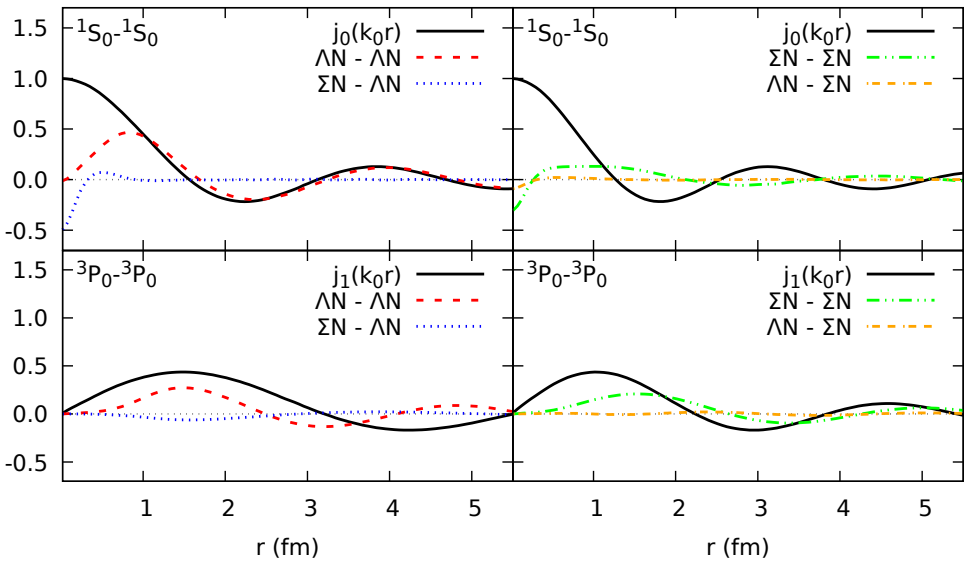

Figure 5.2: Different components of the final state wave function, showing the diagonal $\Lambda N - \Lambda N$ and the $\Sigma N - \Sigma N$ components in dashed red and dot-dot-dashed green, respectively, as well as the off-diagonal $\Sigma N - \Lambda N$ and $\Lambda N - \Sigma N$ terms in dotted blue and dot-dashed orange for the $^1S_0 - ^1S_0$ and $^3P_0 - ^3P_0$ transition channels, for a representative momentum value of $k_0 = 100$ MeV.

5.2 Initial State Interactions

For the initial state interactions a similar framework to that of the Lippmann-Schwinger equation is applied, but considering the fact that the interacting particles feel the presence of the medium where they are embedded. This is known as the Brueckner-Goldstone theory, which considers the interactions of a pair of particles within the Fermi sea, with the collisions fulfilling the requirements of the Pauli principle. We will solve the problem in infinite nuclear matter and the obtained results will be adapted to the finite hypernuclear problem that we are dealing with.

Working within the $\left(\frac{1}{2}\right)^+$ baryon octet, the strange $\Lambda\Lambda$, ΞN and $\Sigma\Sigma$ pairs can couple through the strong interaction to the initial $\Lambda\Lambda$ state. The correlated state, $|\Psi\rangle$, is defined through $G|\Psi\rangle = V|\Phi\rangle$, where $|\Phi\rangle$ is the free-particle state, and G is given in terms of the

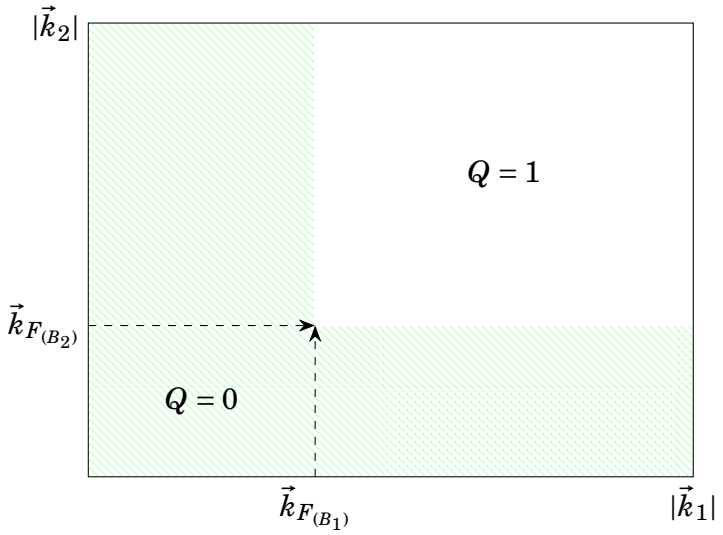

Figure 5.3: Schematic representation of the value of the Pauli operator as a function of the single particle momenta $\vec{k}_1$ and $\vec{k}_2$ with $k_{F_{(B_1)}}$ and $k_{F_{(B_2)}}$ the radii of the Fermi surface.

bare baryon-baryon potential, V, by:

$$G = V + V\frac{Q}{E - H_0 + i\epsilon}G. \tag{5.11}$$

This is an integral equation, where Q corresponds to the Pauli blocking operator, as shown in Fig. 5.3, which restricts the summation to unoccupied states above the Fermi level, and E is the energy of the interacting two-body system.

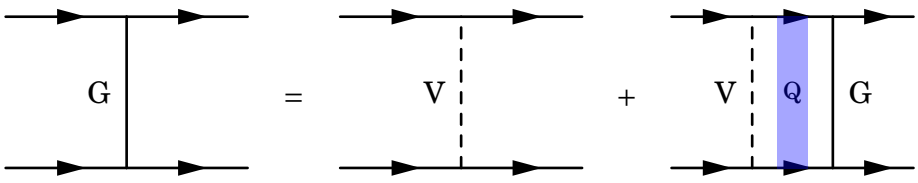

Figure 5.4: Visual representation of the G-Matrix equation.

The correlated state can therefore be written as:

$$|\Psi\rangle = |\Phi\rangle + \frac{Q}{E - H_0 + i\epsilon}G|\Phi\rangle. \tag{5.12}$$

Working in the coupled $(LS)J$ representation, we find

$$\Psi^J_{\tilde{Y}\tilde{L}\tilde{S},\Lambda LS}(k,r) = j_L(kr)\delta_{\Lambda\tilde{Y}}\delta_{L\tilde{L}}\delta_{S\tilde{S}} + \int k'^2 dk' \frac{\langle k'\tilde{Y}(\tilde{L}\tilde{S})JM|G|kY\Lambda(LS)JM\rangle \overline{Q}(k') j_{\tilde{L}}(k'r)}{E(k)-E(k')+i\epsilon}, \tag{5.13}$$

where $\overline{Q}$ stands for the angle-averaged Pauli operator[81], which imposes certain restrictions to the values of the momenta of the involved particles, and the partial wave G-matrix elements fulfill the integral equation:

$$\begin{aligned}\langle k'\tilde{Y}(\tilde{L}\tilde{S})JM|G|k\Lambda(LS)JM\rangle &= \langle k'\tilde{Y}(\tilde{L}\tilde{S})JM|V|k\Lambda(LS)JM\rangle \\ &+ \sum_{L''S''Y''}\int k''^2 dk'' \langle k'\tilde{Y}(\tilde{L}\tilde{S})JM|V|k''Y''(L''S'')JM\rangle \\ &\times \frac{\overline{Q}(k'')\langle k''Y''(L''S'')JM|G|k\Lambda(LS)JM\rangle}{E(k)-E(k'')+i\epsilon}.\end{aligned} \tag{5.14}$$

As before, conservation of angular momentum and parity, together with the fact that the initial $\Lambda\Lambda$ is in a ${}^1S_0$ state, simplifies the above equations considerably, as the only permitted transition is ${}^1S_0 \rightarrow {}^1S_0$.

In order to obtain the wave functions corresponding to a finite hypernucleus a correlation function is defined:

$$f^J_{\Lambda LS}(r) \equiv \frac{\Psi^J_{\Lambda LS,\Lambda LS}(k^*,r)}{j_L(k^*r)}. \tag{5.15}$$

This function ascribes the correlated wave function in nuclear matter, $\Psi^J_{\Lambda LS,\Lambda LS}(k,r)$, with the non-interacting one for a relative momentum k^*, taken to be 100 MeV, which is representative of the average momentum of the $\Lambda\Lambda$ pair in ${}^{\ 6}_{\Lambda\Lambda}$He. The same correlation effects are assumed for finite nuclei, thusly defining the diagonal terms of the relative motion wave function in a finite nucleus as:

$$\Omega^J_{\Lambda LS}(r) \equiv f^J_{\Lambda LS}(r)\Phi_{NL}\left(\frac{r}{\sqrt{2}b}\right), \tag{5.16}$$

where $\Phi_{NL}(r/\sqrt{2}b)$ is the relative harmonic oscillator wave function of the two Λ particles.

For the non-diagonal $\Lambda LS \rightarrow \tilde{Y}\tilde{L}\tilde{S}$ components, we rescale the nuclear matter wave function $\Psi^J_{\tilde{Y}\tilde{L}\tilde{S},\Lambda LS}$ by the same normalisation factor affecting the diagonal components, namely:

$$\Omega^J_{\tilde{Y}\tilde{L}\tilde{S},\Lambda LS}(r) \equiv \frac{\Phi_{NL}(r=0)}{j_L(k^* r=0)} \Psi^J_{\tilde{Y}\tilde{L}\tilde{S},\Lambda LS}(k^*, r), \tag{5.17}$$

as can be inferred upon inspecting Eqs. (5.15) and (5.16).

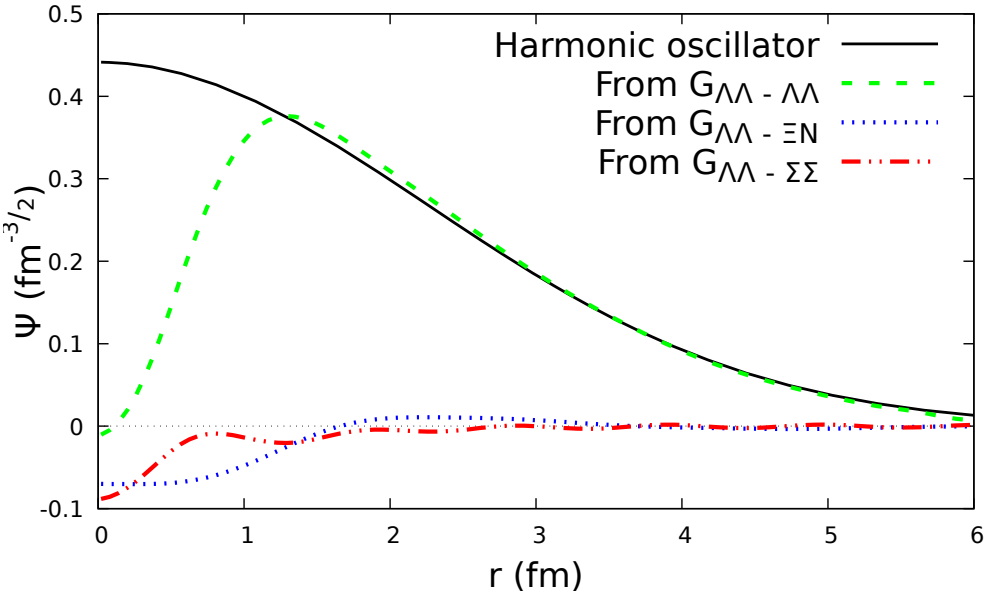

Figure 5.5: Different components of the relative $\Lambda\Lambda$ wave function corresponding to the $^1S_0$ channel, and for a value of the relative momentum of 100 MeV. The uncorrelated H.O w.f is also represented for the sake of comparison.

In Fig. 5.5 we represent the initial $\Lambda\Lambda$ wave function for $N = 1$ and $L = 0$ as a function of the relative distance between the two Λ particles. The black solid line displays the uncorrelated harmonic oscillator wave function, while the green dashed line displays the correlated wave function for the dominant diagonal $\Lambda\Lambda - \Lambda\Lambda$ component. The red dot-dot-dashed and the blue dotted lines represent, respectively, the $\Lambda\Lambda - \Sigma\Sigma$ and the $\Lambda\Lambda - \Xi N$ components. It is clear that the dominant contribution to the $\Lambda\Lambda \rightarrow YN$ decay mode of ${}^{6}_{\Lambda\Lambda}$He will come from the diagonal $\Lambda\Lambda - \Lambda\Lambda$ component of the wave function, which at distances of around 3 fm behaves as the uncorrelated harmonic oscillator w.f., while

at distances below 1.2 fm its strength gets reduced due to the short-distance repulsive behavior of the strangeness $S = -2$ baryon-baryon NSC97f interaction employed [38]. With regard to the non-diagonal components of the wave function one can see that, despite having a comparable size at the origin, the strength of the $\Lambda\Lambda - \Sigma\Sigma$ term is essentially located at distances under 0.5 fm, which will be strongly suppressed by the r^2 factor in the integrand of the two-body matrix element. On the other hand, the $\Lambda\Lambda - \Xi N$ component is still sizable around 1 fm and it is expected to contribute non-negligibly to the $\Lambda\Lambda \to YN$ decay mode of ${}^{\;\;6}_{\Lambda\Lambda}\mathrm{He}$. We will see that, even if non-negligible, this non-diagonal component gives only a ten percent correction to the diagonal contribution, a finding that justifies that in this work we disregard the contributions to the decay coming from the $\Lambda\Lambda - \Sigma\Sigma$ component of the initial $\Lambda\Lambda$ wave function.

CHAPTER 6

RESULTS

The results for the non-mesonic Λ-induced, $\Lambda\Lambda \to YN$, decay rate of ${}^{6}_{\Lambda\Lambda}$He are displayed in Tables 6.1 to 6.7 and are given in terms of the free decay rate of the Λ hyperon, $\Gamma_\Lambda = 3.8 \times 10^9\, s^{-1}$. The possible final states are Λn, $\Sigma^0 n$ and $\Sigma^- p$ but, by virtue of the $\Delta I = 1/2$ rule, isospin coupling algebra relates the decay rates of the two later modes by a factor of 2. Therefore, the $\Lambda\Lambda \to \Sigma^0 n$ and $\Lambda\Lambda \to \Sigma^- p$ channels fulfil $\Gamma_{\Sigma^0 n} = \Gamma_{\Sigma N}/3$ and $\Gamma_{\Sigma^- p} = 2\Gamma_{\Sigma N}/3$, respectively, where $\Gamma_{\Sigma N}$ collects the total ΣN decay rate, which is the one quoted in the Tables. We also give the contribution of each individual meson separately, in order to asses its importance in a given transition, and we add up the contribution of the lightest pseudoscalar mesons sequentially for a better interpretation of our results.

We start by presenting in Table 6.1 the contribution to the $\Lambda\Lambda \to YN$ decay coming from the diagonal $\Lambda\Lambda - \Lambda\Lambda$ component of the initial wave function without the inclusion of final state interactions, followed by the results of Table 6.2 where these effects are considered. The strong coupling constants required to describe the $\Lambda\Lambda \to \Lambda\Lambda \to YN$ transition are taken from the Nijmegen soft-core NSC97f model [38], which has been

Table 6.1: Individual and combined meson-exchange contributions to the non-mesonic decay rate of ${}^{6}_{\Lambda\Lambda}$He, when only the diagonal $\Lambda\Lambda - \Lambda\Lambda$ component of the initial wave function is included, and in the absence of final state interactions. Results given in units of $\Gamma_\Lambda = 3.8 \times 10^9\, s^{-1}$.

Meson	**Λn**	**ΣN**
$\boldsymbol{\pi}$	-	1.94×10^{-2}
$\boldsymbol{K}$	1.45×10^{-3}	2.41×10^{-3}
$\boldsymbol{\eta}$	1.67×10^{-4}	-
$\boldsymbol{\rho}$	-	2.20×10^{-3}
$\boldsymbol{K^*}$	3.32×10^{-4}	2.73×10^{-3}
$\boldsymbol{\omega}$	3.20×10^{-4}	-
$\boldsymbol{\pi + K}$	1.45×10^{-3}	2.69×10^{-2}
$\boldsymbol{\pi + K + \eta}$	1.72×10^{-3}	2.69×10^{-2}
All	2.39×10^{-3}	4.22×10^{-2}

proved to reproduce satisfactorily the scarce YN scattering data, as well as the structure of Λ-hypernuclei and their decay properties. Consequently, the results presented in Tables 6.1 and 6.2 are obtained following the same approach as that of Ref. [35], except for minor changes in the initial $\Lambda\Lambda$ and the final YN wave functions, which have been obtained with higher precision here. Therefore, they have to be considered as benchmark results against which we can later asses the importance of the new $\Lambda\Lambda \to \Xi N \to YN$ transition explored in the present work.

Isospin conservation at the strong vertex excludes the exchange of a π or a ρ meson in the $\Lambda\Lambda \to \Lambda n$ transition presented in Table 6.1, which ignores final strong interaction effects, and this is reflected as a null contribution to the decay rate for those mesons. Instead, we find that the dominant contribution to this decay mode is coming from K exchange, with a rate of $1.45 \times 10^{-3}\Gamma_\Lambda$, corresponding to roughly 60% of the rate obtained when all mesons are considered ($\Gamma_{\Lambda n} = 2.39 \times 10^{-3}\Gamma_\Lambda$). The remaining 40% of the $\Gamma_{\Lambda n}$ rate originates from the exchange of K^*, ω and η mesons, with individual contributions which are one order of magnitude smaller than that for K exchange. Conversely, for ΣN final states, one sees a clear dominance of the π meson contribution, giving practically half of the total ΣN rate of $\Gamma_{\Sigma N} = 4.22 \times 10^{-2}\Gamma_\Lambda$. In this case, and also due to isospin

considerations, the isoscalar η and ω mesons do not contribute, so the remaining rate is provided by the K, ρ and K^* mesons with similar contributions, and again, one order of magnitude smaller. Adding the partial decay rates of the Λn, $\Sigma^0 n$ and $\Sigma^- p$ final states, one obtains a total $\Lambda\Lambda \to YN$ decay rate of $\Gamma_{YN} = 4.46 \times 10^{-2}\Gamma_\Lambda$, distributed into an almost negligible Λn contribution ($\sim 5\%$ of Γ_{YN}) in front of the ΣN one ($\sim 95\%$ of Γ_{YN}).

Table 6.2: Individual and combined meson-exchange contributions to the non-mesonic decay rate of ${}^{\ 6}_{\Lambda\Lambda}$He, when only the diagonal $\Lambda\Lambda - \Lambda\Lambda$ component of the initial wave function is included, and considering final state interactions. Results given in units of $\Gamma_\Lambda = 3.8 \times 10^9\, s^{-1}$.

Meson	**Λn**	**ΣN**
$\boldsymbol{\pi}$	1.35×10^{-4}	7.15×10^{-3}
$\boldsymbol{K}$	2.22×10^{-2}	9.69×10^{-4}
$\boldsymbol{\eta}$	8.95×10^{-4}	7.67×10^{-7}
$\boldsymbol{\rho}$	1.32×10^{-5}	2.37×10^{-6}
$\boldsymbol{K^*}$	4.28×10^{-3}	2.35×10^{-4}
$\boldsymbol{\omega}$	4.95×10^{-5}	1.42×10^{-7}
$\boldsymbol{\pi + K}$	2.17×10^{-2}	6.34×10^{-3}
$\boldsymbol{\pi + K + \eta}$	1.41×10^{-2}	6.29×10^{-3}
All	3.00×10^{-2}	5.81×10^{-3}

As mentioned before, the results of Table 6.2 also correspond to the contributions to the rate from the diagonal $\Lambda\Lambda - \Lambda\Lambda$ component of the wave function, but incorporate the effect of final state interactions, which, as can be seen, reduce the total $\Lambda\Lambda \to YN$ decay rate by about 20% to a value $\Gamma_{YN} = 3.58 \times 10^{-2}\Gamma_\Lambda$. Of special note is the contribution of K exchange to the Λn mode, which gets enhanced by one order of magnitude when final state interactions are implemented, becoming the dominant mechanism for the transition. Note also that a similar enhancement is seen for the contribution of the K^* meson, which represents the second dominant contribution, yet, one order of magnitude smaller than its pseudoscalar partner. In the case of ΣN final states, we observe that final state interactions cause a similar reduction, of about a factor 2.5, for the pseudoscalar π and K contributions, while the reduction is even larger for ρ and K^* vector meson exchange, giving rise to an overall decrease of the ΣN rate by almost one order of

magnitude. Consequently, the inclusion of final state interactions has inverted the relative importance of the decay modes, from 5% to 84% for the $\Lambda\Lambda \to \Lambda n$ channel and from 95% to 16% for the $\Lambda\Lambda \to \Sigma N$ one, increasing the value of the $\Gamma_{\Lambda n}/(\Gamma_{\Sigma^0 n} + \Gamma_{\Sigma^- p})$ ratio by more than a factor 90, from 0.06 to 5.16. Since these decay channels could, in principle, be detected separately in experiments, this ratio could be used to learn about the weak decay mechanism in the strangeness $S = -2$ sector and the role played by the strong interaction in the decay process.

Another change associated to the effect of final state interactions that can be inferred from Table 6.2 is that previously excluded meson exchanges now contribute, albeit in a very moderate manner. This is the case of the π meson, for example, which now contributes to the $\Lambda\Lambda \to \Lambda n$ decay rate through the intermediate weak $\Lambda\Lambda \to \Sigma N$ transition followed by the $\Sigma N \to \Lambda n$ strong one.

Up to this point, our results are totally in line with those found in Ref. [35], as expected, since the only essential difference here is the use of slightly different correlated baryon-baryon wave functions. The novelty of the present work is the consideration of the strong non-diagonal $\Lambda\Lambda - \Xi N$ mixing of the $\Lambda\Lambda$ wave function. However, contrary to the previous case, the new strong coupling constants required for the description of the $\Xi N \to YN$ transition do not have an experimental support. For this reason, we will compare the results obtained when these additional coupling constants are taken either from the same NSC97f model employed in the description of the diagonal $\Lambda\Lambda \to \Lambda\Lambda \to YN$ transition or from the chiral Lagrangians given in the appendix.

When the $\Lambda\Lambda \to \Xi N \to YN$ component is added to the calculations using the strong coupling constants given by the Nijmegen soft-core NSC97f model [38], we obtain the results of Table 6.4. We observe that the only significant effect of the $\Lambda\Lambda - \Xi N$ mixing to the decay into a final Λn state comes from π and K exchanges. Their combined effect ends up decreasing the decay rate by more than a factor two, from $\Gamma_{\Lambda n} = 3.00 \times 10^{-2}\Gamma_\Lambda$ to

$1.31 \times 10^{-2}\Gamma_\Lambda$. The ΣN decay channel experiences an increase of over a factor four, from $\Gamma_{\Sigma N} = 5.81 \times 10^{-3}\Gamma_\Lambda$ to $2.67 \times 10^{-2}\Gamma_\Lambda$. Altogether, the $\Lambda\Lambda - \Xi N$ component of the wave function brings the value of the $\Gamma_{\Lambda n}/(\Gamma_{\Sigma^0 n} + \Gamma_{\Sigma^- p})$ ratio to 0.49, a factor 10 times smaller than that found when this mixing is neglected. Adding the Λn, $\Sigma^0 n$ and $\Sigma^- p$ partial rates, the total $\Lambda\Lambda \to YN$ decay rate amounts to $\Gamma_{YN} = 3.98 \times 10^{-2}\Gamma_\Lambda$, which represents a modest increase of around 10% over the case that ignored the $\Lambda\Lambda - \Xi N$ piece in the initial wave function.

In order to assess the model dependence of the $\Lambda\Lambda - \Xi N$ mixing to the $\Lambda\Lambda \to YN$ decay rate, we perform another calculation which keeps the experimentally constrained NSC97f coupling constants in the description of the weak $\Lambda\Lambda \to YN$ transition but employs, for the $\Xi N \to YN$ one, the decay model developed in this work, based on effective lagrangians, which is described in the appendix. The results of this hybrid model are presented in Table 6.5. We observe that the addition of the partial rates yields a total contribution from the $\Lambda\Lambda \to YN$ decay mode of $\Gamma_{YN} = 2.55 \times 10^{-2}\Gamma_\Lambda$, which represents an overall decrease of around 30% over the rate obtained for the diagonal $\Lambda\Lambda$ channel only. Comparing the results of this hybrid model with those of Table 6.4, obtained with the strong NSC97f coupling constants, we observe a drastic reduction of almost a factor five in the Λn rate. This comes from the reduction by about a factor of two in the K-exchange rate, together with the enhancement of the π- and η-exchange contributions, with which the K-exchange one interferes destructively. The ΣN rate of the hybrid model is only 15% smaller than that of the model employing the strong NSC97f coupling constants. Within the hybrid model we can see that the interferences between the various meson-exchange contributions are such that the final decay rate for the $\Lambda\Lambda \to \Lambda n$ channel decreases a whole order of magnitude with respect to the case that ignores the $\Lambda\Lambda - \Xi N$ mixing, from $\Gamma_{\Lambda n} = 3.00 \times 10^{-2}\Gamma_\Lambda$ to $2.86 \times 10^{-3}\Gamma_\Lambda$. This is partially compensated by a major increase in the ΣN decay, from $\Gamma_{\Sigma N} = 5.81 \times 10^{-3}\Gamma_\Lambda$

to $2.27 \times 10^{-2}\Gamma_\Lambda$. Altogether, the $\Lambda\Lambda - \Xi N$ component of the wave function reduces the value of the $\Gamma_{\Lambda n}/(\Gamma_{\Sigma^0 n} + \Gamma_{\Sigma^- p})$ ratio obtained with only the diagonal $\Lambda\Lambda \to \Lambda\Lambda$ component by a factor of 40, down to a value of 0.13, further highlighting the effect of the $\Lambda\Lambda - \Xi N$ mixing in inverting the dominance with regards to the $\Lambda n/\Sigma N$ decay modes.

The effect of the $\Lambda\Lambda - \Xi N$ mixing to the $\Lambda\Lambda \to YN$ decay modes of ${}^{6}_{\Lambda\Lambda}$He is summarized in Table 6.7, where we observe that, even if it induces a small component in the wave function, this mixing can moderately modify the rate, either by increasing it in about 10% (NSC97f model) or by decreasing it in about 30% (hybrid model). A more substantial change is observed in the relative importance between the Λn and ΣN decay rates, which is inverted drastically, from a factor five in the absence of the $\Lambda\Lambda - \Xi N$ mixing to about 0.5 (NSC97f model) or 0.1 (hybrid model) when this new wave function component is considered. An exclusive measurement of the decay of ${}^{6}_{\Lambda\Lambda}$He hypernuclei into Λn and $\Sigma^- p$ final states would provide valuable information to confirm the importance of the strong interaction mixing effects in the decay mechanism, and could possibly help constraining some of the strong coupling constants involving a Ξ hyperon.

The complete two-body non-mesonic decay rate Γ of ${}^{6}_{\Lambda\Lambda}$He, contains also the processes induced by a ΛN pair and as such one may write $\Gamma = \Gamma_{\Lambda N \to NN} + \Gamma_{\Lambda\Lambda \to YN}$. The decay rate for the $\Lambda N \to NN$ channel has been computed[35] to be $\Gamma_{\Lambda N \to NN} = 0.96\Gamma_\Lambda \approx 2\Gamma\left({}^{5}_{\Lambda}\mathrm{He}\right)$. Comparing this result to those of the $\Lambda\Lambda$ induced mode calculated in the present work, one can see that the decay rate for the $\Lambda\Lambda \to YN$ transition with $\Lambda\Lambda - \Lambda\Lambda$ diagonal correlations amounts to a 3.7% of the one-nucleon induced rate $\Gamma_{\Lambda N \to NN}$, while the inclusion of the $\Lambda\Lambda - \Xi N$ mixing produces a slight increase in this percentage up to 4.1% (NSC97f model) or a decrease down to 2.6% (hybrid model).

Table 6.3: Individual and combined meson-exchange contributions to the non-mesonic decay rate of ${}^{6}_{\Lambda\Lambda}\mathrm{He}$, when only the diagonal $\Lambda\Lambda - \Lambda\Lambda$ component of the initial wave function is included, and in the absence of final state interactions (FSI) as well as considering final state interactions through the use of the NSC97f model. Results given in units of $\Gamma_\Lambda = 3.8 \times 10^9\, s^{-1}$.

1	**No FSI**			**NSC97f**		
Meson	**Λn**	**ΣN**	**Total**	**Λn**	**ΣN**	**Total**
$\boldsymbol{\pi}$	—	1.94×10^{-2}	1.94×10^{-2}	1.35×10^{-4}	7.15×10^{-3}	7.28×10^{-3}
$\boldsymbol{K}$	1.45×10^{-3}	2.41×10^{-3}	3.86×10^{-3}	2.22×10^{-2}	9.69×10^{-4}	2.32×10^{-2}
$\boldsymbol{\eta}$	1.67×10^{-4}	—	1.67×10^{-4}	8.95×10^{-4}	7.67×10^{-7}	8.95×10^{-4}
$\boldsymbol{\rho}$	—	2.20×10^{-3}	2.20×10^{-3}	1.32×10^{-5}	2.37×10^{-6}	1.56×10^{-5}
$\boldsymbol{K^*}$	3.32×10^{-4}	2.73×10^{-3}	3.06×10^{-3}	4.28×10^{-3}	2.35×10^{-4}	4.51×10^{-3}
$\boldsymbol{\omega}$	3.20×10^{-4}	—	3.20×10^{-4}	4.95×10^{-5}	1.42×10^{-7}	4.97×10^{-5}
$\boldsymbol{\pi + K}$	1.45×10^{-3}	2.69×10^{-2}	2.84×10^{-2}	2.17×10^{-2}	6.34×10^{-3}	2.80×10^{-2}
$\boldsymbol{\pi + K + \eta}$	1.72×10^{-3}	2.69×10^{-2}	2.86×10^{-2}	1.41×10^{-2}	6.29×10^{-3}	2.04×10^{-2}
All	2.39×10^{-3}	4.22×10^{-2}	4.46×10^{-2}	3.00×10^{-2}	5.81×10^{-3}	3.58×10^{-2}

Table 6.4: Individual and combined meson-exchange contributions to the non-mesonic decay rate of ${}^{6}_{\Lambda\Lambda}$He, considering final state interactions and both components of the initial wave function, $\Lambda\Lambda - \Lambda\Lambda$ and $\Lambda\Lambda - \Xi N$. The results, given in units of $\Gamma_\Lambda = 3.8 \times 10^9\, s^{-1}$, have been obtained using the strong NSC97f model.

Meson	**Λn**	**ΣN**
$\boldsymbol{\pi}$	3.65×10^{-4}	5.85×10^{-3}
$\boldsymbol{K}$	1.13×10^{-2}	1.37×10^{-2}
$\boldsymbol{\eta}$	8.62×10^{-4}	1.41×10^{-4}
$\boldsymbol{\rho}$	1.31×10^{-5}	1.86×10^{-6}
$\boldsymbol{K^*}$	4.27×10^{-3}	2.31×10^{-4}
$\boldsymbol{\omega}$	4.85×10^{-5}	1.36×10^{-7}
$\boldsymbol{\pi + K}$	7.87×10^{-3}	1.97×10^{-2}
$\boldsymbol{\pi + K + \eta}$	3.66×10^{-3}	2.28×10^{-2}
All	1.31×10^{-2}	2.67×10^{-2}

Table 6.5: Individual and combined meson-exchange contributions to the non-mesonic decay rate of ${}^{6}_{\Lambda\Lambda}$He, considering final state interactions and both $\Lambda\Lambda - \Lambda\Lambda$ and $\Lambda\Lambda - \Xi N$ components of the initial wave function The results, given in units of $\Gamma_\Lambda = 3.8 \times 10^9\, s^{-1}$, have been obtained using the hybrid model discussed in the appendix.

Meson	**Λn**	**ΣN**
$\boldsymbol{\pi}$	9.73×10^{-4}	5.87×10^{-3}
$\boldsymbol{K}$	5.15×10^{-3}	9.54×10^{-3}
$\boldsymbol{\eta}$	2.08×10^{-3}	1.77×10^{-4}
$\boldsymbol{\rho}$	1.31×10^{-5}	1.95×10^{-6}
$\boldsymbol{K^*}$	4.27×10^{-3}	2.32×10^{-4}
$\boldsymbol{\omega}$	4.85×10^{-5}	1.36×10^{-7}
$\boldsymbol{\pi + K}$	1.86×10^{-3}	1.63×10^{-2}
$\boldsymbol{\pi + K + \eta}$	3.75×10^{-4}	1.93×10^{-2}
All	2.86×10^{-3}	2.27×10^{-2}

Table 6.6: Individual and combined meson-exchange contributions to the non-mesonic decay rate of ${}^{6}_{\Lambda\Lambda}\mathrm{He}$, considering final state interactions and both $\Lambda\Lambda - \Lambda\Lambda$ and $\Lambda\Lambda - \Xi N$ components of the initial wave function The results, given in units of $\Gamma_\Lambda = 3.8 \times 10^9 s^{-1}$, have been obtained using the NSC97f model as well as the hybrid model discussed in the appendix.

Meson	**NSC97f**			**Hybrid model**		
	ΛN	**ΣN**	**Total**	**ΛN**	**ΣN**	**Total**
π	3.65×10^{-4}	5.85×10^{-3}	6.22×10^{-3}	9.73×10^{-4}	5.87×10^{-3}	6.84×10^{-3}
K	1.13×10^{-2}	1.37×10^{-2}	2.51×10^{-2}	5.15×10^{-3}	9.54×10^{-3}	1.47×10^{-2}
η	8.62×10^{-4}	1.41×10^{-4}	1.00×10^{-3}	2.08×10^{-3}	1.77×10^{-4}	2.25×10^{-3}
ρ	1.31×10^{-5}	1.86×10^{-6}	1.50×10^{-5}	1.31×10^{-5}	1.95×10^{-6}	1.51×10^{-5}
K^*	4.27×10^{-3}	2.31×10^{-4}	4.50×10^{-3}	4.27×10^{-3}	2.32×10^{-4}	4.50×10^{-3}
ω	4.85×10^{-5}	1.36×10^{-7}	4.86×10^{-5}	4.85×10^{-5}	1.36×10^{-7}	4.86×10^{-5}
$\pi + K$	7.87×10^{-3}	1.97×10^{-2}	2.76×10^{-2}	1.86×10^{-3}	1.63×10^{-2}	1.82×10^{-2}
$\pi + K + \eta$	3.66×10^{-3}	2.28×10^{-2}	2.64×10^{-2}	3.75×10^{-4}	1.93×10^{-2}	1.96×10^{-2}
All	1.31×10^{-2}	2.67×10^{-2}	3.98×10^{-2}	2.86×10^{-3}	2.27×10^{-2}	2.55×10^{-2}

Table 6.7: Total $\Lambda\Lambda \to YN$ contribution to the weak decay rate of ${}^{6}_{\Lambda\Lambda}\mathrm{He}$ and ratio $\Gamma_{\Lambda n}/(\Gamma_{\Sigma^0 n} + \Gamma_{\Sigma^- p})$, considering only the diagonal component of the $\Lambda\Lambda$ wave function and including also the $\Lambda\Lambda - \Xi N$ mixing employing two different models. The rates are given in units of $\Gamma_\Lambda = 3.8 \times 10^9\, s^{-1}$.

Model		Γ_{YN}	$\Gamma_{\Lambda n}/\Gamma_{\Sigma N}$
$\Lambda\Lambda \to \Lambda\Lambda \to YN$		3.58×10^{-2}	5.2
$\Lambda\Lambda \to \Lambda\Lambda \to YN$ $\Lambda\Lambda \to \Xi N \to YN$	(NSC97f)	3.98×10^{-2}	0.49
$\Lambda\Lambda \to \Lambda\Lambda \to YN$ $\Lambda\Lambda \to \Xi N \to YN$	(Hybrid)	2.55×10^{-2}	0.13

CHAPTER 7

CONCLUSIONS

Historically strange systems have been used as a framework for the study of the weak interaction through their leptonic and non-leptonic decay modes. This function is still relevant today, as new technological advances allow for the production of ever increasingly heavier and stranger nuclei.

Indeed the field of experimental strangeness physics is in its heyday, as new proposals for experiments to be carried out at beamlines around the world are discussed yearly. Just last year at J-PARC several experiments were submitted for approval, including: Decay Pion Spectroscopy of ${}^{5}_{\Lambda\Lambda}$H produced by Ξ-hypernuclear Decay[82], Direct measurement of the ${}^{3}_{\Lambda}$H and ${}^{4}_{\Lambda}$H lifetimes using ^{3,4}He $(\pi^-, K^0)^{3,4}_{\Lambda}$H reactions[83] and ${}^{3}_{\Lambda}$H and ${}^{4}_{\Lambda}$H mesonic weak decay lifetime measurement with ^{3,4}He $(K^-, \pi^0)^{3,4}_{\Lambda}$H reaction[84], with more proposals to be submitted in the following months.

Since previous studies of double-Λ hypernuclei decay only included the channels induced by either the ΛN, ΣN or ΛΛ pairs, it became necessary to evaluate the contribution of additional decay modes that arise from the complete consideration of the strong interaction. The microscopic resolution of G-Matrix and T-Matrix equations using

up-to-date and realistic baryon-baryon potentials for the initial and final two-body states respectively, yielded the coupled wave function for the initial $\Lambda\Lambda$ system, which includes $\Lambda\Lambda$, ΞN and $\Sigma\Sigma$ components, as well as for the final hyperon-nucleon wave function, with ΛN and ΣN components, and nucleon-nucleon wave functions.

The first step in this endeavour was the inclusion of the channel induced by the ΞN pair, which has a lower energy threshold than the $\Sigma\Sigma$ one. In order to accomplish this, the two-body potential that governs the ΞN interaction with a change in strangeness of one unit had to be constructed, in order to include it in the computation of the decay of ${}^{\ \ 6}_{\Lambda\Lambda}$He. This potential is based on a meson exchange model which includes the fundamental states of the pseudoscalar and vector meson octets.

The inclusion of the weak transitions corresponding to the Ξ^0n and Ξ^-p intermediate states required the calculation of new coupling constants, which have been derived using chiral Lagrangians and SU(3) flavour symmetry (extended to S(6) flavour-spin symmetry for vector mesons). Additionally, the new transitions that appeared in the isotopic spin space also demanded the construction of new operational structures.

This research and calculation undertaking has been paired with a programming effort, modifying existing FORTRAN code in order to implement in a clear and concise manner all the fragments involved in the computation of the decay rate when the $\Xi\text{N} \rightarrow \text{YN}$ transition is included. A by-product of this refinement is a better interpretation of the underlying physics present in the code, as well as an improvement to the modularity of the program which translates into a greater degree of future-proofing by increasing the flexibility regarding the modification of the elements that are involved in the calculation and paving the way for the incorporation of new ones, such as the weak $\Sigma\Sigma \rightarrow \text{YN}$ channel.

Certainly, regardless of the actual results for the decay rate, the tool developed in this work will provide an easy, fast and reliable way to study the decay of hypernuclei

within a one-meson-exchange model either by allowing a somewhat on-the-fly swapping of coupling constants or by opening the possibility of adding new decay modes to the overall calculation.

As a preceding step to the outright calculation, we have chosen to update our results for the $(\Lambda\Lambda - \Lambda\Lambda) \rightarrow$ YN decay channel using amended wave functions in order to assess the validity of the modifications introduced in the main program and its subroutines. As was to be expected, the obtained results fall in line with previous ones barring some minor discrepancies originating from the use of newer wave functions.

Once everything has been put together one can consider the impact that the inclusion of the strong non-diagonal $\Lambda\Lambda - \Xi$N component of the $\Lambda\Lambda$ wave function has on the decay rate. Not only that, but one can go one step further and consider also possible variations on the results produced by the use of different models for the derivation of the additional coupling constants. In our case we have chosen to keep the coupling constants derived from the NSC97f model that has already been used for the description of the diagonal $(\Lambda\Lambda - \Lambda\Lambda) \rightarrow$ YN transition while implementing the ones derived from the chiral Lagrangians discussed throughout this thesis for the $(\Lambda\Lambda - \Xi N) \rightarrow$ YN channel.

For the direct decay induced by the $\Lambda\Lambda - \Lambda\Lambda$ component of the wave function and disregarding final state interactions for the moment, one finds that the dominant meson-exchange contribution leading to final Λn states is that of the kaon with a rate of $1.45 \times 10^{-3}\Gamma_\Lambda$, with the following three allowed contributions (K^*, ω and η exchanges) amounting to a 40% of the $\Gamma_{\Lambda n}$ rate. In contrast, the leading contribution for ΣN final states is that of the π meson, adding up to half of the total $\Gamma_{\Sigma N} = 4.22 \times 10^{-2}\Gamma_\Lambda$ rate. Comparing these rates one finds that the ΣN final state dominates the total decay rate, contributing at the 95% level.

When one considers the inclusion of final state interactions to the rate induced by the diagonal $\Lambda\Lambda - \Lambda\Lambda$ components of the wave function, it can be immediately seen that

the total rate is reduced by about 20% to a value of $\Gamma_{YN} = 3.58 \times 10^{-2}\Gamma_{\Lambda}$. This inclusion produces an enhancement of the K and K^* contributions to the Λn final state while inhibiting the π, K, K^* and ρ contributions to the ΣN final states, giving rise to an inversion of the relative importance of the partial decay modes, with the $\Lambda\Lambda \rightarrow \Lambda n$ now amounting to a 84% of the total decay rate.

Including the $(\Lambda\Lambda - \Xi N) \rightarrow YN$ wave function component to the calculations and using the strong coupling constants given by the Nijmegen soft-core NSC97f model yields a small effect in the Λn decay rate chiefly through the modification of the π and K exchanges. This combined effect ends up decreasing the decay rate by more than a factor of two, down to $\Gamma_{\Lambda n} = 1.31 \times 10^{-2}\Gamma_{\Lambda}$. Comparatively the decay rate to the ΣN channel experiences an increase up to $\Gamma_{\Sigma N} = 2.67 \times 10^{-2}\Gamma_{\Lambda}$. Adding these partial rates gives $\Gamma_{YN} = 3.98 \times 10^{-2}\Gamma_{\Lambda}$, a 10% increase with respect to to the case without the $\Lambda\Lambda - \Xi N$ component of the wave function.

A second calculation has been performed, this time substituting the strong coupling constants needed for the evaluation of the $(\Lambda\Lambda - \Xi N) \rightarrow YN$ transition with the ones obtained using the decay model developed in this work while keeping the experimentally constrained NSC97f constants describing the $\Lambda\Lambda \rightarrow YN$ transition. Through the use of this hybrid model the total contribution to the rate from the $\Lambda\Lambda \rightarrow YN$ decay mode is of $\Gamma_{YN} = 2.55 \times 10^{-2}\Gamma_{\Lambda}$, a 30% decrease with respect to the consideration of only the diagonal component of the wave function, $(\Lambda\Lambda - \Lambda\Lambda) \rightarrow YN$.

The effect of the $\Lambda\Lambda - \Xi N$ baryon mixing on the $\Lambda\Lambda \rightarrow YN$ decay rate of ${}^{6}_{\Lambda\Lambda}\mathrm{He}$ can either be to increase it by about 10% in the case where the NSC97f model is used, or to decrease it by about 30% when dealing with the hybrid model. The relative importance between the Λn and ΣN decay rates is inverted drastically, from a factor five in the absence of the $\Lambda\Lambda - \Xi N$ mixing to about 0.5 with the NSC97f model or 0.1 using the hybrid model.

The major takeaway is that despite the effect introduced by the inclusion of additional strong states in the decay into the ΛN and ΣN final states being small, it is nonetheless distinguishable. Specifically measurements of the ${}^{6}_{\Lambda\Lambda}\mathrm{He}$ decay would provide much needed insight into the importance of the strong interaction mixing effects and would be useful in confining fundamental physics in different sectors leading to the baryon-baryon-meson coupling constants involving a Ξ hyperon, and constraining which model is best suited for the description of strangeness-changing decays. Prospectively, the inclusion of the $\Sigma\Sigma$ intermediate states will contribute further to our understanding of the physics involved in the strangeness $S = -2$ decay reactions and would require, analogously to the ΞN states, the derivation of new coupling constants and isospin operators.

APPENDIX A

PRACTICAL CASE - THE $\Lambda\Xi^0 \xrightarrow{\pi^0} \Lambda n$ DECAY

In order to improve the understanding of the procedure followed to obtain the coupling constants used in the calculation of the hypernuclear decay rate, the transition from a $\Xi^0 n$ to a Λn final state through the exchange of a π^0 meson will be studied in detail.

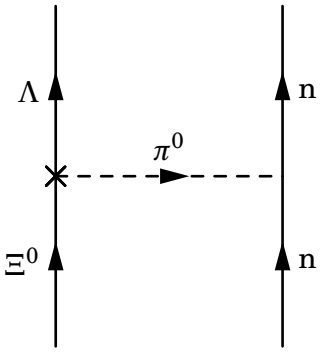

Figure A.1: Diagrammatic representation of the decay. Weak vertex denoted by a cross.

A.1 Strong Vertex

Since only the baryon-baryon-meson vertex is of interest the relevant terms of the Lagrangian (Eq. (4.52) from the relevant section of the main text) are:

$$\mathscr{L}^S_{BB\phi} = D\,\mathrm{Tr}\left[\overline{B}\gamma^\mu\gamma_5\{u_\mu, B\}\right] + F\,\mathrm{Tr}\left[\overline{B}\gamma^\mu\gamma_5[u_\mu, B]\right]. \tag{A.1}$$

where F and D are the octet baryon to meson couplings, γ^μ are the Dirac matrices and B ($\overline{B^i_j} = (B^j_i)^\dagger\gamma_4$) is the matrix representing the inbound (outbound) baryons. The dependence on the meson fields is contained in the u_μ operator:

$$u_\mu = \frac{i}{2}\left(u\partial_\mu u^\dagger - u^\dagger\partial_\mu u\right), \tag{A.2}$$

where u is defined as $u = \mathrm{e}^{i\frac{\phi}{\sqrt{2}f_\pi}}$ which may be expanded and truncated to first order in order to account for the exchange of a single meson:

$$u \simeq 1 + i\frac{1}{\sqrt{2}f_\pi}\phi, \tag{A.3}$$

with f_π the pion decay constant, and ϕ the selfadjoint matrix of inbound pseudoscalar mesons.

Thinking in terms of an inbound baryon and meson the strong vertex is $n\pi^0 \to n$. This gives the following baryon and meson matrices:

$$B = \begin{pmatrix} 0 & 0 & 0 \\ 0 & 0 & n \\ 0 & 0 & 0 \end{pmatrix}, \overline{B} = \begin{pmatrix} 0 & 0 & 0 \\ 0 & 0 & 0 \\ 0 & \overline{n} & 0 \end{pmatrix}, \phi = \begin{pmatrix} \frac{1}{\sqrt{2}}\pi^0 & 0 & 0 \\ 0 & -\frac{1}{\sqrt{2}}\pi^0 & 0 \\ 0 & 0 & 0 \end{pmatrix}. \tag{A.4}$$

The first step in the calculation is computing the value for u_μ, for which we need u as a prerequisite. This yields:

$$u = 1 + \begin{pmatrix} \frac{1}{2f_\pi}\pi^0 & 0 & 0 \\ 0 & -\frac{1}{2f_\pi}\pi^0 & 0 \\ 0 & 0 & 0 \end{pmatrix}, \tag{A.5}$$

which translates into a u_μ value of

$$u_\mu = \frac{i}{2}\left(u\partial_\mu u^\dagger - u^\dagger \partial_\mu u\right) = \begin{pmatrix} \frac{\partial_\mu \pi^0}{2f_\pi} & 0 & 0 \\ 0 & -\frac{\partial_\mu \pi^0}{2f_\pi} & 0 \\ 0 & 0 & 0 \end{pmatrix}. \tag{A.6}$$

Thus, the value for the commutator and the anti-commutator terms are:

$$\mathrm{Tr}\left[\overline{B}\gamma^\mu\gamma_5\{u_\mu, B\}\right] = \mathrm{Tr}\left[\overline{B}\gamma^\mu\gamma_5[u_\mu, B]\right] = -\frac{n\overline{n}\partial_\mu\pi^0}{2f_\pi}, \tag{A.7}$$

which in turn yields the following strong vertex:

$$g_S = -\frac{D+F}{2f_\pi} \tag{A.8}$$

A.2 Weak Vertex

A.2.1 Parity Violating

The parity violating amplitudes can be obtained using the weak Lagrangian at lowest order (Eq. (4.54) in the main text):

$$\mathscr{L}^W_{BB\phi} = \sqrt{2}\left(h_D\,\mathrm{Tr}\left[\overline{B}\left\{\xi^\dagger h\xi, B\right\}\right] + h_F\,\mathrm{Tr}\left[\overline{B}\left[\xi^\dagger h\xi, B\right]\right]\right), \tag{A.9}$$

written in terms of the dimensionless constants h_D and h_F, which can be fitted to reproduce known meson decay amplitudes and the s-wave non-leptonic weak decays of the baryon octet members [68]. The h operator is a 3×3 matrix with a single non-zero element, $h_{23} = 1$, which accounts for strangeness variations of $|\Delta S| = 1$. The operator ξ plays a role equivalent to the one of the u operator in the strong Lagrangian.

For this particular decay the weak vertex may be written as $\Xi^0\pi^0 \to \Lambda$, which means the incoming (B) and outgoing ($\overline{B}$) baryon and meson matrices will be:

$$B = \begin{pmatrix} 0 & 0 & 0 \\ 0 & 0 & 0 \\ 0 & \Xi^0 & 0 \end{pmatrix}, \overline{B} = \begin{pmatrix} \frac{1}{\sqrt{6}}\overline{\Lambda} & 0 & 0 \\ 0 & \frac{1}{\sqrt{6}}\overline{\Lambda} & 0 \\ 0 & 0 & -\sqrt{\frac{2}{3}}\overline{\Lambda} \end{pmatrix}, \phi = \begin{pmatrix} \frac{1}{\sqrt{2}}\pi^0 & 0 & 0 \\ 0 & -\frac{1}{\sqrt{2}}\pi^0 & 0 \\ 0 & 0 & 0 \end{pmatrix}. \tag{A.10}$$

The $\xi^\dagger h \xi$ term is:

$$\xi^\dagger h \xi = h - \frac{i}{\sqrt{2}f}\phi^\dagger h + \frac{i}{\sqrt{2}f} h\phi = \begin{pmatrix} 0 & 0 & 0 \\ 0 & 1+\frac{i\pi^0}{2f} & 0 \\ 0 & 0 & 0 \end{pmatrix}. \tag{A.11}$$

Consequently the commutator and anti-commutator traces are:

$$Tr\left[\overline{B}\left\{\xi^\dagger h \xi, B\right\}\right] = -\frac{\Xi^0\overline{\Lambda}\left(2f + i\pi^0\right)}{2\sqrt{6}f} \tag{A.12}$$

$$\mathrm{Tr}\left[\overline{B}\left[\xi^\dagger h \xi, B\right]\right] = -\frac{\sqrt{3}\Xi^0\overline{\Lambda}\left(2f + i\pi^0\right)}{2\sqrt{2}f} \tag{A.13}$$

Thus, the Lagrangian for this vertex:

$$\mathscr{L} = -\frac{(h_D - 3h_F)\Xi^0\overline{\Lambda}\left(2f + i\pi^0\right)}{2\sqrt{3}f} \tag{A.14}$$

A.2.2 Parity Conserving

As discussed in Section 2.2.2 parity conserving amplitudes cannot be obtained through the use of a weak effective Lagrangian. As such, one may use the pole model in order to extract these coupling constants. The decay, then, may be decomposed into a series of baryon-pole diagrams:

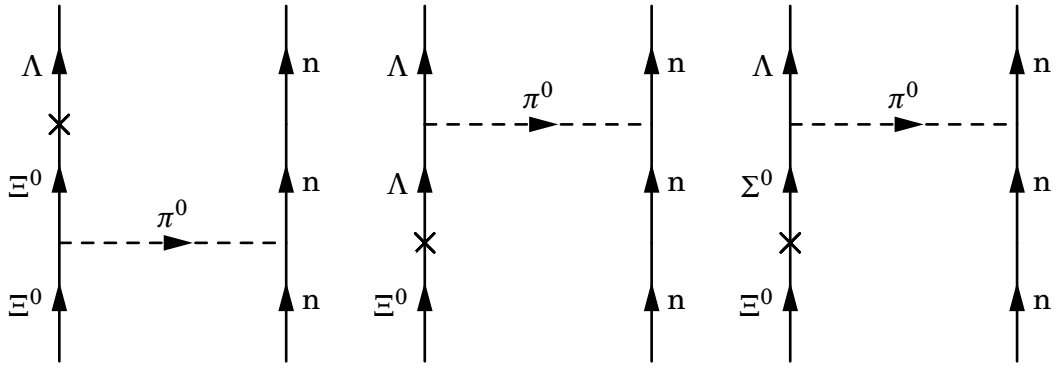

Figure A.2: Baryon-pole model diagrams for the $\Xi^0 n \to \Lambda n$ transition

yields the following expression for the vertex:

$$g^{W}_{\Xi^0\pi^0\overline{\Lambda}} = G_{\Xi^0\Xi^0\pi^0}\frac{1}{m_\Lambda - m_{\Xi^0}}A_{\Xi^0\Lambda} + G_{\Lambda\Lambda\pi^0}\frac{1}{m_{\Xi^0} - m_\Lambda}A_{\Xi^0\Lambda} + G_{\Lambda\Sigma^0\pi^0}\frac{1}{m_{\Xi^0} - m_{\Sigma^0}}A_{\Xi^0\Sigma^0} \tag{A.15}$$

where $G_{B'B\phi}$ correspond to the baryon-baryon-meson ($B'B\phi$) coupling constants obtained from the strong Lagrangian in Eq. (A.1).

For the calculation of the weak pole vertices it is necessary to express the physical states in terms of the baryon octet fields $|B_i\rangle$, as well as the meson states in terms of $|M_i\rangle$[74]. Furthermore, the mesonless weak transition between baryons, $\langle B|H_W(0)|B'\rangle$, can be computed using low-energy theorems for mesons. These theorems express the matrix element for the emission of a meson of zero (or small) four-momentum in terms of the corresponding matrix element in the absence of the soft meson and some equal-time commutators of currents[75]. Therefore, we will be able to relate the strong scattering amplitudes to the weak vertices,

$$\lim_{q\to 0}\langle B \xrightarrow{PV} B'M_i\rangle = \lim_{q\to 0}\langle B'M_i|H_{PV}|B\rangle = -\frac{i}{f_\pi}\langle B'|[F_i, H_6]|B\rangle, \tag{A.16}$$

where, following Cabibbo's theory, we have assumed that the weak hamiltonian transforms like the sixth component of an octet, H_6, according to the CP invariance of $H_W^{\Delta S=1}$, and F_i are the corresponding $SU(3)$ generators.

To compute the last term of Eq. (A.16), one can use the completely antisymmetric, f_{ijk}, and symmetric, d_{ijk}, SU(3) coefficients[76] to express the action of the F_i generator on a baryon field,

$$F_i|B_j\rangle = if_{ijk}|B_k\rangle, \tag{A.17}$$

and the weak transition between baryon fields in terms of two reduced matrix elements, A and B,

$$\langle B_k|H_6|B_j\rangle = iAf_{6jk} + Bd_{6jk}, \tag{A.18}$$

which can be determined by a fit to experimental data for specific parity violating transitions, for which we choose the $\Sigma^+ \to p + \pi^0$ ($A_{\Sigma^+ p}$) and $\Lambda \to p + \pi^-$ ($A_{\Lambda p}$) processes,

$$A_{\Sigma^+ p} = \frac{i}{4 f_\pi}(B - A), \tag{A.19}$$

$$A_{\Lambda p} = -\frac{i}{f_\pi}\frac{-3A - B}{4\sqrt{3}}. \tag{A.20}$$

Combining these expressions, we obtain:

$$-\frac{i}{f_\pi}A = A_{\Sigma^+ p} - \sqrt{3}A_{\Lambda p}, \tag{A.21}$$

$$-\frac{i}{f_\pi}B = -\sqrt{3}A_{\Lambda p} - 3A_{\Sigma^+ p}. \tag{A.22}$$

Let us start with the $A_{\Xi^0\Lambda}$ weak transition:

$$\begin{aligned} A_{\Xi^0\Lambda} = \langle \Lambda\pi^0 \,|\, H_{PV} \,|\, \Xi^0\rangle &= \langle B_8 M_3 \,|\, H_{PV} \,|\, \frac{1}{\sqrt{2}}(|\, B_6\rangle - i \,|\, B_7\rangle)\\ &= \frac{1}{\sqrt{2}}[\langle B_8 M_3 \,|\, H_{PV} \,|\, B_6\rangle - i\langle B_8 M_3 \,|\, H_{PV} \,|\, B_7\rangle]\\ &= -\frac{i}{F_\pi}\frac{1}{\sqrt{2}}[\langle B_8 \,|\, [F_3, H_6] \,|\, B_6\rangle - i\langle B_8 \,|\, [F_3, H_6] \,|\, B_7\rangle]. \end{aligned} \tag{A.23}$$

The commutator terms are:

$$\begin{aligned} \langle B_8 \,|\, [F_3, H_6] \,|\, B_6\rangle &= \langle B_8 \,|\, F_3 H_6 \,|\, B_6\rangle - \langle B_8 \,|\, H_6 F_3 \,|\, B_6\rangle\\ &= \frac{i}{2}\langle B_8 \,|\, H_6 \,|\, B_7\rangle = \frac{i}{2}(iAf_{678} + Bd_{678}) = -\frac{\sqrt{3}}{4}A, \end{aligned} \tag{A.24}$$

$$\begin{aligned} \langle B_8 \,|\, [F_3, H_6] \,|\, B_7\rangle &= \langle B_8 \,|\, F_3 H_7 \,|\, B_6\rangle - \langle B_8 \,|\, H_6 F_3 \,|\, B_7\rangle\\ &= -\frac{i}{2}\langle B_8 \,|\, H_6 \,|\, B_6\rangle = -\frac{i}{2}(iAf_{668} + Bd_{668}) = \frac{i}{4\sqrt{3}}B, \end{aligned} \tag{A.25}$$

which once introduced into the main expression yield:

$$A_{\Xi^0\Lambda} = -\frac{i}{F_\pi}\frac{-3A + B}{4\sqrt{6}} = \frac{1}{2\sqrt{2}}\left[A_{\Lambda p} - \sqrt{3}A_{\Sigma p}\right]. \tag{A.26}$$

For the other weak transition, $A_{\Xi^0\Sigma^0}$:

$$\begin{aligned} A_{\Xi^0\Sigma^0} &= \langle \Sigma^0\pi^0 \mid H_{PV} \mid \Xi^0\rangle = \langle B_3 M_3 \mid H_{PV} \mid \frac{1}{\sqrt{2}}(\mid B_6\rangle - i \mid B_7\rangle) \\ &= \frac{1}{\sqrt{2}}[\langle B_3 M_3 \mid H_{PV} \mid B_6\rangle - i\langle B_3 M_3 \mid H_{PV} \mid B_7\rangle] \\ &= -\frac{i}{F_\pi}\frac{1}{\sqrt{2}}[\langle B_3 \mid [F_3, H_6] \mid B_6\rangle - i\langle B_3 \mid [F_3, H_6] \mid B_7\rangle], \end{aligned} \tag{A.27}$$

$$\begin{aligned} \langle B_3 \mid [F_3, H_6] \mid B_6\rangle &= \langle B_3 \mid F_3 H_6 \mid B_6\rangle - \langle B_3 \mid H_6 F_3 \mid B_6\rangle \\ &= \frac{i}{2}\langle B_3 \mid H_6 \mid B_7\rangle = \frac{i}{2}(iAf_{673} + Bd_{673}) = \frac{1}{4}A, \end{aligned} \tag{A.28}$$

$$\begin{aligned} \langle B_3 \mid [F_3, H_6] \mid B_7\rangle &= \langle B_3 \mid F_3 H_7 \mid B_6\rangle - \langle B_3 \mid H_6 F_3 \mid B_7\rangle \\ &= -\frac{i}{2}\langle B_3 \mid H_6 \mid B_6\rangle = -\frac{i}{2}(iAf_{663} + Bd_{663}) = \frac{i}{4}B. \end{aligned} \tag{A.29}$$

Thus we obtain:

$$A_{\Xi^0\Sigma^0} = -\frac{i}{F_\pi}\frac{A+B}{4\sqrt{2}} = -\frac{1}{2\sqrt{2}}\left[\sqrt{3}A_{\Lambda p} + A_{\Sigma p}\right]. \tag{A.30}$$

APPENDIX B

CONVENTIONS: SU(3) COEFFICIENTS

The values for the SU(3) structure constants[85] used in the soft-meson reduction theorem calculations are collected in Table B.1 of this appendix.

Table B.1: Non-zero SU(3) coefficients

ijk	f_{ijk}	**ijk**	d_{ijk}
123	1	118	$\sqrt{\frac{1}{3}}$
147	$\frac{1}{2}$	146	$\frac{1}{2}$
156	$-\frac{1}{2}$	157	$\frac{1}{2}$
246	$\frac{1}{2}$	228	$\sqrt{\frac{1}{3}}$
257	$\frac{1}{2}$	247	$-\frac{1}{2}$
345	$\frac{1}{2}$	256	$\frac{1}{2}$
367	$-\frac{1}{2}$	338	$\sqrt{\frac{1}{3}}$
458	$\frac{1}{2}\sqrt{3}$	344	$\frac{1}{2}$
678	$\frac{1}{2}\sqrt{3}$	355	$\frac{1}{2}$
		366	$-\frac{1}{2}$
		377	$-\frac{1}{2}$
		448	$-\frac{1}{2\sqrt{3}}$
		558	$-\frac{1}{2\sqrt{3}}$
		668	$-\frac{1}{2\sqrt{3}}$
		778	$-\frac{1}{2\sqrt{3}}$
		888	$-\sqrt{\frac{1}{3}}$

BIBLIOGRAPHY

[1] F. HALZEN AND A. D. MARTIN, *Quarks and Leptons: an introductory course in modern particle physics* (Wiley and Sons, New York, USA, 1984), ISBN 0471887412, 9780471887416.

[2] A. PARREÑO, A. RAMOS, C. BENNHOLD, AND K. MALTMAN, *Violation of the ΔI=1/2 rule in the nonmesonic weak decay of hypernuclei*, Physics Letters B, 435(1), (1998), pp. 1 – 8, ISSN 0370-2693.

[3] S. KANATSUKI ET AL., *Spectroscopic Study of S = -2 Hypernuclei with a New Spectrometer S - 2S*, JPS Conf. Proc., 8, (2015), p. 021018.

[4] K. NAKAZAWA, Y. ENDO, K. HOSHINO, H. ITO ET AL., *Study of Double-strangeness Nuclear Systems with Nuclear Emulsion*, Physics Procedia, 80, (2015), pp. 69 – 73, ISSN 1875-3892.

[5] J. K. AHN ET AL., *Double-Λ hypernuclei observed in a hybrid emulsion experiment*, Phys. Rev., C88(1), (2013), p. 014003.

[6] K. NAKAZAWA, Y. ENDO, S. FUKUNAGA, K. HOSHINO ET AL., *The first evidence of a deeply bound state of Ξ^--^{14} N system*, Progress of Theoretical and Experimental Physics, 2015(3), (2015), p. 033D02.

[7] T. T. SUN, E. HIYAMA, H. SAGAWA, H. J. SCHULZE ET AL., *Mean field approaches*

for Ξ^- hypernuclei and current experimental data, Phys. Rev., C94(6), (2016), p. 064319.

[8] I. VIDAÑA, *Hyperons in Neutron Stars*, Journal of Physics: Conference Series, 668, (2016), p. 012031.

[9] N. CHAMEL, P. HAENSEL, J. L. ZDUNIK, AND A. F. FANTINA, *On the Maximum Mass of Neutron Stars*, Int. J. Mod. Phys., E22, (2013), p. 1330018.

[10] L. TOLOS, M. CENTELLES, AND A. RAMOS, *The Equation of State for the Nucleonic and Hyperonic Core of Neutron Stars*, Publ. Astron. Soc. Austral., 34, (2017), p. e065.

[11] E. HIYAMA, M. KAMIMURA, K. MIYAZAKI, AND T. MOTOBA, *γ transitions in $A = 7$ hypernuclei and a possible derivation of hypernuclear size*, Phys. Rev. C, 59, (1999), pp. 2351–2360.

[12] T. AKAISHI AND K. HAGINO, *Reaction cross sections of hypernuclei and the shrinkage effect*, Phys. Rev. C, 88, (2013), p. 047603.

[13] A. PARREÑO, *Weak Decays of Hypernuclei*, pp. 141–189 (Springer Berlin Heidelberg, Berlin, Heidelberg, 2007), ISBN 978-3-540-72039-3.

[14] E. OSET AND A. RAMOS, *Weak decay of Λ hypernuclei*, Prog. Part. Nucl. Phys., 41, (1998), pp. 191–253.

[15] W. M. ALBERICO AND G. GARBARINO, *Weak decay of Λ hypernuclei*, Phys. Rept., 369, (2002), pp. 1–109.

[16] E. BOTTA, T. BRESSANI, AND G. GARBARINO, *Strangeness nuclear physics: a critical review on selected topics*, Eur. Phys. J., A48, (2012), p. 41.

[17] S. AJIMURA ET AL., *Polarization of ${}^{5}_{\Lambda}$He produced by the (π^+, K^+) reaction*, Phys. Rev. Lett., 80, (1998), pp. 3471–3474.

[18] O. HASHIMOTO ET AL., *Proton Energy Spectra in the Nonmesonic Weak Decay of ${}^{12}_{\Lambda}$C and ${}^{28}_{\Lambda}$Si Hypernuclei*, Phys. Rev. Lett., 88, (2002), p. 042503.

[19] J. H. KIM ET AL., *Neutron energy spectra from the nonmesonic weak decay of ${}^{12}_{\Lambda}$C and ${}^{89}_{\Lambda}$Y hypernuclei*, Phys. Rev., C68, (2003), p. 065201.

[20] S. OKADA ET AL., *Neutron and proton energy spectra from the non-mesonic weak decays of ${}^{5}_{\Lambda}$He and ${}^{12}_{\Lambda}$C*, Phys. Lett., B597, (2004), pp. 249–256.

[21] M. AGNELLO ET AL., *Neutron-proton coincidences from Non-Mesonic Weak Decay of p-shell Λ-hypernuclei and determination of the two-nucleon induced process*, Phys. Lett., B701, (2011), pp. 556–561.

[22] M. AGNELLO ET AL., *First determination of the one-proton induced Non-Mesonic Weak Decay width of p-shell Λ-Hypernuclei*, Phys. Lett., B738, (2014), pp. 499–504.

[23] E. BOTTA, T. BRESSANI, S. BUFALINO, AND A. FELICIELLO, *Status and perspectives of experimental studies on hypernuclear weak decays*, Riv. Nuovo Cim., 38(9), (2015), pp. 387–448.

[24] A. PARRENO, A. RAMOS, AND C. BENNHOLD, *The Weak decay of hypernuclei*, Phys. Rev., C56, (1997), pp. 339–364.

[25] A. RAMOS, M. J. VICENTE-VACAS, AND E. OSET, *Neutron and proton spectra from the decay of Λ hypernuclei*, Phys. Rev., C55, (1997), pp. 735–744, [Erratum: Phys. Rev. C66, 039903 (2002)].

[26] W. M. ALBERICO, G. GARBARINO, A. PARRENO, AND A. RAMOS, *Asymmetries in the non-mesonic weak decay of polarized Λ-hypernuclei*, Phys. Rev. Lett., 94, (2005), p. 082501.

[27] K. SASAKI, M. IZAKI, AND M. OKA, *σ exchange in the nonmesonic decays of light hypernuclei and violation of the* $\Delta I = 1/2$ *rule*, Phys. Rev., C71, (2005), p. 035502.

[28] K. ITONAGA, T. MOTOBA, T. UEDA, AND T. A. RIJKEN, *Role of the axial vector a1-meson exchange in hypernuclear nonmesonic weak decays*, Phys. Rev., C77, (2008), p. 044605.

[29] J.-H. JUN, *Four-baryon point* ΛN → NN *interaction for the nonmesonic weak decay of the hypernuclei* ${}^{4}_{\Lambda}$H, ${}^{4}_{\Lambda}$He, ${}^{5}_{\Lambda}$He, *and* ${}^{12}_{\Lambda}$C, Phys. Rev., 63, (2001), p. 044012.

[30] A. PARRENO, C. BENNHOLD, AND B. R. HOLSTEIN, *The* ΛN —> *NN weak interaction in effective field theory*, Phys. Rev., C70, (2004), p. 051601.

[31] A. PEREZ-OBIOL, A. PARRENO, AND B. JULIA-DIAZ, *Current constraints on the EFT for the* $\Lambda N \to NN$ *transition*, Phys. Rev., C84, (2011), p. 024606.

[32] A. PÉREZ-OBIOL, D. R. ENTEM, B. JULIÁ-DÍAZ, AND A. PARREÑO, *One-loop contributions in the EFT for the* $\Lambda N \to NN$ *transition*, Phys. Rev., C87, (2013), p. 044614.

[33] E. BAUER AND G. GARBARINO, *Microscopic Approach to Nucleon Spectra in Hypernuclear Non-Mesonic Weak Decay*, Phys. Lett., B698, (2011), pp. 306–310.

[34] E. BAUER, G. GARBARINO, AND C. A. RODRÍGUEZ PEÑA, *Nonmesonic weak decay of* Λ *hypernuclei: The three-nucleon induced mode*, Phys. Lett., B766, (2017), pp. 144–148.

[35] A. PARRENO, A. RAMOS, AND C. BENNHOLD, *Novel weak decays in doubly strange systems*, Phys. Rev., C65, (2002), p. 015205.

[36] K. SASAKI, T. INOUE, AND M. OKA, *The ΛΛ —> Y N weak transition in double Λ hypernuclei*, Nucl. Phys., A726, (2003), pp. 349–355.

[37] E. BAUER, G. GARBARINO, AND C. A. RODRÍGUEZ PEÑA, *Nonmesonic weak decay of double-Λ hypernuclei: A microscopic approach*, Phys. Rev., C92(1), (2015), p. 014301.

[38] V. G. J. STOKS AND T. A. RIJKEN, *Soft core baryon baryon potentials for the complete baryon octet*, Phys. Rev., C59, (1999), pp. 3009–3020.

[39] J. BERINGER, J. F. ARGUIN, R. M. BARNETT, K. COPIC ET AL., *Review of Particle Physics*, Phys. Rev. D, 86, (2012), p. 010001.

[40] J. BALEWSKI, A. BUDZANOWSKI, H. DOMBROWSKI, W. EYRICH ET AL., *Total cross section of the reaction $pp \rightarrow pK^+\Lambda$ close to threshold*, Physics Letters B, 420(1), (1998), pp. 211 – 216, ISSN 0370-2693.

[41] S. SEWERIN, G. SCHEPERS, J. T. BALEWSKI, A. BUDZANOWSKI ET AL., *Comparison of Λ and Σ^0 Production near Threshold in Proton-Proton Collisions*, Phys. Rev. Lett., 83, (1999), pp. 682–685.

[42] P. KOWINA, M. WOLKE, H. H. ADAM, A. BUDZANOWSKI ET AL., *Energy dependence of the Λ/Σproduction cross-section ratio in p-p interactions*, The European Physical Journal A - Hadrons and Nuclei, 22(2), (2004), pp. 293–299, ISSN 1434-601X.

[43] J. GRÄTER, R. BILGER, H. CLEMENT, R. MEIER ET AL., *"The $^4He(\pi^+,\pi^-)$ reaction at low energies"*, Physics Letters B, 420(1), (1998), pp. 37 – 42, ISSN 0370-2693.

[44] M. ABDEL-BARY, S. ABDEL-SAMAD, K.-T. BRINKMANN, H. CLEMENT ET AL., *Evidence for a narrow resonance at $1530MeV/c^2$ in the K^0p-system of the reaction*

$pp \to \Sigma^+ K^0 p$ from the COSY-TOF experiment, Physics Letters B, 595(1), (2004), pp. 127 – 134, ISSN 0370-2693.

[45] A. GASPARYAN, J. HAIDENBAUER, C. HANHART, AND J. SPETH, *How to extract the ΛN scattering length from production reactions*, Phys. Rev. C, 69, (2004), p. 034006.

[46] A. M. GASPARYAN, J. HAIDENBAUER, AND C. HANHART, *Scattering lengths of strangeness $S = -2$ baryon-baryon interactions*, Phys. Rev. C, 85, (2012), p. 015204.

[47] S. R. BEANE, E. CHANG, W. DETMOLD, H. W. LIN ET AL., *Deuteron and exotic two-body bound states from lattice QCD*, Phys. Rev. D, 85, (2012), p. 054511.

[48] S. R. BEANE, E. CHANG, S. D. COHEN, W. DETMOLD ET AL., *Hyperon-Nucleon Interactions from Quantum Chromodynamics and the Composition of Dense Nuclear Matter*, Phys. Rev. Lett., 109, (2012), p. 172001.

[49] A. PARREÑO, A. RAMOS, N. G. KELKAR, AND C. BENNHOLD, *Weak strangeness production reaction $pn \to p\Lambda$ in a one-boson-exchange model*, Phys. Rev. C, 59, (1999), pp. 2122–2129.

[50] T. KISHIMOTO, *Weak and electromagnetic interactions in nuclei*, in *World Scientific* (edited by H. EJIRI, T. KISHIMOTO, AND T. SATO), p. 514 (1995).

[51] J. HAIDENBAUER, K. HOLINDE, K. KILIAN, T. SEFZICK ET AL., *Weak strangeness production in nucleon-nucleon scattering*, Phys. Rev., C52, (1995), p. 3496.

[52] E. BOTTA, T. BRESSANI, AND G. GARBARINO, *Strangeness in nuclear physics: a critical review on selected topics*, Eur. Phys. J., A48, (2012), pp. 41–99.

[53] R. SHYAM, K. TSUSHIMA, AND A. W. THOMAS, *Production of Ξ^- hypernuclei via the (K-,K+) reaction within a quark-meson coupling model*, Nucl. Phys., A881, (2012), pp. 255–268.

[54] S. DAIRAKU ET AL., *Measurement of X-Rays from Ξ^- Atom* (2006), proposal for J-PARC 50 GeV Proton Synchrotron.

[55] M. KOTULLA ET AL., *Technical progress report for: PANDA Strong Interaction Studies with Antiprotons* (2005), PANDA Collaboration.

[56] M. GELL-MANN, *A schematic model of baryons and mesons*, Physics Letters, 8(3), (1964), pp. 214 – 215, ISSN 0031-9163.

[57] G. ZWEIG, *An SU(3) model for strong interaction symmetry and its breaking. Version 1*.

[58] E. NOETHER, *Invariante Variationsprobleme*, Nachrichten von der Gesellschaft der Wissenschaften zu Göttingen, Mathematisch-Physikalische Klasse, 1918, (1918), pp. 235–257.

[59] M. GELL-MANN, R. J. OAKES, AND B. RENNER, *Behavior of Current Divergences under* $SU_3 \times SU_3$, Phys. Rev., 175, (1968), pp. 2195–2199.

[60] S. COLEMAN, J. WESS, AND B. ZUMINO, *Structure of phenomenological Lagrangians. 1*, Phys. Rev., 177, (1969), p. 2239.

[61] C. CALLAN, S. COLEMAN, J. WESS, AND B. ZUMINO, *Structure of phenomenological Lagrangians. 2*, Phys. Rev., 177, (1969), p. 2247.

[62] Y. GOTO, N. HAYASHI, M. HIRAI, H. HORIKAWA ET AL., *Polarized parton distribution functions in the nucleon*, Phys. Rev. D, 62, (2000), p. 034017.

[63] G.-S. YANG AND H.-C. KIM, *Meson–baryon coupling constants of the SU(3) baryons with flavor SU(3) symmetry breaking*, Physics Letters B, 785, (2018), pp. 434 – 440, ISSN 0370-2693.

[64] M. BANDO, T. KUGO, S. UEHARA, K. YAMAWAKI ET AL., Phys. Rev. Lett., 54, (1985), p. 1215.

[65] S. OKUBO, *φ meson and unitary symmetry model*, Phys. Lett., 5, (1963), pp. 165–168.

[66] K. P. KHEMCHANDANI, H. KANEKO, H. NAGAHIRO, AND A. HOSAKA, *Vector meson-baryon dynamics and generation of resonances*, Phys. Rev., D83(114041).

[67] E. E. JENKINS AND A. V. MANOHAR, *Baryon chiral perturbation theory using a heavy fermion Lagrangian*, Phys. Lett., B255, (1991), pp. 558–562.

[68] R. P. SPRINGER, *Heavy baryon chiral perturbation theory and the weak nonleptonic p wave decays of the baryon octet*, Phys. Lett., B461, (1999), pp. 167–174.

[69] R. E. MARSHAK, RIAZUDDIN, AND C. P. RYAN, *Theory of weak interactions in particle physics* (Wiley-Interscience, John Wiley and Sons Inc., 1969).

[70] F. E. CLOSE, *An introduction to quarks and patrons* (Academic Press Inc (London), 1979).

[71] B. DESPLANQUES, J. F. DONOGHUE, AND B. R. HOLSTEIN, *Unified treatment of the parity violating nuclear force*, Annals of Physics, 124(2), (1980), pp. 449 – 495, ISSN 0003-4916.

[72] J. F. DONOGHUE, E. GOLOWICH, AND B. R. HOLSTEIN, *Dynamics of the Standard Model* (Cambridge University Press, 1992).

[73] J. F. DONOGHUE, E. GOLOWICH, AND B. HOLSTEIN, *Low-energy weak interactions of quarks*, Physics Reports, 131(5), (1986), pp. 319 – 428, ISSN 0370-1573.

[74] L. DE LA TORRE, *On particle mixing and hypernuclear decay*, Ph.D. thesis, UMI Dissertation Information Service (1982).

[75] S. L. ADLER AND R. F. DASHEN, *Current algebras and applications to particle physics* (W.A. Benjamin, INC. Publishers, 1968).

[76] M. GRIGORESCU, *SU(3) Clebsch-Gordan coefficients*, Stud. Cercetari Fiz., 36, (1984), p. 3.

[77] J. CARO, C. GARCIA-RECIO, AND J. NIEVES, *Double Λ hypernuclei and the nuclear medium effective $\Lambda\Lambda$ interaction*, Nucl. Phys., A646, (1999), pp. 299–342.

[78] M. BANDO, T. KUGO, S. UEHARA, K. YAMAWAKI ET AL., *Is the ρ Meson a Dynamical Gauge Boson of Hidden Local Symmetry?*, Phys. Rev. Lett., 54, (1985), pp. 1215–1218.

[79] A. PARREÑO, *The nonmesonic weak decay of hypernuclei*, Ph.D. thesis, Universitat de Barcelona (1997).

[80] T. A. RIJKEN, V. G. J. STOKS, AND Y. YAMAMOTO, *Soft core hyperon - nucleon potentials*, Phys. Rev., C59, (1999), pp. 21–40.

[81] I. VIDAÑA HARO, *Description of hyperonic matter and hypernuclei within the Brueckner-Hartree-Fock theory*, Ph.D. thesis, Barcelona U., ECM (2001).

[82] H. FUJIOKA ET AL., *Decay Pion Spectroscopy of ${}^{5}_{\Lambda\Lambda}H$ produced by Ξ^-–hypernuclear Decay* (2019), proposal for J-PARC 50 GeV Proton Synchrotron.

[83] M. AGNELLO ET AL., *Direct measurement of the ${}^{3}_{\Lambda}H$ and ${}^{4}_{\Lambda}H$ lifetimes using ${}^{3,4}He(\pi^-,K^0){}^{3,4}_{\Lambda}H$ reactions* (2019), proposal for J-PARC 50 GeV Proton Synchrotron.

[84] H. ASANO ET AL., ${}^{3}_{\Lambda}H$ *and* ${}^{4}_{\Lambda}H$ *mesonic weak decay lifetime measurement with* ${}^{3,4}He(K^-,\pi^0)^{3,4}_{\Lambda}H$ *reaction* (2019), proposal for J-PARC 30 GeV Proton Synchrotron.

[85] S. WEINBERG, *The Quantum theory of fields. Vol. 1: Foundations* (Cambridge University Press, 2005), ISBN 9780521670531, 9780511252044.